The key role of crevasse splays in prograding river systems

Analysis of evolving floodplain accommodation and its implications for architecture and reservoir potential

van Toorenenburg, Koen

DOI
10.4233/uuid:28ce86f1-ab43-44fa-a1a6-e8a2f917c9ce

Publication date
2018

Document Version
Final published version

Citation (APA)
van Toorenenburg, K. (2018). *The key role of crevasse splays in prograding river systems: Analysis of evolving floodplain accommodation and its implications for architecture and reservoir potential*. [Dissertation (TU Delft), Delft University of Technology]. https://doi.org/10.4233/uuid:28ce86f1-ab43-44fa-a1a6-e8a2f917c9ce

Important note
To cite this publication, please use the final published version (if applicable).
Please check the document version above.

The key role of crevasse splays in prograding river systems

Analysis of evolving floodplain accommodation and its implications for architecture and reservoir potential

The key role of crevasse splays in prograding river systems

Analysis of evolving floodplain accommodation and its implications for architecture and reservoir potential

Proefschrift

ter verkrijging van de graad van doctor
aan de Technische Universiteit Delft,
op gezag van de Rector Magnificus prof. dr. ir. T.H.J.J. van der Hagen,
voorzitter van het College voor Promoties,
in het openbaar te verdedigen op donderdag 18 oktober 2018 om 12:30 uur

door

Koen Arnoldus VAN TOORENENBURG

Ingenieur in de Technische Aardwetenschappen
aan de Technische Universiteit Delft, geboren te Leiden, Nederland.

Dit proefschrift is goedgekeurd door de promotoren:

Dr. M.E. Donselaar
Prof. dr. G.J. Weltje

Samenstelling promotiecommissie:

Rector Magnificus,	voorzitter
Dr. M.E. Donselaar,	Technische Universiteit Delft, promotor
Prof. dr. G.J. Weltje,	Katholieke Universiteit Leuven, promotor
Onafhankelijke leden:	
Prof. dr. A.W. Martinius,	Technische Universiteit Delft
Prof. dr. C.R. Fielding,	University of Nebraska-Lincoln
Prof. dr. A. Amorosi,	Università di Bologna
Dr. E.A. Hajek,	Pennsylvania State University
Dr. R.A.F. Dalman,	TNO Nederland
Prof. dr. G. Bertotti,	Technische Universiteit Delft, reservelid

Keywords: Crevasse splays, prograding river systems, floodplain evolution, low net-to-gross fluvial stratigraphy, reservoir potential

Printed by: Gildeprint

Front & Back: Stylised kite aerial imagery of the Río Colorado, Bolivia

ISBN 978-94-6366-084-6

An electronic version of this dissertation is available at
http://repository.tudelft.nl/

cre·vas·se splay

noun [C] /krəˈvæs spleɪ/
sedimentary fluvial deposit which forms when a stream breaks its natural or artificial levees and deposits sediment onto a floodplain

Contents

Summary

Crevasse splays play a crucial role in the development of prograding fluvial fans, manifested in the aggradation of alluvial ridges and the subsequent autogenic switching (i.e., avulsion) of river paths. Despite this being generally acknowledged, the underlying processes have remained underexplored and are often represented only in overly simplified parametrisations. Few studies are dedicated to crevasse splays, most of which are focused towards depositional processes and lack a comprehensive integration with the parent river system. A thorough appreciation of how crevasse splays interact with their fluvial environment is key to understanding the mechanisms that shape prograding fluvial systems and their preserved stratigraphy. This provides valuable constraints for palaeo-reconstructructions of (subsurface) fluvial intervals and the assessment of their (hydrocarbon) reservoir potential.

This Thesis concerns the spatial and temporal evolution of crevasse splays, their role in the autogenic development of fluvial fans, and the resultant sedimentary architecture. Data were acquired from complementing settings in order to include all spatial and temporal dimensions needed for a systematic analysis. The presently active Río Colorado fluvial system (Altiplano Basin, Bolivia) allowed to make snapshot observations of fluvial (overbank) processes, sediment distribution, and surface geomorphology at the time of deposition. Outcrops of the Miocene Huesca fluvial fan (Ebro Basin, Spain) provided insights over a longer period of deposition, exposing the preserved sedimentary architecture in outcrop. The pseudo-three-dimensional outcrop view was linked to subsurface fluvial stratigraphy and petrophysical properties encountered in wells (i.e., cores and well logs) that penetrate the gas-prone margins of the Southern Permian Basin (Central Europe) and Triassic West Netherlands Basin (The Netherlands). This multi-perspective workflow supported the formulation of a comprehensive depositional model and a generic life cycle for crevasse splays, integrated into the parent fluvial environment. It enabled a thorough evaluation of the fundamental role that crevasse splays play in progradational avulsion processes. The study ultimately serves to assess the resultant sedimentary architecture and properties, having been conceived to investigate the reservoir potential and exploratory value of crevasse splays in the deep subsurface.

A generic life cycle applies to crevasse splays in non-degradational fluvial systems, typically ending in backfilling and abandonment. Crevasse-splay channels adjust to a graded equilibrium profile through proximal erosion and distal deposition, with their prograding distal termini acting as a local base level. When proximal incision advances to below the maximum level of floodplain inundation, a reflux of floodwater occurs during the waning stage of flooding. The resultant decrease in gradient ultimately leads to the backfilling and abandonment of a crevasse splay, provided that the elevation at its distal fringe remains higher than that of the parent channel floor. Consecutive crevasse splays form an alluvial ridge through lateral

amalgamation and subsequent vertical stacking, perching the active river above the surrounding floodplain. Avulsion occurs when super-elevation and gradient reduction of the channel thalweg advance to the point where a crevasse channel constitutes a hydrodynamically more-favourable flow path.

A high-resolution morphological reconstruction of the Río Colorado fluvial fan has been established to test the proposed life cycle of crevasse splays and evaluate its role in progradational avulsions and the autogenic organisation of the fluvial system. An avulsion can only occur when an overbank path of steepest descent reaches a base level in a shorter distance than the along-channel distance. Crevasse splays prograde along this overbank flow path and capture an increasing portion of the total discharge, accelerating their development. When the crevasse apex incises down to or below its trunk channel thalweg, the avulsion is complete. The overbank path of steepest descent (i.e., avulsion path) is governed by floodplain topography, which is largely comprised of abandoned alluvial ridges. This leads to compensational stacking of successive prograding channel belts, resulting in fan of amalgamated ridges that may be inaccurately identified as a distributary fluvial system.

Crevasse splays may constitute (additional) reservoir capacity in fluvial subsurface intervals, forming thin, but laterally extensive sediment bodies of up to $\sim 10^5$ m^3 in volume. Lateral amalgamation and subsequent vertical stacking of crevasse splays in alluvial ridges creates sand-on-sand contact between individual units, resulting in combined volumes of up to $\sim 10^7$ m^3. Avulsion-induced channel incision and onlapping of consecutive alluvial ridges may further increase the interconnected sand volume to $>10^8$ m^3. In outcrop stratigraphy, stacked crevasse splays form intervals of up to several metres thick that can be correlated over several kilometres distance and reflect parent channel dimensions.

Preliminary work appended to this Thesis shows that sediment dispersal in crevasse splays is essentially governed by stream power during short episodes of peak runoff preceding unconfined overbank flow. Sediment is sourced from both the parent channel and incision (i.e., reworking) of levee and substrate material near the crevasse apex and subsequently transported and deposited further onto the adjacent floodplain. The resultant grain-size distribution is bimodal. Deposition of the relatively coarser fraction is governed by flow energy, which is longer-retained in the distributary crevasse-splay channels and rapidly decreases when leaving confinement. The grain-size distribution of this end member can be parametrised as a bivariate function of transport distance along-channel and outside the splay channels, although repeated switching and amalgamation over multiple flooding events add complexity to this depositional model. A finer-grained fraction settles from standing water during floodplain inundation, draping over the coarser-grained fraction and locally removed over subsequent flooding events.

Initial studies on reservoir potential show that the petrophysical properties of crevasse splays are suitable for the production of natural gas. The contribution of overbank deposits should be considered in volumetric estimates of conventional fluvial reservoir intervals. Moreover, previously bypassed intervals of fine-grained floodplain stratigraphy may be developed using existing infrastructure at low rein-

vestment costs, prolonging gas production and postponing abandonment.

Floodplain intervals containing crevasse splays could help to constrain well-based (i.e., sub-seismic) reconstructions of their associated fluvial system, provided that individual river fans can be reliably correlated between wells. Within such correlated intervals, normalised well-log responses representative of sediment size could be used to derive the relative position of each penetration within the system and estimate the associated river dimensions, based on the insights presented in this Thesis. This would ultimately help to constrain approximations of size, orientation, and connectivity of the fluvial system, aiding exploration and productivity assessments.

Samenvatting

Crevassewaaiers spelen een sleutelrol in de ontwikkeling van prograderende rivierwaaiers. Dit komt tot uiting in de aggradatie van rivierruggen en de daaropvolgende autogene verlegging van rivierpaden (i.e., avulsie). Ondanks het feit dat dit breed erkend wordt zijn de onderliggende processen onderbelicht gebleven en worden die vaak voorgesteld met overeenvoudige parametrisaties. Een klein aantal studies heeft zich volledig toegelegd op crevassewaaiers, waarvan het overgrote deel zich richt op afzettingsprocessen en een volledige integratie met het fluviatiele moedersysteem mist. Een doorgronding van de wisselwerking tussen crevassewaaiers en hun rivieromgeving is essentieel om de mechanismen te begrijpen die prograderende rivierwaaiers en hun gepreserveerde stratigrafie vormen. Dit biedt waardevolle aanknopingspunten voor palaeo-reconstructies van (ondergrondse) fluviatiele intervallen en de beoordeling van hun reservoirpotentie (voor koolwaterstoffen).

Dit Proefschrift richt zich op de evolutie van crevassewaaiers in ruimte en tijd, hun rol in de autogene ontwikkeling van prograderende rivierwaaiers en de resulterende sedimentaire architectuur. Om alle voor een systematische analyse benodigde dimensies in ruimte en tijd te kunnen beschouwen zijn gegevens verzameld uit elkaar aanvullende omgevingen. Het hedendaagse Río Colorado riviersysteem (Altiplanobekken, Bolivia) stond het toe momentopnames te maken van fluviatiele (overstromings)afzettingen, sedimentdistributie en oppervlaktegeomorfologie ten tijde van afzetting. Ontsluitingen van de Miocene Huesca rivierwaaier (Ebrobekken, Spanje) gaven inzicht in langere periodes van depositie door de resulterende stratigrafie bloot te stellen. Deze pseudo-driedimensionale ontsluiting werd gekoppeld aan fluviatiele stratigrafie en petrofysische eigenschappen in de ondergrond, zoals aangetroffen in boorputten (i.e., kernen en putlogs) die de gashoudende randen van het Zuid-Permische Bekken (Centraal Europa) en het Triassische West Nederland Bekken (Nederland) penetreren. Deze meerzijdige werkwijze leidde tot het formuleren van een veelomvattend afzettingsmodel en een generieke onwikkelingscyclus van crevassewaaiers die is geïntegreerd in de rivieromgeving. Dit maakte het mogelijk om de fundamentele rol die crevassewaaiers spelen in prograderende avulsieprocessen grondig te analyseren. Uiteindelijk dient deze studie om de resulterende sedimentaire architectuur en eigenschappen te beoordelen, met als doel om de reservoirpotentie en exploratiewaarde van crevassewaaiers in de diepe ondergrond te onderzoeken.

Crevassewaaiers in prograderende riviersystemen doorgaan een generieke ontwikkelingscyclus die normaal gesproken eindigt in opvulling en verlating. Crevassegeulen passen zich aan aan een gegradeerd equilibriumprofiel door middel van proximale erosie en distale sedimentafzetting. Daarbij dienen hun prograderende distale termini als een lokaal basisniveau. Wanneer proximale insnijding tot onder

het maximale overstromingspeil komt zal een terugstroom van vloedwater optreden zodra het waterpeil zakt. De daaruit voortkomende reductie in gradiënt leidt uiteindelijk tot opvulling en verlating van de crevassewaaier, mits de distale waaierrand hoger ligt dan de bodem van de moedergeul. Opeenvolgende crevassewaaiers vormen een rivierrug door laterale amalgamatie en verticale opeenstapeling. Daardoor wordt de actieve geul verheven boven de omliggende overstromingsvlakte. Een avulsie vindt plaats wanneer superelevatie en afvlakking van het geulprofiel ertoe leiden dat een crevassegeul een hydrodynamisch aantrekkelijker stroompad vormt.

Er is op hoge resolutie een morfologische reconstructie van de Río Colorado rivierwaaier gemaakt om de voorgestelde ontwikkelingscyclus van crevassewaaiers te testen, alsook om de rol daarvan bij progradatiegestuurde avulsies en de autogene ontwikkeling van het fluviatiele systeem te analyseren. Een avulsie kan alleen dan plaatsvinden wanneer een buitengeuls steilste stroompad een basisniveau bereikt in een kortere afstand dan de hoofdgeul. Een crevassewaaier bouwt uit langs dit buitengeulse stroompad en vangt een steeds groter deel van het totale debiet waardoor de ontwikkeling verder versneld. Wanneer de crevasse-apex tot beneden de bodem van de moedergeul insnijdt is de avulsie compleet. Het buitengeulse steilste stroompad (i.e., avulsiepad) wordt bepaald door de topografie van de overstromingsvlakte die grotendeels bestaat uit verlaten rivierruggen. Dit leidt tot compensatiestapeling van opeenvolgende rivierpaden, hetgeen resulteert in een waaier van geamalgameerde ruggen waarin abusievelijk een distributief riviersysteem kan worden herkend.

Crevassewaaiers kunnen aanvullende reservoircapaciteit vormen in fluviatiele intervallen in de ondergrond. Zij vormen dunne, maar lateraal uitgestrekte sedimentlichamen tot $\sim 10^5$ m^3 in volume. Laterale amalgamatie en verticale opeenstapeling vormen zand-op-zand contact, wat resulteert in gecombineerde volumes tot $\sim 10^7$ m^3. Door avulsie veroorzaakte geulinsnijdingen en overlapping van opeenvolgende rivierruggen zou het onderling verbonden zandvolume verder kunnen opstuwen naar $>10^8$ m^3. In gesteenteontsluitingen vormen gestapelde crevassewaaiers intervallen tot enkele meters dikte die over een aantal kilometers afstand gecorreleerd kunnen worden en schalen met de dimensies van de moedergeul.

Voorlopige onderzoeksresultaten die bij dit Proefschift zijn aangehecht laat zien dat de sedimentverdeling in crevassewaaiers primair bepaald wordt door stromingskracht gedurende korte periodes van piekdebiet voorafgaand aan onbeperkte overstroming. Sediment wordt zowel aangevoerd door de moedergeul als gemobiliseerd uit het substraat bij de crevasse-apex en wordt vervolgens naar de naastgelegen overstromingsvlakte vervoerd en afgezet. De resulterende korrelgrootteverdeling is bimodaal. Afzetting van relatief grovere korrels wordt bepaald door stromingskracht, hetgeen langer vastgehouden wordt in de distributieve crevassegeulen en daarbuiten snel afneemt. De korrelgrootteverdeling van dit eindelement kan worden geparametriseerd als een bivariate functie van transportafstand door de crevassegeul(en) en die daarbuiten, alhoewel herhaaldelijke verlegging en amalgamatie gedurende meerdere overstromingen leiden tot een complexere verdeling. Een relatief fijnere korrelgroottefractie daalt neer wanneer de overstromingsvlakte onder

water staat en wordt over de grovere fractie heen gedrapeerd. Deze laag wordt lokaal weer gemobiliseerd bij volgende overstromingen.

Inleidende studies naar reservoirpotentieel laten zien dat de petrofysische eigenschappen van crevassewaaiers geschikt zijn voor de productie van aardgas. De bijdrage van overstromingsafzettingen zou in overweging genomen moeten worden bij volumetrische schattingen van conventionele fluviatiele reservoirintervallen. Verder kunnen eerder gemiste intervallen van fijnkorrelig overstromingssediment met gebruikmaking van bestaande infrastructuur mogelijk economisch ontwikkeld worden waardoor de gasproductie wordt verlengd en putverlating wordt uitgesteld.

Overstromingsafzettingen met daarin crevassewaaiers kunnen helpen bij het maken van op boorputten gebaseerde (sub-seismische) reconstructies van het moederriviersysteem, mits individuele rivierwaaiers goed gecorreleerd kunnen worden tussen de boorputten. Binnen dergelijke gecorreleerde intervallen kunnen genormaliseerde putlogs die de sedimentgrootte vertegenwoordigen worden gebruikt om de relatieve positie van elke penetratie binnen het systeem te achterhalen en rivierdimensies te kunnen schatten op basis van de inzichten die in dit Proefschrift worden gepresenteerd. Dit kan uiteindelijk helpen bij het inschatten van de grootte, oriëntatie en connectiviteit van het fluviatiele systeem, hetgeen bijdraagt aan exploratie en beoordelingen van productiviteit.

1

Introduction

1

Research in the field of fluvial sedimentology mainly concerns the channel domain, which typically constitutes the most energetic and dynamic environment in river systems and carries the coarsest sediments. The overbank realm is given comparatively less attention (Bridge, 2006), although its influence on fluvial development has been acknowledged in system-scale studies (e.g., Hajek and Wolinsky, 2012). In fact, overbank sedimentation generally forms a volumetrically significant part of fluvial deposits in filling aggradational basins, which is evidenced by the widespread occurrence of preserved floodplain stratigraphy in the rock record (e.g., Wright and Marriott, 1993). These comparatively fine-grained intervals may have predictive value in the reconstruction of their associated fluvial system and contain thin-bedded sandstone units (Figure 1.1) that could have (secondary) reservoir potential in gas-prone subsurface intervals. A thorough appreciation of the overbank domain is required to develop a comprehensive understanding of sedimentary processes and preserved architecture in fluvial depositional systems.

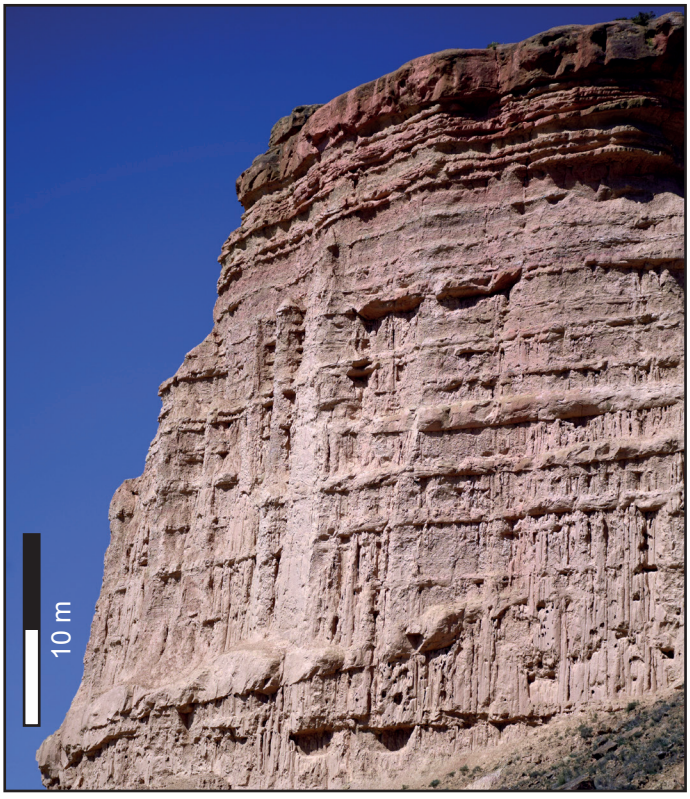

Figure 1.1: Floodplain stratigraphy in an outcrop of the Huesca fluvial fan (Ebro Basin, Spain) near the *Embalse del Torrollón*, containing thin-bedded sandstone sheets.

1.1. Context and rationale

Floodplains develop through a complex interplay of processes, some of which are specific to the environmental setting. By definition, floodplains are subjected to episodic river flooding, the frequency of which is dominantly controlled by runoff variability (mainly as a function of climate and hinterland vegetation) and fluvial morphology. Sediment is supplied to the floodplain as sediment-laden water spills out of confinement when river discharge exceeds the bankfull channel capacity or spills through levee breaches. The coarsest of these sediments are deposited as the overbank flow decelerates, forming fluvial levees and crevasse splays adjacent to their parent channel. Finer sediments subsequently settle from standing floodwater across the inundated floodplain. In between successive flooding events, subaerial exposure of the floodplain typically leads to its alteration by non-depositional processes. These may include desiccation, aeolian deflation and deposition, bioturbation, pedogenesis (i.e., soil formation), and early diagenesis (e.g., compaction, cementation). Vegetation may rapidly occupy overbank accommodation space and increase bank stability in humid climates. As a result, the inherently heterogeneous floodplain stratigraphy comprises an intercalation of relatively coarse-grained beds (i.e., levees and crevasse splays), finer-grained inundation deposits (i.e., floodplain fines), and (if present) coal seams and other non-fluvial sedimentary interbeds. The long-term preservation of floodplain sediment is primarily dependent upon accommodation space, as prolonged lateral migration and switching of fluvial channels may erode and remove previously deposited overbank sediment over shorter timescales.

Compared to other fluvial overbank deposits, levees and crevasse splays represent the highest clastic accumulation rates, occurring in relative proximity to their parent channel as a function of flow energy (e.g., Törnqvist and Bridge, 2002; Adams et al., 2004; Shen et al., 2015). Levees develop during unconfined overbank flow, building continuous ridges along both river banks (Brierley et al., 1997). They are then (partially) removed and redeposited by crevasse splays, which extend further onto the adjacent floodplain and form laterally extensive lobes of relatively coarse-grained sediment (e.g., Smith and Pérez-Arlucea, 1994; Tooth, 2005; Burns et al., 2017). The consequent near-channel differential elevation of floodplain topography is associated with the development of alluvial ridges (e.g., Bridge, 1984; Törnqvist and Bridge, 2002; Van Toorenenburg et al., 2016, 2018). Moreover, crevasse splays have been identified as a mechanism for avulsion (e.g., Smith et al., 1989; Smith and Pérez-Arlucea, 1994; Bristow et al., 1999; Mohrig et al., 2000; Farrell, 2001; Slingerland and Smith, 2004; Tooth, 2005; Hampton and Horton, 2007; Dalman and Weltje, 2008; Buehler et al., 2011; Hajek and Wolinsky, 2012; Bernal et al., 2013; Kleinhans et al., 2013; Yuill et al., 2016). It is, therefore, evident that these overbank deposits have a substantial influence on river (system) dynamics and the resultant fluvial stratigraphy.

Research detailing the development and sedimentary architecture of levees and crevasse splays is limited and often lacks a comprehensive integration with its fluvial context. As a result, depositional models have long remained rudimentary

(Bridge, 2006) and are only recently receiving more attention. A critical review by Brierley et al. (1997) addresses the uncertainties in the definition and identification of levees, stating that their inferred significance in fluvial geomorphology justifies further research. Progress since then is helpfully summarised by, e.g., Bridge (2003) and Miall (2014). Crevasse splays are similarly underrepresented in fluvial research, whereas their relative complexity merits more attention. Existing studies on crevasse splays include observations in modern-day river systems (e.g., Arndorfer, 1973; O'Brien and Wells, 1986; Smith et al., 1989; Van Gelder et al., 1994; Bristow et al., 1999; Farrell, 2001; Tooth, 2005; Cahoon et al., 2011; Donselaar et al., 2013; Li and Bristow, 2015; Shen et al., 2015; Joeckel et al., 2016; Yuill et al., 2016; Millard et al., 2017) and examples of preserved stratigraphy in outcrop (e.g., Platt and Keller, 1992; Mjøs et al., 1993; Hornung and Aigner, 1999; Anderson, 2005; Fisher et al., 2007; Hampton and Horton, 2007; Jones and Hajek, 2007; Nichols and Fisher, 2007; Ghazi and Mountney, 2009; Pranter et al., 2009; Ford and Pyles, 2014; Gulliford et al., 2014; Sahoo et al., 2016; Van Toorenenburg et al., 2016; Burns et al., 2017) or in the subsurface (e.g., Pranter et al., 2008; McKie, 2011b; Keeton et al., 2015).

1.2. Research scope and approach

The aim of this Thesis is to investigate the role that crevasse splays play in the autogenic development of prograding fluvial systems. To this end, it is crucial to establish a depositional model that captures the full evolution of crevasse splays in both space and time, and includes non-depositional processes such as the incision of crevasse-splay channels. A generic life cycle for crevasse splays (i.e., from the initial levee breach until splay abandonment) will be proposed and presented in the context of fluvial aggradation and subsequent avulsion of the parent channel. The identification of governing mechanisms and their subsequent sediment dispersal patterns furthers a comprehensive understanding of the autogenic processes that shape prograding fluvial systems. The study serves to enable quantitative reconstructions of the sedimentary architecture and properties of crevasse splays in subsurface floodplain stratigraphy, having been conceived to investigate their hydrocarbon (i.e., natural gas) reservoir potential. Other applications may include the formulation of additional constraints for the palaeo-reconstruction of (subsurface) fluvial successions, the advancement of sediment transport models, and the prediction of river system evolution.

Data for this study were acquired from complementing settings in order to include all spatial and temporal dimensions needed for a systematic analysis (Figure 1.2). The presently active Río Colorado fluvial fan (Altiplano Basin, Bolivia) allows to observe snapshots of fluvial (overbank) processes, sediment distribution, and surface geomorphology at the time of deposition. These can be used to constrain forward models (e.g., *Delft3D*) in order to validate the inferred sedimentary mechanisms that occur during flooding events. Outcrops of the Miocene Huesca fluvial fan (Ebro Basin, Spain) expand the window to a longer period of deposition, exposing the preserved sedimentary architecture in outcrop. This three-dimensional

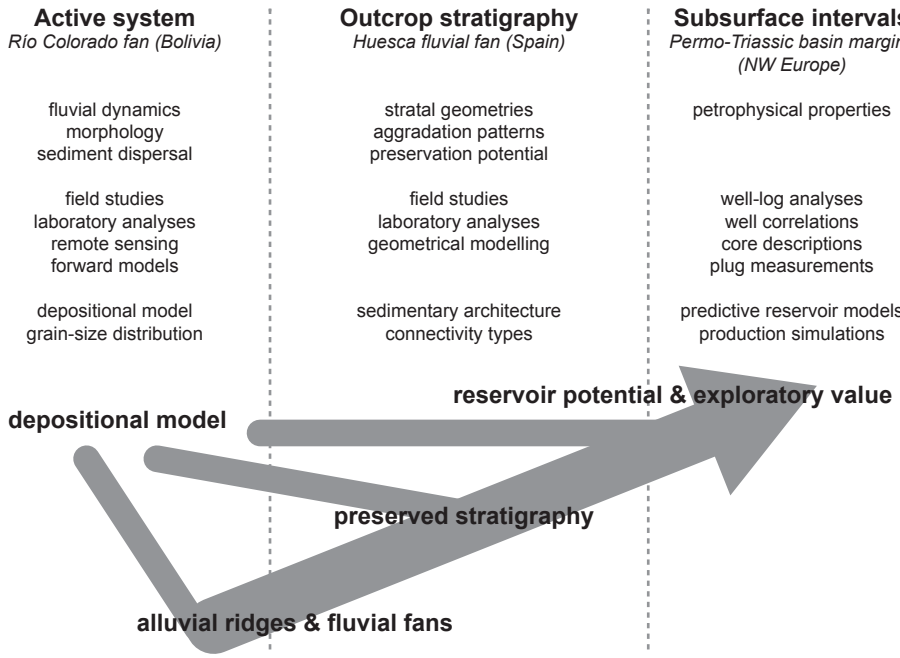

Figure 1.2: Schematic visualisation of the research workflow, divided over columns representative of data sources.

view links to subsurface floodplain stratigraphy encountered in wells (i.e., cores and well logs) in the Southern Permian Basin (Central Europe) and Triassic West Netherlands Basin (The Netherlands). These settings combine to support a comprehensive depositional model of crevasse splays within its fluvial context, as well as an assessment of its hydrocarbon reservoir potential in the subsurface.

1.3. Geological setting

The research presented here is focused on overbank sedimentation in low-gradient river systems that develop along the margins of semi-arid endorheic basins. The climatological setting and absence of eustacy in these inland basins promote a low-stand configuration (i.e., prograding fans punctuated by occasional high-amplitude lake level fluctuations that lead to rapid transgression-regression cycles), leading to the subaerial termination of unconfined dryland river systems into fluvial fans (Figure 1.3). This allows for a comprehensive account of fluvial sediment (i.e., negligible bypass), which may comprise >90% of floodplain deposits near the system terminus (e.g., Hirst, 1991). In addition, the studied setting suppresses any influence of vegetation, base level changes, and lateral confinement on fluvial geomorphology. Similar depositional and climatological conditions characterised Permo-Triassic basins throughout the Central and North Atlantic margins (Williams and

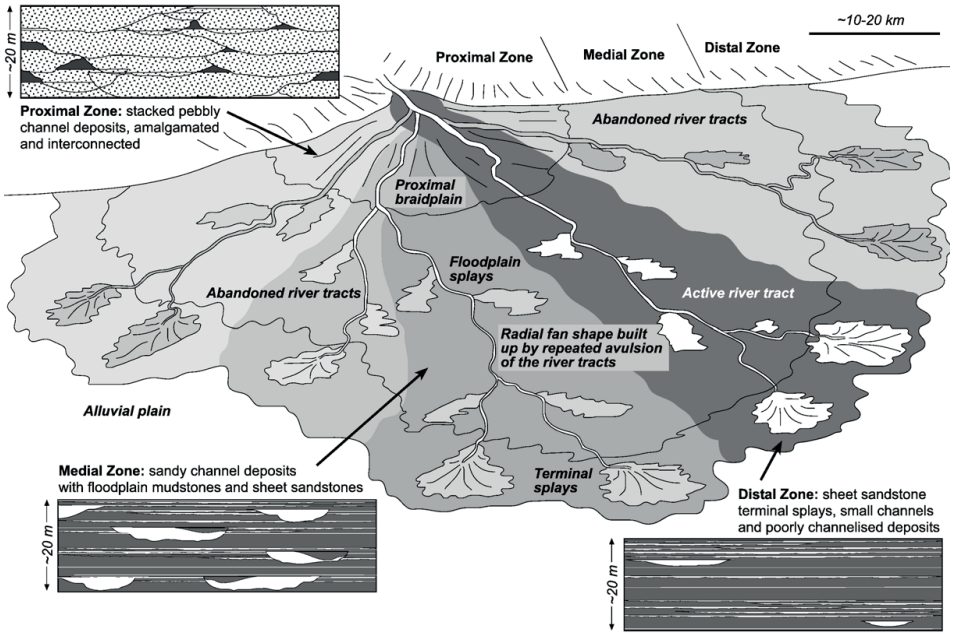

Figure 1.3: Schematic representation of a fluvial fan, formed by repeated avulsions of a single-thread river. After Nichols and Fisher (2007).

McKie, 2009; McKie, 2011a), including now gas-prolific plays in Northwest Europe (e.g., Geluk, 2007a, 2007b; Donselaar et al., 2011). This specific setting thus facilitates the assessment of undisturbed fluvial processes and deposits, whilst serving as a reservoir analogue.

1.3.1. Present-day Río Colorado fluvial fan

The Río Colorado drains into the Altiplano Basin; a large (~$2.0 \cdot 10^5$ km^2) N–S elongated endorheic basin that extends across Peru, Bolivia, Argentina, and Chile and is surrounded by the Cordilleran mountain ranges (Figure 1.4). Tectonically, the basin forms part of the Central Andean ocean-continent convergent margin. The basin is a high-altitude (3650–4200 m above mean sea level) hinterland plateau that formed during the Andean Orogeny (Cretaceous–present) in response to the eastward subduction on the Nazca oceanic Plate under the South American Plate and the related uplift of the Andean orogenic belt (Argollo and Mourguiart, 2000; Horton et al., 2001; Rigsby et al., 2005; Risacher and Fritz, 2009). From the Cretaceous onwards, the basin is filled with volcanoclastics and lacustrine and alluvial sediment (Elger et al., 2005). At present, it lies in the rain shadow of the Eastern Cordillera and has an overall semi-arid climate. Large salt lakes occupy depressions in the southern part of the basin. Towards the north, these pass into ephemeral lakes and a permanent lake (Lago Titicaca) in response to a precipita-

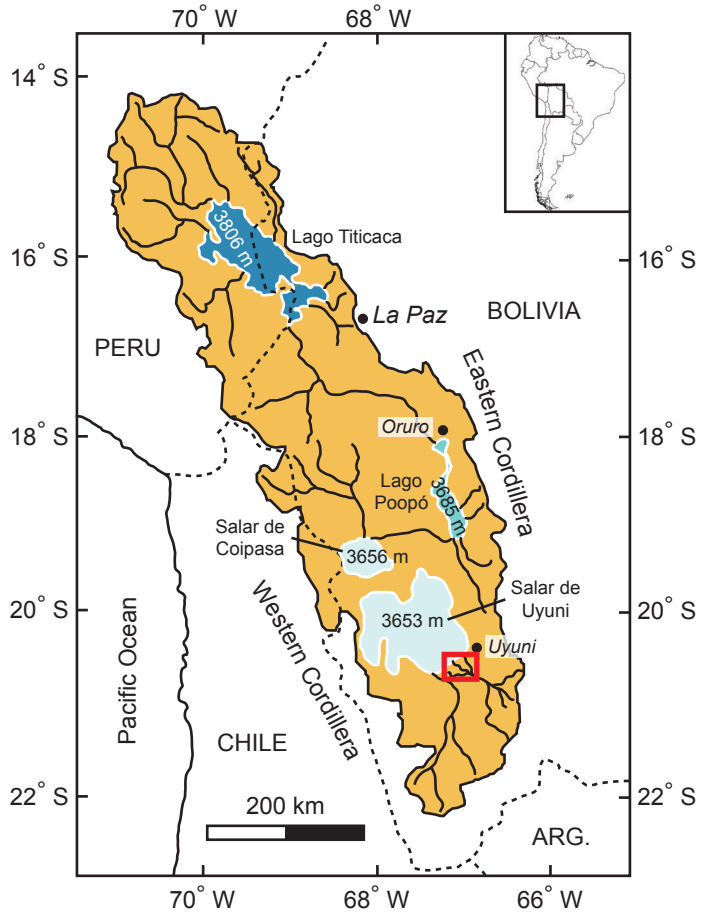

Figure 1.4: Overview of the Altiplano Basin (yellow) showing the internal drainage pattern, southward decrease in lake water levels (dark to light blue), and study area (red box). Inset: location in South America. Modified from Donselaar et al. (2013).

tion gradient across the basin length, from 200 mm yr^{-1} in the south to 800 mm yr^{-1} in the north (Argollo and Mourguiart, 2000). Past wetter climate periods have been recorded; these are characterized by short periods of rapid lake expansion (Servant et al., 1995; Sylvestre et al., 1999; Baker et al., 2001; Fornari et al., 2001; Chepstow-Lusty et al., 2005; Rigsby et al., 2005; Placzek et al., 2006). An example of such wetter climate period is the Tauca phase (26,100–14,900 cal. yr before present), when a large part of the basin was covered with lacustrine water (Donselaar et al., 2013) and the lake level rose to 127 m above the present-day lowstand level (Baker et al., 2001).

The Río Colorado fluvial system on the southeastern fringe of the Altiplano Basin has its catchment in the Eastern Cordillera (Figure 1.5). Absolute age dating using optically stimulated luminescence (OSL) reveals that the river system has been

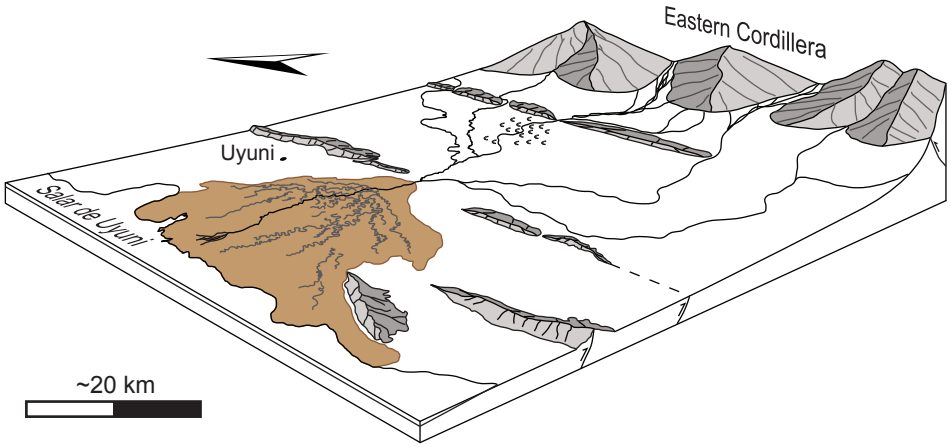

Figure 1.5: Schematic diagram of the Río Colorado fluvial system. The studied distal (depositional) part is indicated in brown; arrow indicates north. Modified from Donselaar et al. (2013).

active for ~12 kyr (Donselaar et al., 2017), gradually prograding towards the salt lake. The river flows to the northwest onto the low-gradient alluvial plain at the edge of the Salar the Uyuni Sub-Basin, where it is mostly single-thread (Donselaar et al., 2013). Crevasse splays extend from both sides of the main channel, generally increasing in frequency downstream (Li and Bristow, 2015).

1.3.2. Miocene Huesca fluvial fan

The Huesca fluvial fan is located on the northern fringe of the Ebro Foreland Basin in northeast Spain (Figure 1.6). The basin formed during the Cenozoic in the Pyrenean Phase of the Alpine Orogeny. It is bounded by the Sierras Marginales thrust front to the north and the Iberian and Catalan coastal ranges to its SW and SE, respectively. From the late Oligocene to the late Miocene, the centre of the basin was occupied by a lake undergoing cycles of water-level fluctuations, which caused km-scale migrations of the shoreline over a low-gradient coastal plain. Alternations of lacustrine clastic sequences with carbonates and evaporites led Arenas and Pardo (1999) to associate high lake levels with a relatively humid paleoclimate, whereas low lake levels were linked to a more arid playa-lake environment.

The Huesca fluvial system derived its sediment from the high Pyrenees as well as the uplifted South Pyrenean Foreland Basin to its north. Sediments of the Huesca fluvial system entered the Ebro basin through a 15–20 km wide gap formed by a fractured zone in the Sierras Marginales thrust sheet, which acted as its line source (Donselaar and Schmidt, 2005). The fan has a ~60 km radius and shows a change in fluvial style from amalgamated braided streams in its proximal reaches to meandering channels and eventually unconfined terminal lobes towards its distal fringe (Fisher et al., 2007; Nichols and Fisher, 2007) (Figure 1.6).

Low net-to-gross floodplain deposits are abundant in the distal part of the fluvial

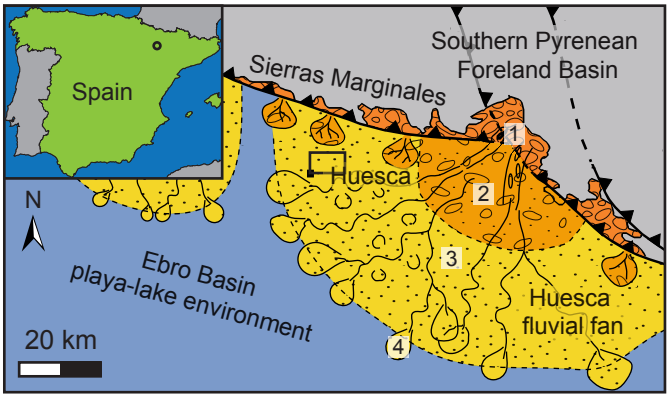

Figure 1.6: Miocene paleogeography of the Huesca fluvial fan showing its source (1), proximal braid plain (2), distal meandering channels (3), and terminal lobes at the fan fringe (4) (modified from Donselaar and Schmidt, 2005). Inset: map of Spain; black circle indicates location of paleogeographic map.

system (Nichols and Fisher, 2007). Here, channel deposits comprise <10% of the overall stratigraphy (Hirst, 1991). Their low-sinuous ribbon geometry (width-to-thickness ratio <15) has been attributed to a limited longevity, as channels avulsed prior to any substantial lateral migration (e.g., Friend et al., 1979; Hirst, 1991; Nichols and Fisher, 2007). Thin-bedded sandstone sheets are common and frequently extend from the top of channel deposits as 'wings', continuing into the channel-fill sandstone (Friend et al., 1986; Hirst, 1991; Fisher et al., 2007; Nichols and Fisher, 2007). These laterally extensive sandstone bodies have been interpreted as the result of unconfined sheet flow (Friend et al., 1986), i.e., overbank levees and crevasse splays (Hirst, 1991; Fisher et al., 2007).

1.4. Thesis outline

This Thesis is structured along its research workflow (Figure 1.2), starting with the definition of a generic depositional model for crevasse splays, subsequently broadening its context to alluvial ridges and fluvial fans, and concluding with a reconstruction of sedimentary architecture and an assessment of its hydrocarbon reservoir potential. A generic life cycle for crevasse splays is proposed in Chapter 2, based on geomorphological and sedimentological observations and playing a key role in the aggradation of alluvial ridges. Chapter 3 is a review of the proposed governing mechanisms for the development of crevasse splays in the context of their parent fluvial system based on a high-resolution geomorphological reconstruction and discusses its implications for autogenic switching of super-elevated river channels. Chapter 4 discusses the sedimentary architecture of amalgamated crevasse-splay intervals in fluvial stratigraphy and its implications for reservoir connectivity. The Thesis is concluded with a synthesis, discussion of its applicability and limitations, and future scope.

The appendices are mainly a preview of initial work towards the application of

the findings presented in this Thesis. Appendix A is focused on sediment dispersal in individual splays, supported by grain-size samples, process-based models, and analogies to channelised fans and lobes. Appendix B links the results of this Thesis to the subsurface expression and reservoir potential of crevasse splays within their fluvial context. Appendix C details the methodology underlying the resampled digital surface models in Chapter 3.

2

The life cycle of crevasse splays

A generic life cycle applies to crevasse splays in prograding river systems, starting with a levee breach and ending with healing of the crevasse. Understanding this mechanism is key to recognising the role that overbank deposition plays in the development of alluvial ridges and subsequent avulsion of the active river.

This Chapter is based on Van Toorenenburg, K. A., Donselaar, M. E., Weltje, G. J. (2018). The life cycle of crevasse splays as a key mechanism in the aggradation of alluvial ridges and river avulsion, *Earth Surface Processes and Landforms* **43**: 2409–2420.

2.1. Introduction

Fluvial research generally focuses on the (near) channel domain, which generally represents the most dynamic environment in river systems. Sedimentation in the unconfined distal part of low-gradient fluvial fans, however, is dominated by floodplain deposition (e.g., Nichols and Fisher, 2007). Here, floodplain evolution has a significant influence on river dynamics, constituting a dynamic boundary condition for the development of the system. Relative to other depositional floodplain processes (i.e., disregarding vegetation cover), fluvial levees and crevasse splays represent the highest accumulation rates (e.g., Törnqvist and Bridge, 2002; Adams et al., 2004; Shen et al., 2015).

On low-gradient alluvial plains, away from topographic confinement, levees likely grow by advection as a water-surface gradient is established between the channel and the adjacent floodplain when peak discharge results in unconfined overbank flow (Adams et al., 2004; Cahoon et al., 2011). Sediment mobilised by the increased in-channel stream power is redeposited in these broad low-gradient levees, decreasing in grain size with distance from the main channel (Adams et al., 2004). Floodplain inundation allows finer sediment to settle from suspension over a large area (Nicholas and Walling, 1997).

The formation of crevasse splays is conditional upon the presence of levees and initiates from a breach point (e.g., Tooth, 2005). The acute onset of crevassing can be arbitrary and has been attributed to fluvial spillover (e.g., Smith et al., 1998; Li and Bristow, 2015), local depressions or weaknesses in the levee crest (Smith et al., 1998; Slingerland and Smith, 2004; Kleinhans et al., 2013), and downstream narrowing (e.g., Li et al., 2014) or blockage of the main channel caused by, e.g., bank collapse or obstruction by foreign objects (Keller and Swanson, 1979; Slingerland and Smith, 2004; Bridge, 2006; Bernal et al., 2013). Initially, the overbank surface gradient and breach-point focusing of floodwater lead to erosion and incision of crevasse-splay channels (Yuill et al., 2016), remobilising levee sediment and the underlying substrate. Deposition occurs where the flow decelerates due to a transition from confined to unconfined flow (cf. Sheets et al., 2002), a decrease in gradient (cf. Bull, 1979), or the floodwater entering a standing body of water (Bristow et al., 1999; Pérez-Arlucea and Smith, 1999; Bridge, 2006; Millard et al., 2017). The splay is deposited as a complex of small lobes that amalgamate as crevasse-splay channels switch and bifurcate (Smith et al., 1989; Tooth, 2005). It expands and progrades further onto the floodplain over the course of consecutive flooding events, its size and floodwater capacity dependent on the overbank morphology and crevasse dimensions (Yuill et al., 2016). The aerial extent of crevasse splays is up to several km^2 (Burns et al., 2017), depending primarily on sediment size and floodplain-drainage conditions (Millard et al., 2017). Crevasse splays extend from both sides of the main channel, generally increasing in frequency downstream (Li and Bristow, 2015). Crevasse-splay channels may be reused by return flow of floodwater to their trunk river during the waning stage of flooding, leading to the development of sinuous rill channels where surface runoff enters a channel depression (Zwoliński, 1992; Donselaar et al., 2013). This reflux causes backstepping

erosion of the hanging crevasse-splay channel floor at its confluence with the main river and in-channel deposition of sedimentary lobes downstream of the channel junction (Donselaar et al., 2013).

Existing research with a dedicated focus on crevasse splays generally concerns depositional processes and (preserved) sedimentary architecture. These studies are based on observations in modern-day river systems (e.g., Arndorfer, 1973; O'Brien and Wells, 1986; Smith et al., 1989; Van Gelder et al., 1994; Bristow et al., 1999; Farrell, 2001; Tooth, 2005; Cahoon et al., 2011; Li et al., 2015; Shen et al., 2015; Joeckel et al., 2016; Millard et al., 2017) and examples of ancient deposits in outcrop (e.g., Platt and Keller, 1992; Mjøs et al., 1993; Hornung and Aigner, 1999; Anderson, 2005; Fisher et al., 2007; Hampton and Horton, 2007; Jones and Hajek, 2007; Nichols and Fisher, 2007; Ghazi and Mountney, 2009; Pranter et al., 2009; Ford and Pyles, 2014; Gulliford et al., 2014; Sahoo et al., 2016; Van Toorenenburg et al., 2016; Burns et al., 2017) or in the subsurface (e.g., Pranter et al., 2008; McKie, 2011a Keeton et al., 2015). Yuill et al. (2016) point out that despite being given minor attention, erosional processes play an important role in the initial phase of crevasse-splay development.

The evolution of crevasse splays is often associated with avulsion of the main river (e.g., Smith et al., 1989; Smith and Pérez-Arlucea, 1994; Bristow et al., 1999; Mohrig et al., 2000; Farrell, 2001; Slingerland and Smith, 2004; Tooth, 2005; Hampton and Horton, 2007; Dalman and Weltje, 2008; Buehler et al., 2011; Hajek and Wolinsky, 2012; Bernal et al., 2013; Kleinhans et al., 2013; Yuill et al., 2016). However, the majority of crevasse splays do not lead to an avulsion of their parent channel. Instead, their activity eventually ceases due to an aggradation-induced decrease in floodwater through-put and backfilling (i.e., healing) of the crevasse-splay channels (e.g., Roberts, 1997; Slingerland and Smith, 2004).

This Chapter presents a detailed analysis of different stages in the evolution of crevasse splays based on observations made in the distal part of the pristine modern-day Río Colorado dryland fluvial system, fringing the endorheic Altiplano Basin in Bolivia. A generic life cycle is proposed and presented as a key building mechanism in the aggradation of alluvial ridges in low-gradient fluvial fans, and its role in the subsequent autogenic switching (i.e., avulsion) of the river path is discussed. The semi-arid lowstand basin setting and consequent sub-aerial termination of the studied system allows for an assessment of fluvial processes in absence of any influence from vegetation, base level changes, or lateral confinement. Moreover, it can serve as an analogue for gas-bearing Permo-Triassic fluvial successions with high proportions of preserved floodplain deposits along the Central and North Atlantic margins (e.g., Williams and McKie, 2009; Donselaar et al., 2011; McKie, 2011a).

2.2. Methodology

The study area entails the pristine distal (depositional) part of the Río Colorado fluvial system (Section 1.3.1) (Donselaar et al., 2013; Li and Bristow, 2015), covering an area of ~500 km^2 southwest of the city of Uyuni in the Potosí depart-

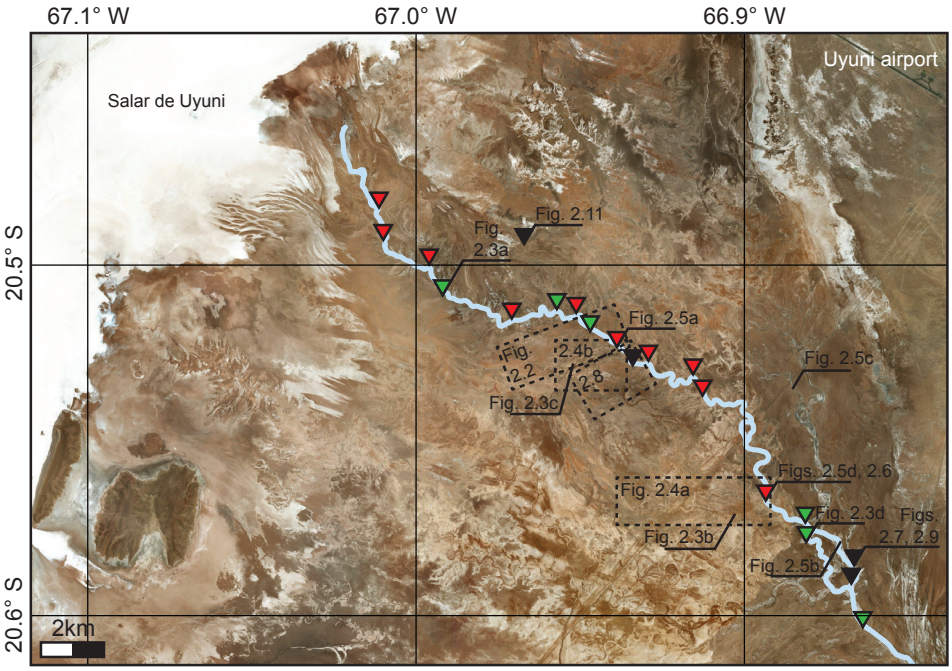

Figure 2.1: Satellite image of the study area (dated 2017; *Bing Maps*) showing the single-thread active river (light blue), morphological classification of observed crevasse splays (triangles in green: unidirectional drainage; red: bidirectional drainage; black: abandoned), and the locations of Figures 2.2–- 2.11.

ment of Bolivia (Figures 1.5 and 2.1). Field campaigns were carried out in the months of October and November of 2014 and 2016, at the end of the dry (winter) season when the river was at its low-flow stage and the area was best accessible.

Google Earth Pro provided a time-lapse overview of the system morphology over the period 2004–2016 with a maximum resolution of ~0.5 m pixel^{-1} (i.e., *WorldView* and *Quickbird* satellite images). Given the high dynamicity of the fluvial environment (Li et al., 2014), kite aerial photography (KAP; Smith et al., 2009) was employed to obtain contemporary aerial imagery at several locations. This was subsequently used to make georeferenced photogrammetric projections in *Agisoft PhotoScan Pro*. A *Trimble 5700* differential-GPS (dGPS) set was used to adequately measure subtle floodplain topography with sub-centimetre accuracy (e.g., Parkinson and Enge, 1996; Chan and Baciu, 2012). Sections were recorded using either a hand-held or vehicle-borne setup of the dGPS rover within a <5 km radius from its base station. This yielded detailed elevation profiles of crevasse splays, their channels, and the surrounding floodplain (subject to a structural +44.4 m vertical datum shift relative to Figure 1.4. All aerial and satellite imagery and dGPS data were combined in a geographic information system (GIS) for comprehensive analysis (Figure 2.1). Sample pits were dug in order to record sedimentary logs comprising bed thickness, nature of contacts, grain size, colour, and sedimentary structures. Sediment samples were collected for grain-size analyses using a *He-*

los KR Sympatico laser particle sizer (Blott et al., 2004), in order to quantify the preserved (i.e., end-member) range in sediment size.

2.3. Morphological observations

Three configurations of crevasse splays are distinguished based on their inferred hydrological role: (1) facilitating unidirectional drainage, (2) facilitating bidirectional drainage, and (3) post-active abandonment. These classifications follow from observations of the crevasse-splay channel gradient and relevant geomorphological features.

2.3.1. Unidirectional drainage

Crevasse splays favouring one-directional flow comprise bifurcating and locally anastomosing low-sinuosity channels with an observed gradient of up to $4 \cdot 10^{-4}$ dipping away from the main river and towards the floodplain (Figure 2.2). These channels are proximally erosive and contain basal scours indicative of outward flow, i.e., away from their parent channel (Figure 2.3a). Their depth and gradient decreases from proximal to distal, leading to an increase in their width-to-depth ratio (Figure 2.2). Subtle levees (Figure 2.3b) and elongate terminal lobes (Figure 2.3c) occur mainly in the distal part of the crevasse splay, resulting from net deposition alongside and at the end of the channels, respectively. Rill channels are absent and there is no evidence for deposition or return flow at the apex of the crevasse splay (Figure 2.3d).

2.3.2. Bidirectional drainage

Bidirectional flow in crevasse splays is accommodated by the near-horizontal thalweg of the lower-order crevasse-splay channels, constituting an absence of gradient ($0–1.5 \cdot 10^{-4}$; Figure 2.4). These channels are more sinuous than those favouring unidirectional drainage and are generally erosive, especially in the proximal reaches of the crevasse splay where they incise deep into the substrate (Figure 2.4) which exhibits a subtle gradient ($2–4 \cdot 10^{-4}$) away from the main river. Basal scours confirm the occurrence of both outflow and reflux (Figure 2.5a) of floodwater. Higher-order crevasse-splay channels with a hanging floor may have a gradient dipping away from their respective lower-order parent channel, locally showing features associated with outflow of floodwater (Figure 2.4a). Contrarily, the presence of rill channels with small sediment lobes at their base suggests a reflux of water from the inundated floodplain into the relative depression of crevasse-splay channels (Figure 2.5b,c). The latter occurs on a larger scale at the junction of the apical crevasse and its associated parent channel, where an asymmetric sediment lobe is found in the main river (Figures 2.2, 2.5a and 2.6). The locus of deposition is partially downstream of the crevasse, causing a local narrowing of the parent channel (Figures 2.5a and 2.6). This results in abundant scouring alongside

and at the downstream end of the lobe (Figure 2.6). The upstream part of the lobe is covered by climbing ripples (Figure 2.5d), ascending its sloped surface oblique to the parent-channel axis as a result of decreasing sediment transport capacity due to flow deceleration.

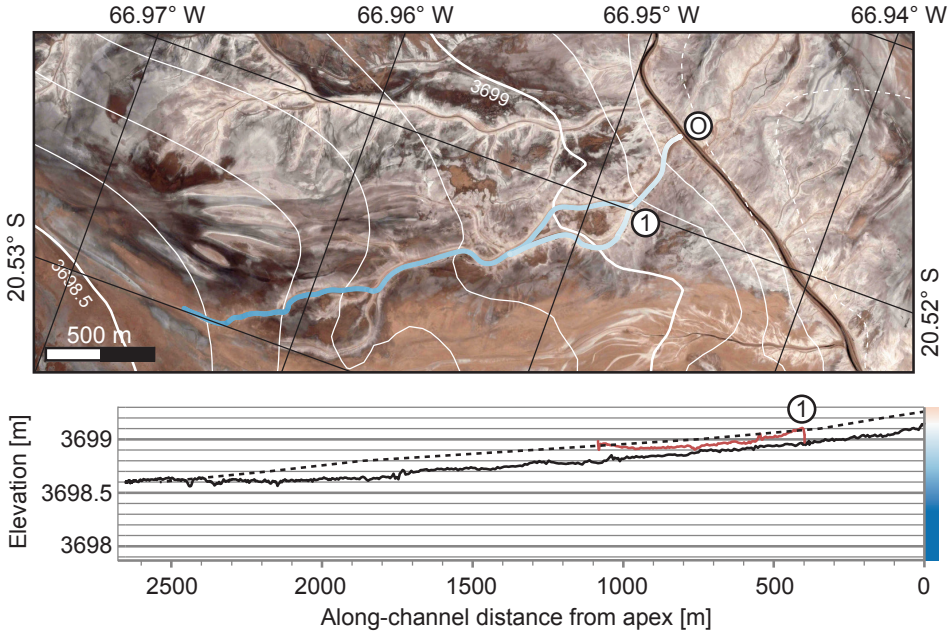

Figure 2.2: Satellite image (dated March 2016; *Google Earth Pro*) and along-channel elevation profile of a crevasse splay facilitating unidirectional drainage. The image shows the elevation of the channel floor relative to the apex (coloured lines; see corresponding colour bar next to profile) and dGPS-based surface topography (white contours). The profile shows the along-channel elevation of the first-order (black) and second-order (red; number corresponds to satellite image) channel floor, and the surface topography alongside the first-order channel (dashed line). x-axis origin corresponds to 'O'; y-axis origin is levelled with the parent-channel floor.

2.3.3. Abandoned crevasse splays

Ample evidence of abandoned and backfilled crevasse-splay channels is visible in the cut banks of the main river (Figure 2.7). The surface expression of crevasse splays in this stage is subtle, ranging from planar to convex and with an overall gradient dipping away from the parent channel (Figure 2.8). Their thickness can range up to 0.25 m for non-channelised sheet deposits proximal to the crevasse-splay channels, thinning towards its distal rims. Remnant depressions of crevasse-splay channels are smoothed out or absent (Figure 2.8). Accretion surfaces within the fill of these channels (Figure 2.7) suggest that sediment entered at an angle to their remnant channel axis (i.e., lateral infill). Climbing ripples overlain by clay drapes provide evidence for short periods of channel reactivation (Figure 2.9), whereas small reflux lobes are also encountered. Preserved grain sizes range from clay to

very-fine sand, ~60% of which is silt (Wentworth, 1922) (Figure 2.10).

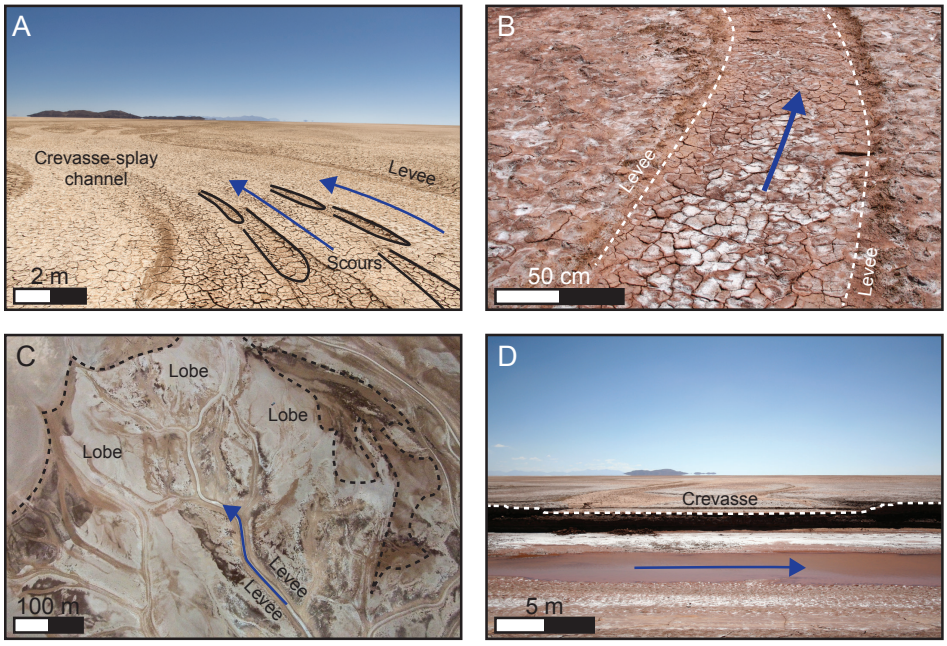

Figure 2.3: Features of crevasse splays facilitating unidirectional drainage. Blue arrows indicate flow direction. (a) Scours (~1 dm deep) indicative of flow towards the floodplain. (b) Subtle levees (~1 cm high levee top) alongside a crevasse-splay channel. (c) KAP orthophoto showing levees and amalgamated lobes at the termini of crevasse-splay channels. (d) Crevasse apex seen from its parent channel (unincised cutbank is ~1.4 m high).

A distinctive type of derelict crevasse splays is found along the remnant depressions of abandoned river channels. Its channels show evidence of backstepping erosion (Figure 2.11) and contain basal scours indicative of flow from the floodplain towards the abandoned main channel. The crevasse-splay channel floor steps down, resulting in an overall gradient dipping towards its former apex and the abandoned trunk channel, acting as a floodplain drainage system.

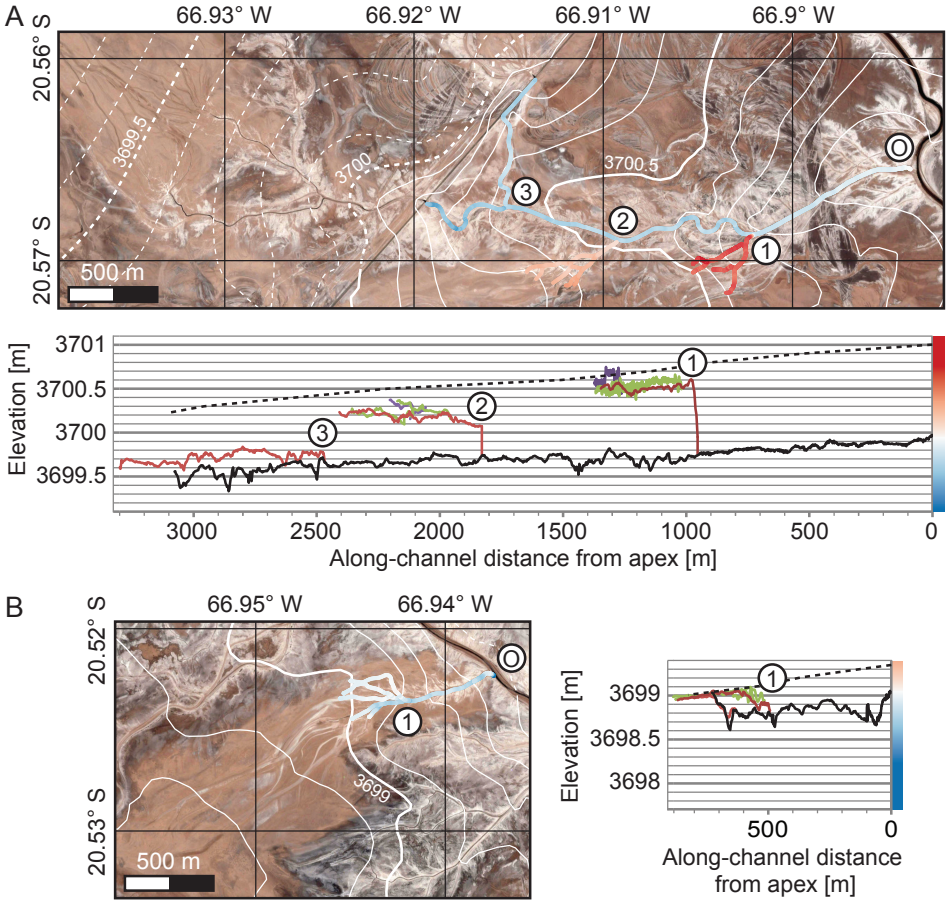

Figure 2.4: Satellite images (dated March 2016; *Google Earth Pro*) and along-channel elevation profiles of crevasse splays facilitating bidirectional drainage. The images show the elevation of the channel floor relative to the apex (coloured lines; see corresponding colour bars next to their associated profiles) and dGPS-based surface topography (white contours). The profiles show the along-channel elevation of first-order (black), second-order (red; number corresponds to satellite image), third-order (green), and fourth-order (purple) channel floor, and the surface topography alongside the first-order channel (dashed). x-axis origin corresponds to 'O'; y-axis origin is levelled with the parent-channel floor. (a) Apex has incised significantly deeper (~1 m) into the river bank and the remaining floodplainward gradient is low. Note that the elevation at the termini is still ~0.5 m above the parent-channel floor. (b) Horizontal and partly reversed channel-floor gradient.

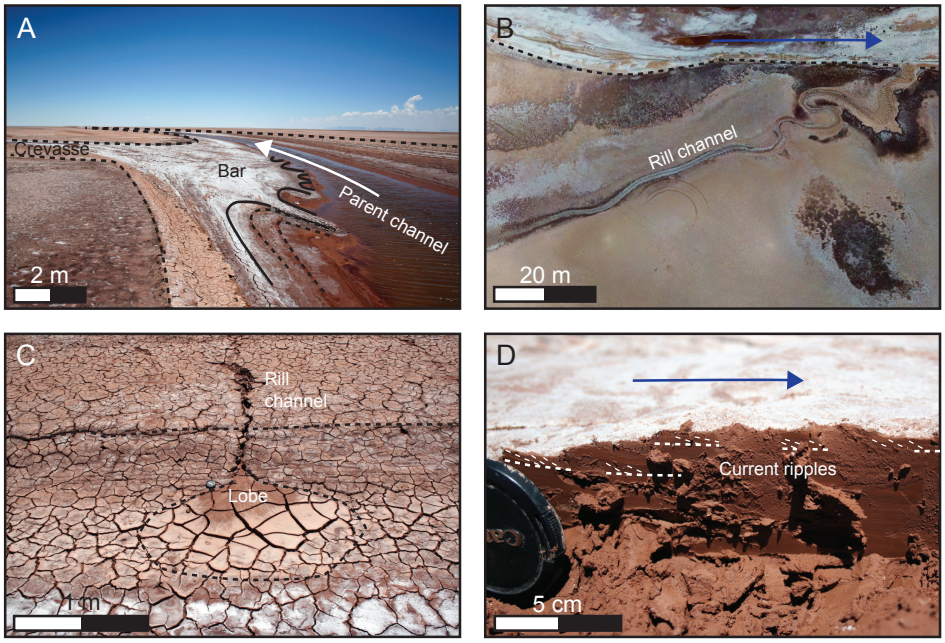

Figure 2.5: Crevasse splays facilitating bidirectional drainage. White/blue arrows indicate flow direction. (a) Reflux lobe in the parent channel (associated with the crevasse splay in Figure 2.4b) with scours indicating return flow at the crevasse-splay apex. (b) KAP orthophoto of a large sinuous rill channel draining into the main river. (c) Depositional lobe at the base of a small rill channel as it enters a channel depression. (d) Current ripples on a reflux lobe (associated with the crevasse splay in Figure 2.4a).

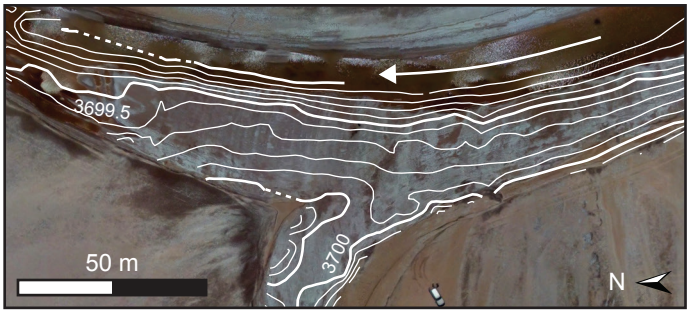

Figure 2.6: KAP orthophoto of an assymetrical reflux lobe (associated with the crevasse splay in Figure 2.4a) showing surface topography (white contours). White arrow indicates flow direction in the parent channel.

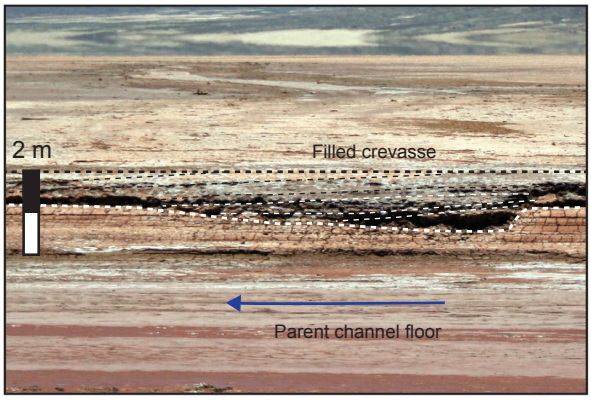

Figure 2.7: Filled crevasse-splay channel with a hanging channel floor in the banks of its parent channel. Note the inclined surfaces indicating lateral infill. Blue arrow indicates flow direction.

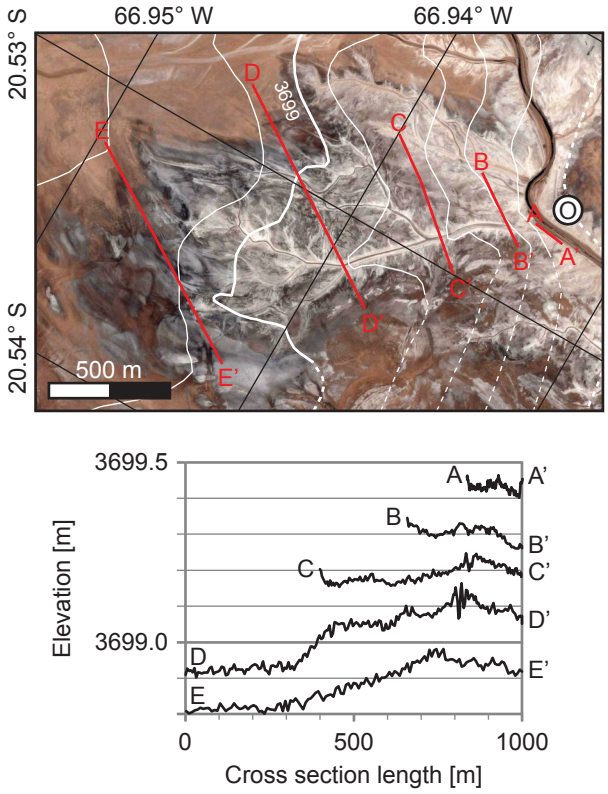

Figure 2.8: Satellite image (dated March 2016; *Google Earth Pro*) and elevation profiles of a post-active crevasse splay. The image showings surface topography (white contours) and the location of profiles A–E (in red). The profiles shows surface topography from proximal (A–A') to distal (E–E').

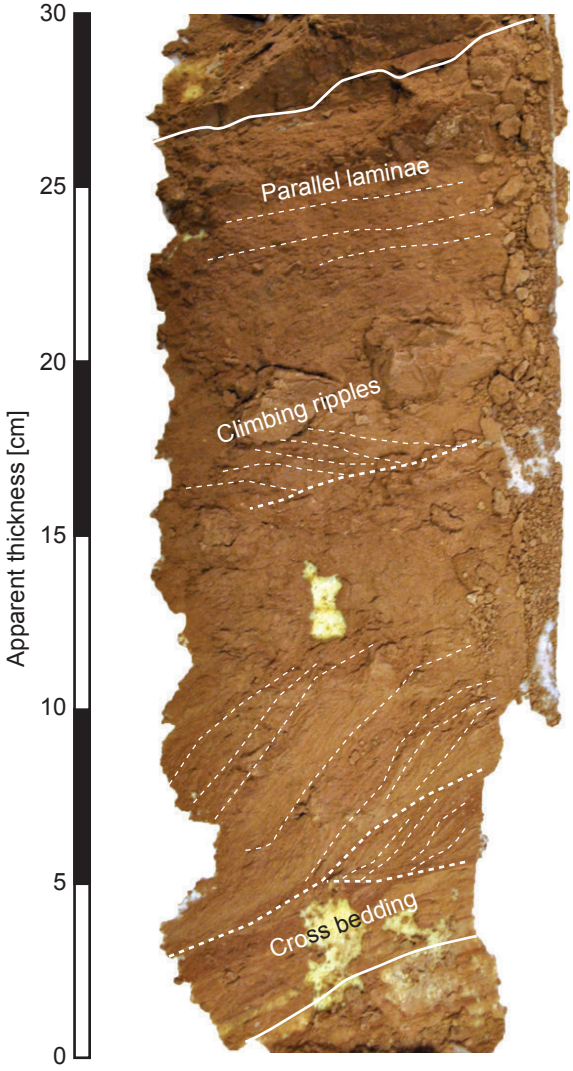

Figure 2.9: Lacquer peel from a post-active crevasse-splay channel showing sedimentary structures.

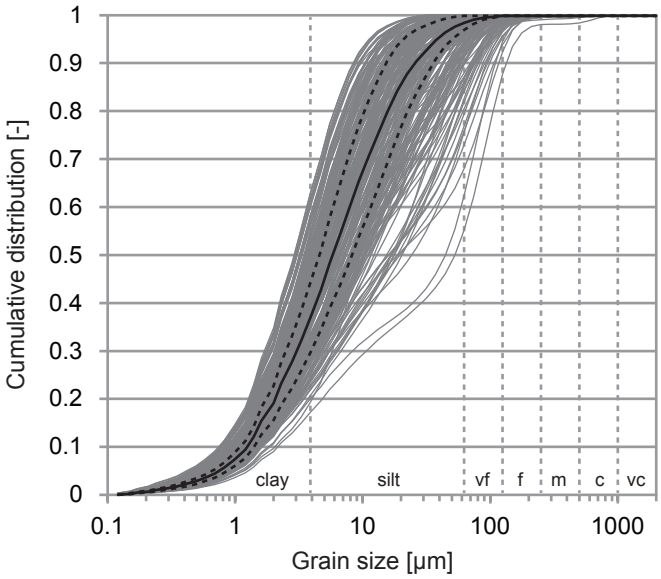

Figure 2.10: Cumulative distribution of 261 grain-size samples from crevasse splays after laser particle sizer analysis showing the median (black) and the median absolute deviation (MAD; dashed lines). Grain-size classes are indicated with dashed grey lines; vf: very fine; f: fine; m: medium; c: coarse; vc: very coarse.

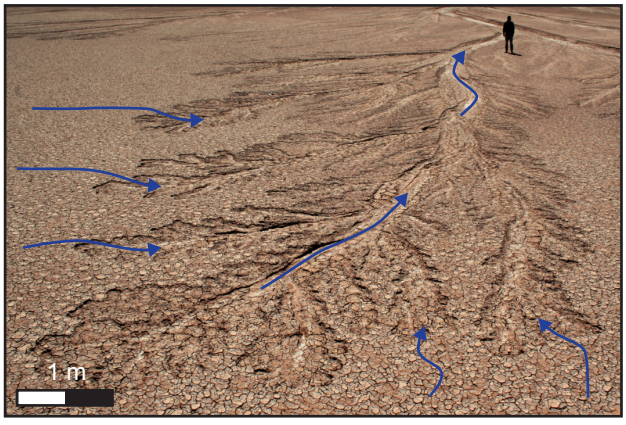

Figure 2.11: Backstepping erosion in a post-active crevasse splay reused for floodplain drainage into an abandoned channel. Blue arrow indicates flow direction. Person for scale (~1.75 m).

2.4. Crevasse-splay life cycle

A generic pattern in the development of crevasse splays can be inferred from the observed configurations and their associated mechanisms. The proposed life cycle applies to all crevasse splays in the river system, provided that their parent channel remains active throughout.

2.4.1. Crevassing and splay equilibration

The formation of a crevasse splay is initiated by a levee breach, allowing water to spill onto the adjacent floodplain even before the river exceeds bankfull discharge (i.e., preceding unconfined overbank flooding) (Figure 2.12a,b). The floodwater drains from the top part of the main stream, which is undersaturated with sediment (Meselhe et al., 2012), and subsequently encounters an overbank gradient down the outside levee and aggraded fluvial ridge (~2–4 · 10^{-4}) that may be steeper than that of the river profile (ranging from <3.3 · 10^{-4} near the fan apex to 0 at the river terminus, averaging ~1 · 10^{-4}; see Chapter 3). The erosive capacity of the floodwater both deepens and widens the initial crevasse (Yuill et al., 2016), confining outflow at the crevasse-splay apex. Combined with the floodplainward gradient of the substrate, this causes the floodwater to retain its flow energy for longer and transport suspended and newly eroded sediment further onto the floodplain (cf. Bull, 1979). Crevasse-splay channels incise and stabilise through headward incision, extending from the crevasse-splay apex. Deposition occurs in the distal part of the crevasse splay, causing localised elevation of the floodplain (O'Brien and Wells, 1986; Tooth, 2005) (Figure 2.12b) which leads to channel bifurcation and switching (Smith et al., 1989; Bristow et al., 1999; Slingerland and Smith, 2004) (Figure 2.3c).

Proximal erosion and distal deposition allow crevasse-splay channels to adjust their flow path towards a graded equilibrium profile (cf. Mackin, 1948), with the lower-lying floodplain at their distal termini as the local base level. Over the course of consecutive flooding events, the crevasse splay progrades further onto the floodplain (O'Brien and Wells, 1986; Smith et al., 1998; Adams et al., 2004; Bernal et al., 2013; Colombera et al., 2013) to a degree that depends on, e.g., floodplain morphology (i.e., gradient and drainage capacity) and grain size (Millard et al., 2017), and the hydraulic capacity of the crevasse (Yuill et al., 2016). This process lengthens the equilibrium profile of the crevasse-splay channels whilst raising its local base level through distal aggradation, effectively reducing its gradient (Figure 2.12b).

2.4.2. Reflux and infill

When river discharge recedes to below bankfull capacity following a flooding event (waning flow stage), it drains more efficiently (i.e., its water level falls more rapidly) than the inundated floodplain (e.g., Dalman and Weltje, 2008). The resulting water-surface gradient may not be able to overcome the river levees and its aggraded fluvial ridge, in which case the floodplain is drained by basinward overland

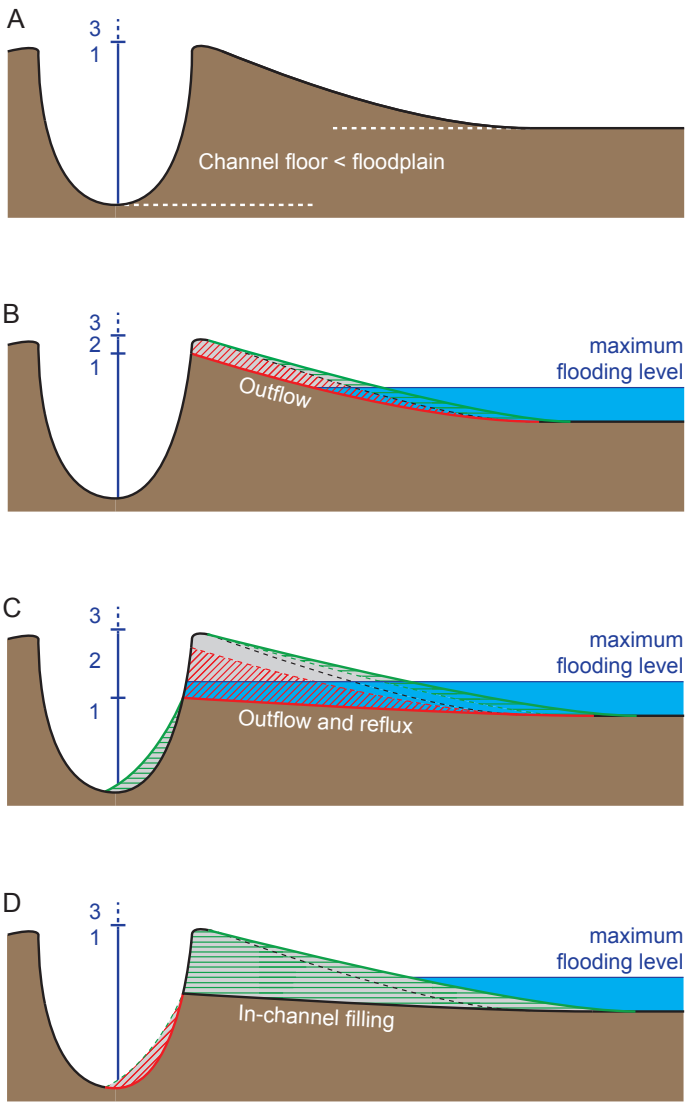

Figure 2.12: Schematic representation of the generic life cycle of a crevasse splay (not to scale). Incision of the (crevasse-splay) channel floor and adjacent deposition of crevasse-splay levees and lobes is indicated in red and green, respectively. Black dashed line indicates the adjacent floodplain topography. Parent-channel runoff stage is subdivided in confined in-channel flow (1), crevasse-confined flooding (2), and unconfined overbank flooding (3). (a) Parent-channel floor elevation is lower than the floodplain adjacent to the alluvial ridge. (b) Levee topping the fluvial ridge is breached, after which the crevasse-splay channel starts incising towards a graded equilibrium profile. Deposition occurs alongside and at the termini of the crevasse-splay channels. As the apex is higher than the maximum flooding level, there is no return flow of floodwater. (c) Continued incision and deposition puts the crevasse apex below the maximum flooding level, facilitating return flow of floodwater and sediment back into the parent channel during the waning stage of flooding, forming a reflux lobe. (d) The reduced gradient causes flow deceleration, leading to in-channel deposition and, ultimately, deactivation of the crevasse splay. The reflux lobe in the parent channel is eroded by sustained lower-order flow.

flow and floodwater capture into the remnant depressions of abandoned channels and their derelict crevasse splays (Figure 2.11), as well as through infiltration and evaporation. However, the topographic barrier between the river and the floodplain is locally removed where continued profile equilibration of crevasse-splay channels causes the apical hanging floor of the crevasse to incise deeper than the maximum flooding level (Figure 2.12c). The now-unobstructed hydrological gradient induces a return flow of floodwater through the crevasse-splay channels back into the main river.

Undersaturated floodwater re-entering the relative depression of crevasse-splay channels cuts out rill channels in the adjacent splay deposits (O'Brien and Wells, 1986; Zwoliński, 1992; Bridge, 2006), remobilising sediment and transporting it back towards the main river (Donselaar et al., 2013) (Figure 2.5c). This return flow causes backstepping erosion at junctions of different-order channels, where the higher-order channel typically has a hanging floor (Figure 2.4). In-channel redeposition of sediment occurs downstream of each such confluence (i.e., in the lower-order channel). This is most evident at the junction of the crevasse and the main river, where it forms an asymmetrical lobe (Donselaar et al., 2013) (Figures 2.6 and 2.12c).

The reflux of floodwater causes the crevasse-splay channel network to adjust towards a reversed equilibrium profile with the trunk-channel floor as its base level, eroding and depositing sediment upstream and downstream of each break in slope (i.e., junction of different-order channels), respectively (Figure 2.12c). The relative concentration of suspended sediment in successive outflow increases as the hanging floor of the crevasse incises deeper into the main channel bank (Figure 2.4), causing its erosive potential to decrease (Meselhe et al., 2012). The floodwater decelerates earlier as the crevasse-splay gradient has been reduced or reversed (i.e., no longer exceeds that of the parent channel) by return flow from the preceding flooding event, resulting in transmission loss and, hence, in-channel deposition of suspended sediment (cf. Schumm, 1993; Bull, 1979; Field, 2001; Slingerland and Smith, 2004). Over consecutive flooding events, this mechanism fills in the crevasse-channel depressions, effectively shutting down the crevasse splay (Figure 2.12d).

2.4.3. Preserved overbank sediment

As the process of crevassing implies reworking of levee sediment, the preservation potential of fluvial levees is low where crevassing is abundant. This is in accordance with their underrepresentation in the rock record, as observed in earlier studies (e.g., Brierley et al., 1997). The majority of preserved crevasse-splay sediment consists of amalgamated splay lobes, fining up in grain size (e.g., Mjøs et al., 1993; Bristow et al., 1999; Fisher et al., 2007; Burns et al., 2017) and blanketed by floodplain fines (Bridge, 2006; McKie, 2011b; Dalman et al., 2015). Crevasse-splay channels constitute a relatively small proportion of preserved sediment, decreasing in proportion from proximal to distal (e.g., Tooth, 2005; Burns et al., 2017). Their fill is heterogeneous (Figure 2.10), consisting mainly of sediment (re)deposited un-

der a waning flow regime during outflow (Tooth, 2005), and pelagic floodplain fines (Bristow et al., 1999; Fisher et al., 2007). The preservation potential of deposits associated with return flow of floodwater (i.e., in-channel reflux lobes) is assumedly low due to subsequent erosion by sustained lower-order flow (Figure 2.12d).

2.5. Role in fluvial aggradation

The deposition of crevasse splays is a principal mechanism for near-channel overbank aggradation in the unconfined distal part of low-gradient fluvial fans, where floodplain sedimentation rates are generally low (e.g., Leeder, 1975; Shen et al., 2015). Their proposed life cycle provides new insights into their role in the aggradation and subsequent abandonment (by avulsion) of alluvial ridges. This ultimately leads to an improved understanding of preserved stratigraphy in fluvial successions with high proportions of floodplain deposits.

2.5.1. Alluvial ridges and avulsion

Over the course of their life cycle, crevasse splays form a dm-scale positive relief (i.e., splay) extending up to several km^2 across the floodplain near the main river. Consecutive crevasse splays interact with adjacent splays in a process of compensational stacking (Donselaar et al., 2013; Li et al., 2014), amalgamating in their erosive proximal reaches and conformably onlapping towards their distal fringes. This mechanism creates a continuous elevated rim alongside the main river, laterally expanding levee topography through redeposition and establishing a alluvial ridge up to several km wide. The consequent rise in bankfull height of the main river corresponds to the aggradation of its channel floor, assuming that its local hydraulic capacity remains more or less constant (Chapter 4). Episodes of unconfined overbank flow continue to deposit levees on top of the aggrading alluvial ridge. These are in turn redeposited by crevasse splays prograding over their precursors off a gradually increasing slope (Chapter 4). This vertical stacking of crevasse splays sustains the aggradation of the alluvial ridge, which becomes increasingly superelevated above the distant floodplain (Figure 2.13a).

Given that its parent channel remains active, each crevasse splay will complete its entire life cycle on the condition that its crevasse-splay channels do not incise down to the channel floor of its parent river (i.e., remain hanging). This is dependent upon the elevation of the distal termini (i.e., local base level) of the crevasse-splay channels relative to that of their trunk channel. When the thalweg of the parent river has super-elevated to above the distal reach of a crevasse splay, equilibration of the crevasse-splay channels ultimately leads to headward incision down to or below its channel floor. At the same time, the crevasse splay will capture an increasing proportion of the total discharge and sediment, accelerating its development. If the gradient of one or more crevasse-splay channels has remained steeper than that of the main channel once incision reaches its channel floor, the river avulses (i.e., low-flow stage discharge is rerouted through the crevasse splay) (Figure 2.13b). This process is amplified by backwater effects induced by the down-

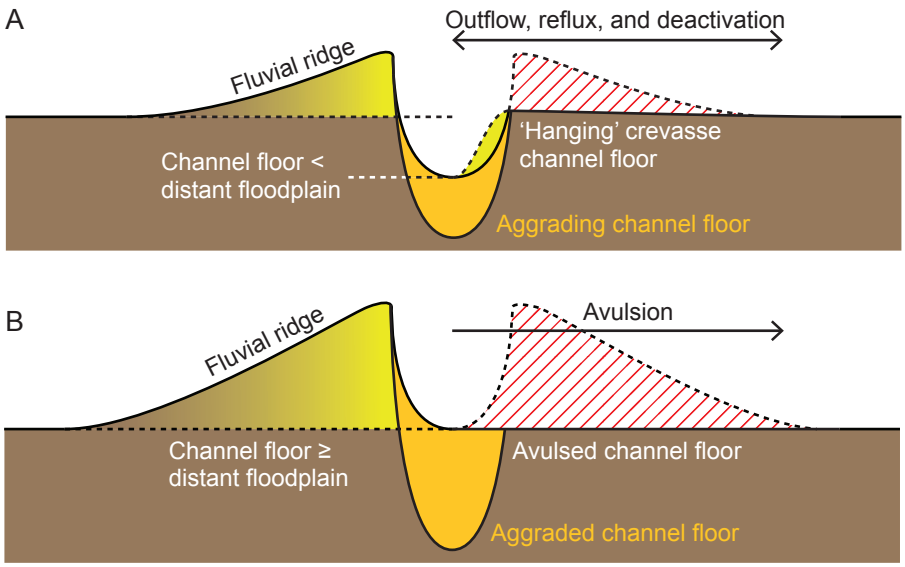

Figure 2.13: Schematic cross section of an aggrading alluvial ridge (not to scale). Maximum incision of the crevasse-splay channel floor is indicated in red. (a) As long as the crevasse-splay channel floor remains 'hanging', the crevasse splay will complete its life cycle (Figure 2.12). (b) When headward incision of a crevasse-splay channel advances to below the trunk channel floor, the river (partially or fully) avulses.

stream reduction in hydraulic capacity of the main river (e.g., flow constriction by in-channel reflux deposits). The proposed mechanisms are in accordance with the avulsion criteria suggested by Mohrig et al. (2000), Slingerland and Smith (2004), and Dalman and Weltje (2008), as summarised in a review by Hajek and Wolinsky (2012).

2.5.2. Generic relevance and implications

The mechanisms proposed in this study exclusively concern self-regulating fluvial processes. The specific configuration of the observed Río Colorado fluvial fan eliminates any significant influence from external factors such as vegetation (barren floodplain), lateral constraint (unconfined alluvial plain), or base-level change (lowstand endorheic basin). The dryland character of the system favours a single-thread river decreasing in hydraulic capacity downstream (e.g., North and Warwick, 2007; Donselaar et al., 2013), preventing multi-channel interference and promoting overbank deposition. The system autogenically creates accommodation space by prograding across the low-gradient basin fringe, and its subaerial termination ensures that all sediment is captured, allowing for a comprehensive account of its distribution.

The mechanisms proposed in this study are relevant to fluvial settings that facilitate progradational avulsions (cf. Hajek and Edmonds, 2014). Floodplain aggra-

dation (and preservation) in such environments requires positive accommodation space in a relatively low-energy environment (i.e., low-gradient and unconfined) (Nichols and Fisher, 2007). The subsequent occurrence of crevasse splays is promoted by relatively coarse-grained suspended sediment (during peak runoff) and effective floodplain drainage (Millard et al., 2017).

In humid environments, river discharge variations are significantly smaller than those in arid or semi-arid settings (McMahon et al., 1987), stream capacity does not decrease downstream (Tooth, 2000), and vegetation may increase bank stability (Simon and Collinson, 2002). Although this may moderate the frequency of flooding and the occurrence of crevasse splays, it does not change the inherently episodic mechanism of crevasse-splay channels adjusting to a graded equilibrium profile and, hence, the life cycle proposed in this study. However, floodplain morphodynamics (i.e., availability of accommodation space and drainage conditions) may be significantly influenced by non-depositional factors such as prolific vegetation and ponding of floodwater (Millard et al., 2017; Nienhuis et al., 2018).

2.5.3. Implications for connected sand volumes

Given their relatively rapid accumulation rate and high preservation potential, crevasse splays form an important constituent of stratigraphy associated with the distal part of low-gradient fluvial fans, for which the studied system qualifies as a modern-day analogue. Comprising sand and silt, their contribution to connected sand volumes (which may constitute hydrocarbon reservoirs) has been acknowledged in previous studies (e.g., Jordan and Pryor, 1992; Pranter et al., 2008; McKie, 2011b), albeit to a limited extent. The heterolithic fill of crevasse-splay channels connects individual splays to their coeval trunk channel, which constitutes the main hydrocarbon reservoir. The proposed role of crevasse splays in building alluvial ridges entails lateral amalgamation and vertical stacking of individual units, creating sand-on-sand contact. This implies that fluvial ridges comprise interconnected crevasse splays, combining into large connected sediment volumes. Truncation of fluvial deposits by younger channels may further enhance connectivity. These inferences are in accordance with the nature and types of crevasse-splay connectivity described in Chapter 4, based on observations in outcrop stratigraphy. Crevasse splays effectively connect otherwise-isolated channel deposits, even when their deposition was not coeval. They should therefore be included in net volume estimations and production models of fluvial successions that contain hydrocarbon reservoirs in order to avoid underestimations.

2.6. Conclusions

A generic life cycle applies to crevasse splays in aggrading alluvial ridges; its expression dependent on floodplain conditions (i.e., drainage, vegetation). Initial development is dominantly controlled by the outflow of floodwater, promoting erosion near the crevasse apex and deposition towards the splay fringes as the crevasse-splay channels adjust towards a graded equilibrium profile with their dis-

tal termini acting as a local base level. When proximal incision advances to below the maximum level of floodplain inundation, return flow occurs during the waning stage of flooding. This floodwater reflux leads to a temporary repositioning of the local base level to the deeper trunk channel thalweg and consequent reversal of the graded equilibrium profile. The resultant decrease in crevasse-splay channel gradient ultimately leads to backfilling and abandonment of the crevasse splay.

Consecutive crevasse splays form an alluvial ridge through lateral amalgamation and subsequent vertical stacking. As the alluvial ridge becomes increasingly perched above the distant floodplain, splay equilibration may cause incision of the levee crevasse down to or below its trunk channel thalweg, leading to an avulsion.

The mechanisms proposed in this study are relevant to fluvial settings promoting progradational avulsions. The relatively rapid accumulation rate and high preservation potential of crevasse splays in this setting makes them an important constituent of the resultant fluvial stratigraphy. Hence, their contribution to net sand volumes in hydrocarbon bearing successions should be considered.

3

The role of crevasse splays in autogenic river avulsions

A high-resolution morphological snapshot of the Río Colorado fluvial fan shows the autogenic organisation of subtle alluvial ridges. It allows reconstruct floodplain drainage patterns and deduce where the next avulsion of the main river could take place.

3.1. Introduction

Crevasse splays are often associated with progradational avulsions (e.g., Slingerland and Smith, 2004; Hajek and Edmonds, 2014), forming a precursor to an alternate river path (e.g., Smith et al., 1989; Farrell, 2001). The probability of a crevasse initiating a full or partial channel switch is conditional upon reaching a locally critical setup, for which various thresholds have been formulated (Hajek and Wolinsky, 2012). These criteria include super-elevation of the active channel above the distant floodplain (e.g., Mohrig et al., 2000; Slingerland and Smith, 2004; Jerolmack and Paola, 2007; Straub et al., 2009; Dalman et al., 2015), the ratio between along-channel slope and cross-floodplain gradient (e.g., Törnqvist and Bridge, 2002; Bridge, 2006; Van Dijk et al., 2009), and crevasse transport capacity (e.g., Smith et al., 1989; Tooth, 2005; Kleinhans et al., 2008; Dalman and Weltje, 2008). These largely interdependent parameters for avulsion proneness are believed to govern when and where a perched channel switches to a hydrodynamically more-favourable path, shifting the locus of deposition and, hence, affecting the resultant sedimentary architecture.

Despite their implicated role in fluvial aggradation and river switching, the morphodynamical development of crevasse splays remains inadequately understood (e.g., Bridge, 2006). As a result, system-scale forward models generally use geometric rules to simulate overbank deposition, rather than process-based algorithms. Moreover, avulsions are reproduced using simplified expressions of the underlying fluvial dynamics in order to reduce the computational load (Kleinhans et al., 2008; Hajek and Wolinsky, 2012). Various approaches to these parameterisations produce inconsistent modelling results, particularly with regard to the spatial arrangement of successive channel belts. This has been attributed to an imprecise representation of floodplain topography (e.g., Jerolmack and Paola, 2007; Hajek and Wolinsky, 2012), which is a dominant control on the development of crevasse splays and, consequently, the routing of avulsion paths. Detailed quantitative input from system-scale field studies is needed to better validate the interactive dynamics between the often-subtle floodplain terrain and crevasse morphodynamics (e.g., Dalman et al., 2015), advancing the appreciation of avulsion processes and thresholds, and the resultant system architecture.

This Chapter combines a high-resolution morphological reconstruction of the modern-day Río Colorado fluvial fan with new insights into the development of crevasse splays (Chapter 2), aiming to clarify the autogenic processes that lie at the basis of progradational avulsions. These include the role of overbank morphodynamics in the aggradation of alluvial ridges and subsequent river switching, as well as its implications for the self-organised compensational stacking of successive channel belts. The work serves to improve insights into generic mechanisms for avulsion and their subsequent expression as part of a fluvial depositional system.

3.2. Methodology

The study area covers the entire depositional fan of the Río Colorado fluvial system (Section 1.3.1), extending across an area of ~500 km^2 southwest of the city of Uyuni in the Potosí department of Bolivia. Field data were collected at the end of the dry austral winter season in October and November of 2014 and 2016, when the floodplain was best passable and the river was at its low-flow stage.

A *Trimble 5700* differential-GPS (dGPS) set was used to record geospatial data with sub-centimetre accuracy (i.e., standard deviation σ < 1 cm in all dimensions). Detailed profiles of floodplain topography were obtained by driving a vehicle-borne setup of the dGPS set across the fluvial fan (Figure 3.1). River cross sections were acquired by traversing the channel perpendicular to its axis (accurate to ±5°; i.e., <0.4% error in profile length) on foot whilst carrying a hand-held dGPS rover. An automated routine was scripted in Python in order to geometrically analyse each of these channel profiles (Figure 3.2), accounting for the propagation of measurement errors (mainly for lateral distances). An additional vertical uncertainty ϵ_z < 0.05 m was introduced for the channel floor (i.e., lowest point in each profile) due to its soft consistency. The bankfull height was equated to the lowest of the two levee tops on either side of the channel; a range or minimum level was specified where the least-elevated or neither levee crest was not captured in the profile. This level was used to establish the bankfull channel depth, width, and width-to-depth (W/D) ratio. The hydraulic area was calculated by applying the trapezoidal rule for all measurements between both levee crests and below the bankfull height (Figure 3.2). All geometrical river properties were plotted against along-channel distance, measured from Google Earth Pro satellite imagery in a geographic information system (GIS; Figure 3.1).

The reconstruction of overbank drainage patterns required a digital elevation model (DEM) with a sufficiently high vertical resolution to capture the subtle floodplain topography whilst spanning the entire fluvial fan (i.e., including areas where dGPS measurements are sparse or absent; Figure 3.1). The *JAXA ALOS World 3D-30* (AW3D30) global digital surface model (DSM) was selected as the most accurate base topography available free of charge (Santillan and Makinano-Santillan, 2016), with a horizontal resolution d = 1 arc-second (~30 m) and a global vertical standard deviation σ_z = 4.38 m (Tadono et al., 2016). A comprehensive collection of >34,000 dGPS floodplain measurements in the study area (Figure 3.1) was used as ground-based control points to determine the local vertical standard deviation $\sigma_{z,loc}$ = 0.81 m. The DSM was then resampled to achieve the required topographic precision, exchanging horizontal resolution for vertical accuracy (see Appendix C). Aiming to capture floodplain gradients $\nabla \geq 2 \cdot 10^{-4}$ (based on the observations in Chapter 2), this resulted in a 400-m horizontal resolution DEM with a vertical margin of error MOE = 0.08 m within a confidence interval CI = 0.95. The vertically enhanced DEM was subsequently calibrated using the before-mentioned collection of ground-based control points, employing a minimum curvature algorithm for the residual surface. Local depressions (sinks) in the resultant DEM were filled (flooded) to the lowest neighbouring spill point using *QGIS GRASS*, after which overbank drainage

patterns were identified. Potential avulsion paths were traced along least-cost flow lines initiating from each dGPS river cross section.

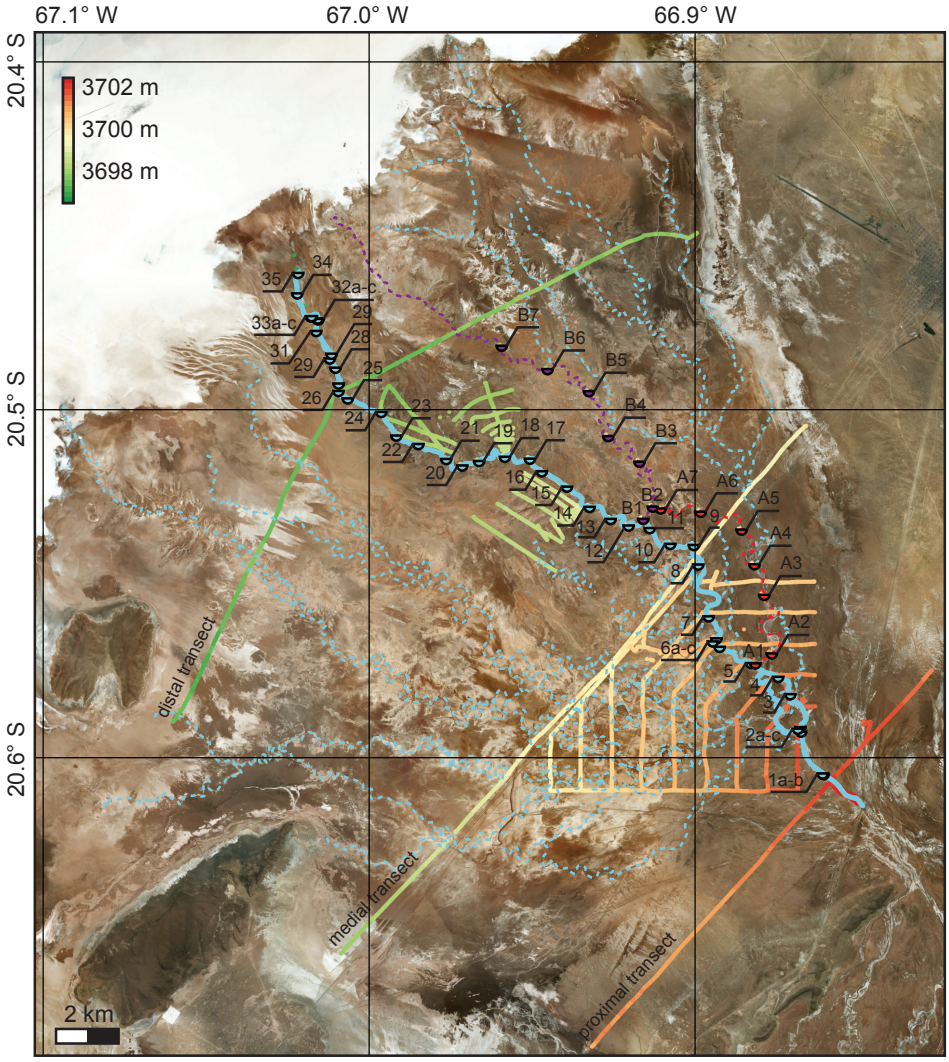

Figure 3.1: Overview of the Río Colorado fluvial fan showing the spatial distribution of dGPS measurements (colours according to elevation scale) and (post-)active river paths (continuous and dashed blue lines). Numbered semicircles denote the location of channel cross-sections (remnant channel A and B in red and purple, respectively).

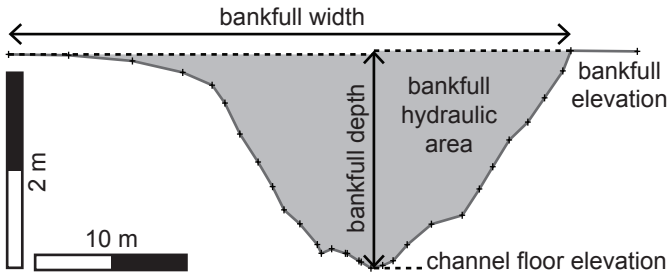

Figure 3.2: Example of a channel cross-section (9 in Figure 3.1) showing the measures for the automated geometrical analysis. Note the vertical exaggeration.

3.3. Geomorphological reconstruction

The analysis constitutes a high-resolution morphological snapshot of fluvial fan evolution. Channel geometry is quantified for both the active river and various post-avulsion (i.e., abandonment) stages. A detailed characterisation of floodplain topography allows to distinguish depositional patterns and reconstruct drainage paths.

3.3.1. Channel morphology

The active river is mostly single thread and has a sinuosity index (SI) of 1.3. The elevation of its channel floor shows a downstream slope, decreasing in gradient from $\geq 1 \cdot 10^{-4}$ near the fan apex to $\leq 0.25 \cdot 10^{-4}$ towards its distal terminus (Figure 3.3), which is level with the salt flat surface. The along-channel gradient of bankfull elevation is more constant, gradually decreasing downstream from $\sim 2 \cdot 10^{-4}$ to $\sim 1 \cdot 10^{-4}$ before increasing again to $> 2.5 \cdot 10^{-4}$ within 3.5 km from the river terminus (Figure 3.3a), i.e., representing a terminal splay. Bankfull depth in the first 16 km from the fan apex varies between 1.5–2.5 m, after which it decreases gradually from 1.5 to 1 m before rapidly shallowing out in the final 2 km (Figure 3.3b). Channel width shows an overall downstream decrease from ~75 to ~5 m (Figure 3.3c). The resultant width-to-depth (W/D) ratio decreases from 40 to 20 within the first 10 km from the fan apex, levelling out and steadily reducing to 10 before rising dramatically where the channel fans out (Fig. Figure 3.3d). The downstream loss in hydraulic area of the channel gradually decreases from ~4 m^2 km^{-1} near the fan apex to ~1.5 m^2 km^{-1} towards the river terminus (Figure 3.3e). Significant variations from these general trends in channel geometry mainly occur where the active channel is transiently divided (i.e., local avulsion; see Figure 3.1 at cross sections 2b–4, 8, and 32b–33a) or where it connects to an alternative drainage conduit (i.e., the remnant depression of a previously avulsed channel or a large crevasse).

The remnant depressions of previously avulsed river paths (cross section series A and B in Figures 3.1 and 3.3) have an SI of 1.8 and 2.0, respectively. Both feature a hanging channel floor (i.e., elevated relative to that of the currently active

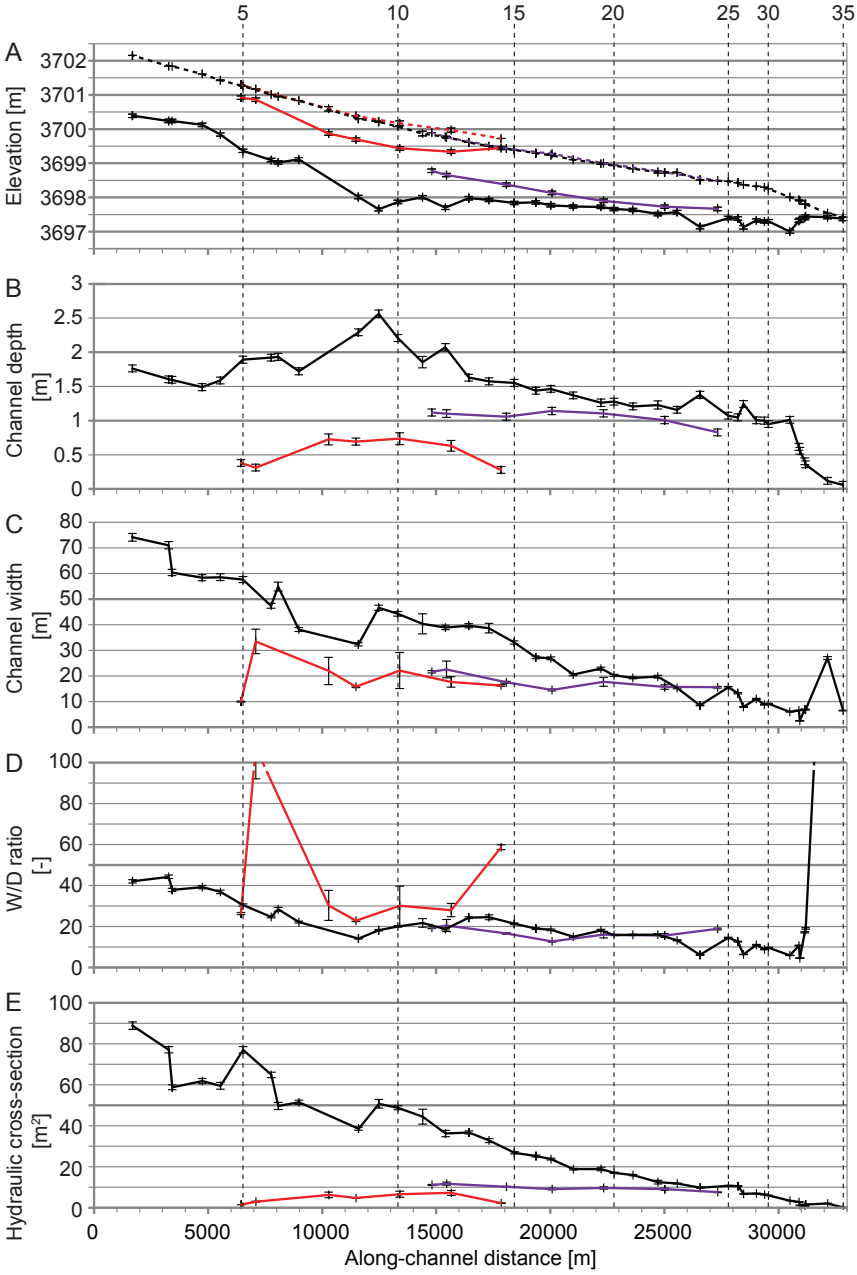

Figure 3.3: Along-channel profiles of the active river (black) and two abandoned rivers (A- in red; B- in purple) showing (a) absolute elevation of the channel floor (continuous lines) and bankfull level (dashed lines), (b) bankfull channel depth, (c) bankfull channel width, (d) bankfull width-to-depth ratio, and (e) bankfull hydraulic cross-section. Note the vertical exaggeration and vertical reference lines numbered corresponding to the section indices in Figure 3.1.

river) at their apex, the downstream slope of which is initially steeper than the equivalent profile of the active channel, levelling out short of descending below it (Figure 3.3a). The downstream decrease in bankfull elevation corresponds to that of the active channel without exceeding it (Figure 3.3a). Channel dimensions remain constant or increase (i.e., deepen and widen) in the proximal part, shallowing and gently narrowing further downstream (Figure 3.3b,c). The W/D ratio is approximately constant, except where the channel width increases dramatically, directly downstream of the apex and where the channel shallows towards its terminus (Figure 3.3d). The hydraulic area remains approximately constant, incidentally even increasing in the first kilometres from the channel apex (Figure 3.3e).

3.3.2. Floodplain topography and drainage

A detailed record of floodplain topography is shown in the dGPS profiles spanning the proximal, medial, and distal part of the fluvial fan perpendicular to its general flow direction (Figure 3.4e). The relative elevation of the profiles shows a basinward descent of ≤4.9 m over a minimum distance of ~21 km (i.e., from the highest point to the salt lake fringe, defining the axial gradient). The floodplain gradient ranges from $0–6 \cdot 10^{-4}$, with the steepest slopes occurring directly adjacent and perpendicular to perched channel depressions. Individual peaks are clearly discernible in the distal profile, ranging up to 2 km in width, but appear to merge into neighbouring highs in the proximal and medial profiles.

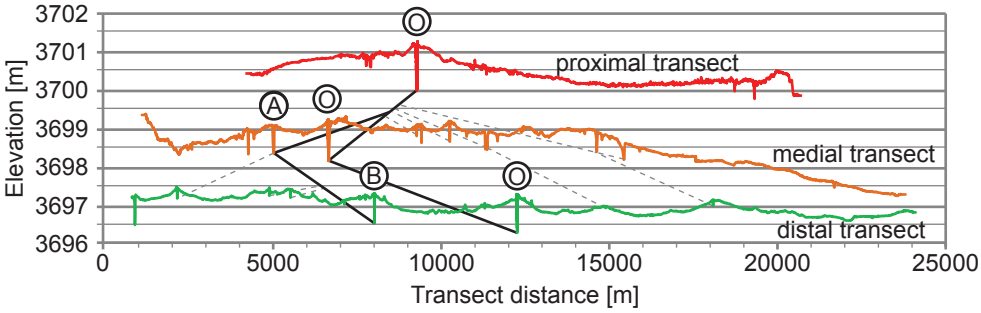

Figure 3.4: Detailed topographic cross-sections across the fluvial fan perpendicular to the general flow direction. Location of the active channel denoted 'O', abandoned channels denoted 'A' and 'B', respectively. Continuous black lines and dashed grey lines indicate corresponding channel depressions. Note the vertical exaggeration.

The vertically enhanced DEM of the fluvial fan (Figure 3.5) reveals ridges that correspond to the peaks in the dGPS profiles (Figure 3.4). These ridges can be linked to river paths (both active and abandoned) interpreted from satellite imagery (Figure 3.1). Organised in a dendritic pattern radiating out from the fan apex, the ridges separate and finger out towards the distal fan fringe. The orientation of individual ridges appears to be governed by the placement of adjoining ridges, especially in the distal part.

The reconstructed overbank drainage patterns follow the path of steepest descent into the inter-ridge depressions where the individual flow lines join in a convergence of floodwater (Figure 3.6). Plotting the floodplain elevation along the drainage paths against the along-channel elevation of the active river shows that the overbank flow paths initiate at bankfull level (Figure 3.7). The overbank gradient is typically higher than that of the river, but the drainage path never descends to below the equivalent river profile. The overbank flow lines initiating from river cross sections 6 and 7 (orange and yellow dashed lines, respectively, in Figures 3.6 and 3.7) come closest to doing so.

3.4. Implications for fluvial system development

The detail and comprehensive coverage of the geomorphological observations in this study support the reconstruction of autogenic processes that shape the fluvial fan. These include the aggradation of alluvial ridges and subsequent avulsion of the active channel, leading to the self-regulated organisation of river deposits.

3.4.1. Development of alluvial ridges

Active channel belts in fluvial fans aggrade in response to basinward lengthening of their fluvial equilibrium profile (i.e., progradation) over a less-steeply inclined surface, which promotes along-river deposition (cf. Dalman et al., 2015). Aggradation is manifested by alluvial ridges (Figures 3.4 and 3.5) forming through overbank deposition of levees and crevasse splays (e.g., Shen et al., 2015) (Chapter 2) and a corresponding rise of the channel thalweg (Chapter 4). Over the course of their development, alluvial ridges super-elevate the active river above the surrounding floodplain. The perched river path lengthens through meandering (here, the SI increases from ≤1.3 to ≥1.8) and continued basinward progradation at its terminus, leading to a decrease in along-channel gradient.

The aggradation of alluvial ridges through overbank deposition may be accelerated by large variations in runoff (i.e., intermittent or ephemeral streams) and a downstream decrease in flow capacity, both of which are typically associated with dryland conditions (e.g., Tooth, 2000). Peak discharge events cause surges in water level that cannot be contained by the low-gradient active river, leading to massive overbank flooding. The results of this study (Figure 3.3) suggest that the downstream transmission loss is dominantly controlled by capture of river water through crevasses and the remnant depressions of abandoned channels during (near) bankfull discharge of a (mostly) single-thread river. High rates of infiltration and evapo-transpiration (e.g., Donselaar et al., 2013) may contribute to the downstream decrease in flow volume, albeit to a lesser degree and mainly during the low-flow stage of river discharge.

3.4.2. Autogenic avulsion processes

Super-elevation and a decrease in along-channel gradient lead to instability of the active river tract, eventually causing it to switch to a hydrodynamically more-favourable path (i.e., avulsion; Figure 3.8). Previous studies were aimed at identifying quantitative criteria for avulsion to occur, pointing to a threshold in super-elevation (e.g., Mohrig et al., 2000; Slingerland and Smith, 2004), cross-floodplain gradient (e.g., Jones and Schumm, 1999), or conductive capacity of crevasse splays. Here, a mechanism is proposed that combines these insights in conjunction with the reconstructed floodplain drainage patterns (Figures 3.6 and 3.7) and the geomorphological evolution (life cycle) of crevasse splays described in Chapter 2.

Aggrading rivers do not get feedback on their avulsion potential, other than through overbank flow. The channels in crevasse splays may form prototypes for alternative flow paths, effectively testing the avulsion proneness of the trunk river. Once a splay channel presents a hydrodynamically more-favourable tract, it can (gradually) take over the function of its parent channel.

Crevasse splays prograde onto the subtle floodplain topography along the path of steepest descent, following floodplain drainage patterns (Figure 3.6). Its channels adjust to a graded equilibrium profile, constrained by the floodplain elevation at their advancing termini (Chapter 2). The river will only avulse when headward incision at the crevasse apex can advance to below its superelevated thalweg (cf. Dalman et al., 2015) whilst its along-channel gradient (i.e., downstream of the crevasse) remains lower than that of the equilibrating splay channels (Figure 3.7). Providing a more-efficient drainage path, the crevasse splay may capture an increasing share of the total runoff, further accelerating its development. The most-competent splay channel will adjust its hydraulic capacity to accommodate the additional stream volume, eventually concentrating flow into a new (single-tread) river (cf. Smith et al., 1989; Farrell, 2001; Field, 2001; Buehler et al., 2011).

The now-abandoned former river continues to receive sediment-laden runoff until its connection to the new river path is completely shut off by in-channel deposition near the avulsion point (red and purple lines in Figure 3.3), which is caused by flow deceleration due to the local increase in hydraulic area (i.e., that of the abandoned and new channel combined) and gradient-induced backwater effects. Further downstream, a water-starved remnant depression may coexist with the active river for an extended period of time, acting as a floodplain drainage system (Bernal et al., 2013) which is slowly backfilled with overbank sediment. The avulsion processes discussed here are gradual rather than abrupt, and are governed by morphodynamic feedback from crevasse splays.

3.4.3. Self-organisation of fluvial fans

Repeated switching of the active river path causes compensatory radial shifts in the locus of deposition, forming a fan of successive alluvial ridges (Figure 3.5). The avulsions appear to be mostly random rather than nodal (cf. Dalman et al., 2015) and successive paths of the single-thread active channel form a dendritic

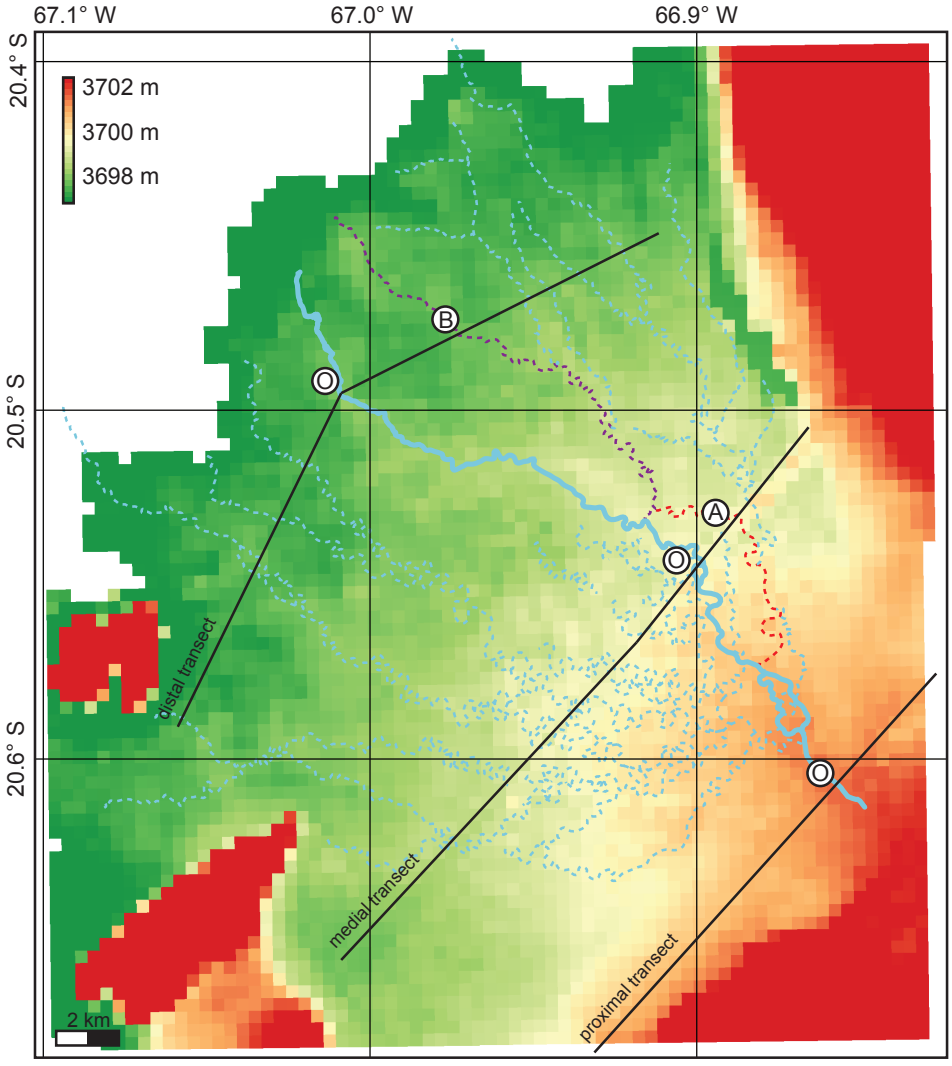

Figure 3.5: Vertically enhanced DEM of the study area showing subtle floodplain topography (colours according to elevation schale) with an overlay of active and abandoned river paths (continuous and dashed blue lines, respectively) and fan-scale cross sections (Figure 3.4).

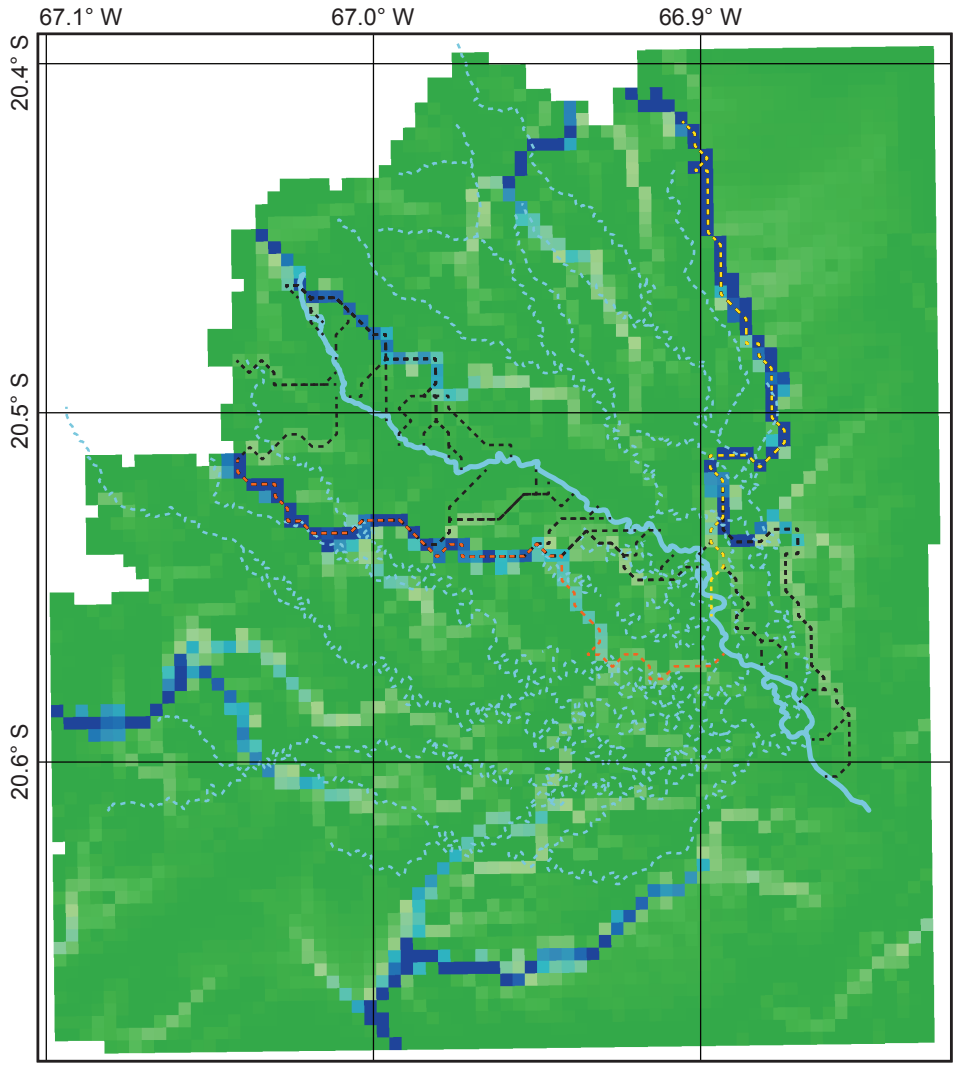

Figure 3.6: Overbank drainage-accumulation pattern (catchment increases from green to blue) with an overlay of active and abandoned river paths (continuous and dashed blue lines, respectively) and floodplain drainage paths (black, orange, and yellow dashed lines) originating from each of the channel cross-sections (Figure 3.3).

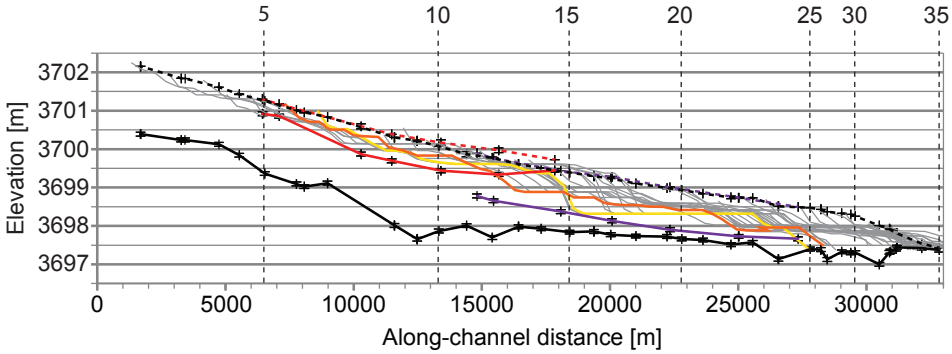

Figure 3.7: Along-channel profiles of the active and abandoned channels (black, red, and purple, respectively) and each of the reconstructed drainage routes (grey, orange, and yellow lines corresponding to Figure 3.6). The yellow and orange lines indicate possible avulsion paths.

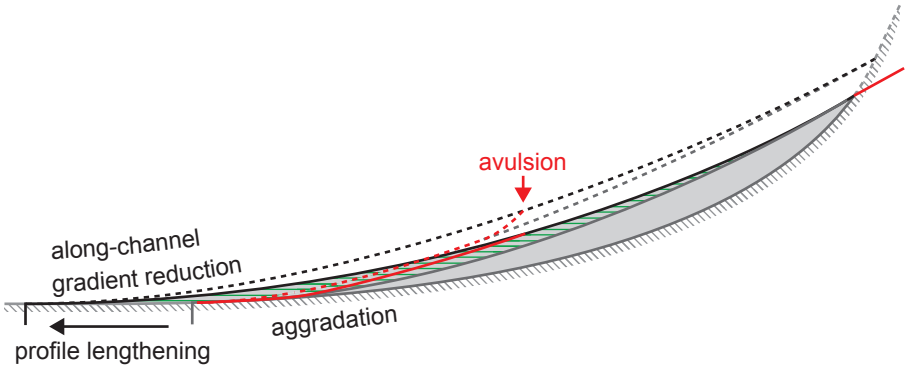

Figure 3.8: Schematic representation of fluvial progradation from the fan apex (right) to its terminus (left). Initial channel floor (continuous) and bankfull (dashed) profile are indicated in grey lines. Prograded profiles in black. Substrate and previous deposits indicated in grey at base. Dashed red line indicates avulsion profile (i.e., shorter path to system base level). Not to scale.

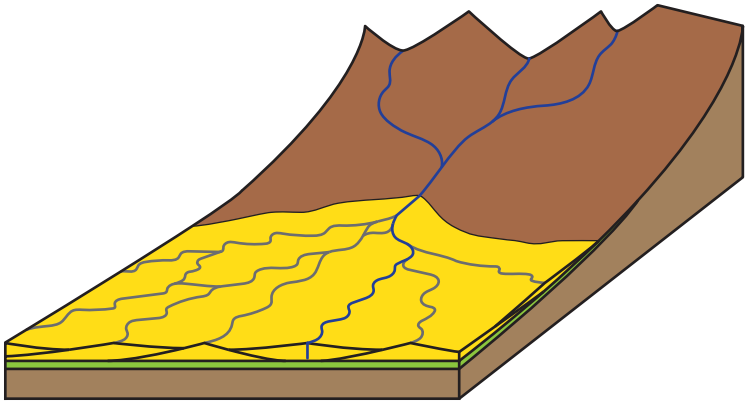

Figure 3.9: Schematic representation of compensational stacking following autocyclic switching of the active aggrading channel belt. Active river in blue; abandoned rivers in grey. Not to scale.

pattern (Figure 3.5), which may imply that the frequency of avulsion increases downstream (cf. Dalman and Weltje, 2008). This could be linked to the basinward decrease in bankfull channel depth (Figure 3.3b), which constitutes an approximate measure for critical super-elevation (e.g., Mohrig et al., 2000). If the corresponding aggradation rate remains relatively more constant, or even increases towards the river terminus, it follows that it takes less time to meet the conditions for avulsion in the distal part of the fluvial system. It is, however, not possible to verify relative aggradation rates of the active channel on the basis of the acquired data. The along-channel decrease in hydraulic area (Figure 3.3e) may be used as a proxy for overbank sediment supply, but it requires a quantification of bankfull stream velocity to derive the overbank transmission loss (cf. Hajek and Wolinsky, 2012). The proposed downstream increase in avulsion frequency does appear to be reflected in the SI of former river tracts (Figure 3.5), which is assumedly indicative of the duration of lateral accretion prior to channel abandonment.

Consecutive alluvial ridges may adjoin, but rarely intersect one another (Figure 3.5). This is inherent to the avulsion process, wherein the precursory crevasse channel develops along the path of steepest descent. Previously aggraded channel belts each form a positive relief (Figures 3.4 and 3.5), governing floodplain drainage patterns through deflection and focusing of flow. The course of a newly avulsed river will thus be governed by preceding alluvial ridges, causing onlap of overbank deposits where the interspace is limited (Figure 3.9). Repeated shifts in the locus of deposition constitute a process of compensational stacking (Straub et al., 2009), resulting in a radial distribution of fluvial sediment.

The resultant fluvial fan comprises consecutive river paths that are organised in a seemingly dendritic pattern, radiating out from the fan apex and bifurcating downstream (Figure 3.5). Although this configuration could be erroneously identified as a distributary channel network (e.g., North and Warwick, 2007; Fielding et al., 2012), it is the product of repeated (gradual) avulsions of a mostly single-tread active channel. Fluvial progradation may persist as long as sediment supply

exceeds accommodation space at the river terminus, except when the equilibrium profile is lower than the surface gradient (i.e, when the base level falls below a shelf break; (e.g., Koss et al., 1994).

It should be noted that preserved stratigraphy may not be governed by solely autogenic processes. For example, rapid retrogradation occurs when accommodation increase (e.g., a climate-induced rise in lake level) surpasses the throughput of fluvial sediment, resulting in a km-scale landward migration of the shoreline across the low-gradient basin margin. Such incursions form laterally continuous drapes of lacustrine sediment, blanketing the underlying fans with an almost isochronous surface.

3.5. Conclusions

Fluvial progradation across an unconfined low-gradient plain results in the formation of a fan, comprised of successive alluvial ridges. The mostly single-thread active river aggrades through overbank deposition of levees and crevasse splays in response to basinward lengthening of its equilibrium profile. Super-elevation and a decrease in along-channel gradient lead to instability, eventually causing the channel to avulse to a morphodynamically more favourable path.

Crevasse splays play an important role in the autogenic switching of rivers, constituting prototypes for alternative flow paths. When equilibration of a crevasse channel provides a more-efficient drainage path, it receives an increasing proportion of the total runoff. The former channel is abandoned and serves as a floodplain drainage system until it is completely backfilled. The avulsion process is gradual rather than abrupt.

Repeated switching of the single active river path forms a fan of successive alluvial ridges, radiating from a single apex as a product of compensational stacking. The avulsion frequency likely increases downstream, resulting in a dendritic pattern of abandoned river paths. Fluvial progradation may persist as long as sediment supply exceeds accommodation space.

4

Connectivity of amalgamated crevasse-splay complexes

Crevasse splays are thin, but laterally extensive, and interconnected with the (parent) river system. They may form additional reservoir capacity that has previously been overlooked. Studying the reservoir architecture helps predict volumes and the possible contribution to natural gas production.

This Chapter is based on Van Toorenenburg, K. A., Donselaar, M. E., Noordijk, N. A., Weltje, G. J. (2016). On the origin of crevasse-splay amalgamation in the Huesca fluvial fan (Ebro Basin, Spain): Implications for connectivity in low net-to-gross fluvial deposits, *Sedimentary Geology* **343**: 156–164.

4.1. Introduction

Floodplain deposits in low net-to-gross fluvial stratigraphy contain fine-grained reservoir bodies (e.g., Donselaar et al., 2011; McKie, 2011b; Ford and Pyles, 2014). These sub-seismic-resolution deposits are difficult to distinguish on well logs (e.g., Passey et al., 2004; Bridge, 2006) and are thought to represent a relatively small proportion of overall sandstone volumes with a reservoir quality that is generally lower than that of coarser-grained fluvial facies (e.g., Pranter et al., 2008). As a result, intervals of floodplain deposits have been discarded as 'waste zones' in conventional reservoir development (Donselaar et al., 2011) and published research on their accumulation and reservoir architecture is limited (Bridge, 2006). Smith et al. (1989), Van Gelder et al. (1994), Tooth (2005), Donselaar et al. (2013), and Li et al. (2014) have studied the deposition of crevasse splays in active river systems through field work and time-lapse satellite data analysis. Fisher et al. (2007), Hampton and Horton (2007), Jones and Hajek (2007), Nichols and Fisher (2007), and Gulliford et al. (2014) have provided qualitative characterisations of ancient fluvial floodplain deposits exposed in outcrop and proposed and/or applied conceptual models for their stratigraphic evolution. Jordan and Pryor (1992), Pranter et al. (2008, 2009), McKie (2011b), and Ford and Pyles (2014) have presented quantitative reservoir-architecture studies of heterogeneous fluvial intervals based on outcrop and subsurface data. These authors have acknowledged the contribution of crevasse-splay sheet sands to connected reservoir volumes, but focussed on channel and bar deposits which constitute the highest-quality reservoir sandstones. A dedicated study of overbank splay geometries has been conducted by Mjøs et al. (1993), who established geometric ratios and rudimentary volume estimates based on outcrop analogues. A more in-depth examination is needed to better assess the (secondary) reservoir potential of crevasse splays and their impact on reservoir connectivity.

Floodplain deposits are abundant in the distal part of low-gradient dryland river systems fringing endorheic basins, such as the Huesca fluvial fan, Ebro Basin, Spain (e.g., Nichols and Fisher, 2007). The distal part of the fluvial system was characterised by one single active channel with a downstream-decreasing bankfull capacity (Tooth, 2000, 2005; Nichols and Fisher, 2007; Weissmann et al., 2010; Donselaar et al., 2013; Li and Bristow, 2015). This has been attributed to: (1) a downstream reduction in slope (and, hence, flow energy), and (2) a transmission loss due to high infiltration and evapo-transpiration rates. The downstream decrease in cross-sectional area makes the channel prone to extensive overbank deposition during short episodes of peak discharge (Donselaar et al., 2013). Similar depositional and climatological conditions characterised Permo-Triassic basins throughout the Central and North Atlantic margins (Williams and McKie, 2009; McKie, 2011a), including now gas-prolific plays in Northwest Europe (e.g., Geluk, 2007a, 2007b; Donselaar et al., 2011) such as the fringes of the Southern Permian Basin and West Netherland Basin.

In this Chapter, an analysis is presented of thin-bedded floodplain deposits in the distal part of the Huesca fluvial fan (Section 1.3.2 Figure 4.1a). Depositional

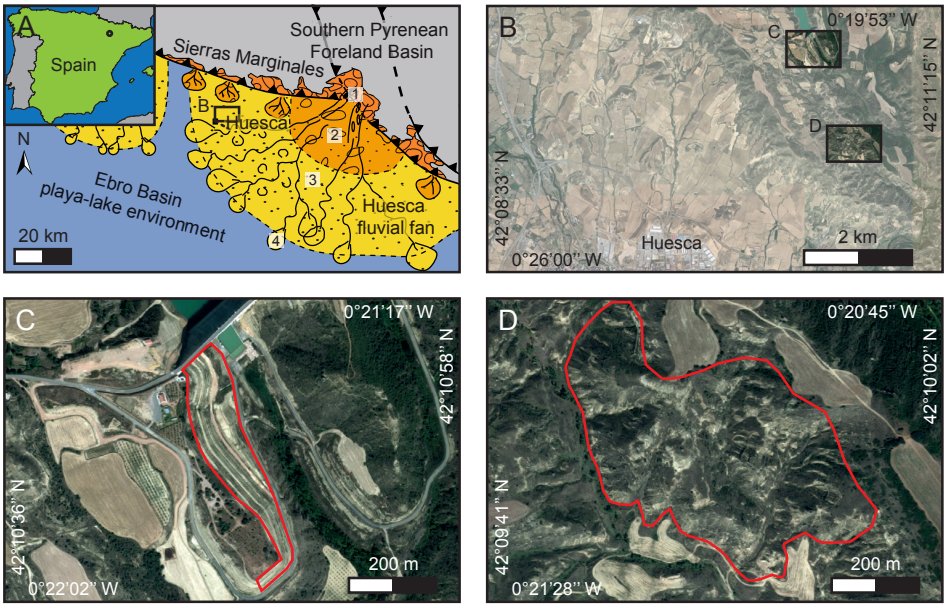

Figure 4.1: Study area. (a) Miocene paleogeography of the Huesca fluvial fan showing its line source (1), proximal braid plain (2), distal meandering channels (3), and terminal lobes at the fan fringe (4) (modified from Donselaar and Schmidt, 2005). Inset: map of Spain; black circle indicates location of paleogeographic map. (b) Overview map of outcrop localities NE of Huesca, indicated by boxes (*Google Earth Pro*). (c) Satellite image of the *Presa de Montearagón* outcrop locality, with the western cut slope encircled in red (*Google Earth Pro*). (d) Satellite image of the *Castillo de Montearagón* outcrop locality, with the studied cliff faces encircled in red (*Google Earth Pro*).

mechanisms explaining the occurrence of intervals of stacked crevasse splays will be proposed. Understanding these processes and their preserved sedimentary architecture improves connectivity estimations of subsurface floodplain reservoirs and aids in the interpretation of low net-to-gross fluvial stratigraphy.

4.2. Methodology

The study area is located to the northeast of Huesca and comprises two outcrop localities spaced approximately 1.6 km apart (Figure 4.1b). Natural cliff faces at 1.3 km to the NNW of the *Castillo de Montearagón* fortress (Figure 4.1d) cover an approximately 35 m thick interval (Figure 4.2a) over an area of 0.2 km2. The western cut slope of the *Presa de Montearagón* reservoir dam (Figure 4.1c) exposes a 52 m thick succession (Figure 4.1b) over a length of 550 m.

The local structural dip was reconstructed in order to accurately correlate data between outcrop localities. A well-developed paleosol at the base of the succession was chosen as a reference horizon, based on the assumption that it developed on a near-horizontal floodplain during a sustained period of inactivity (Kraus, 2002). Sixteen point locations were measured along this horizon with sub-centimetre accu-

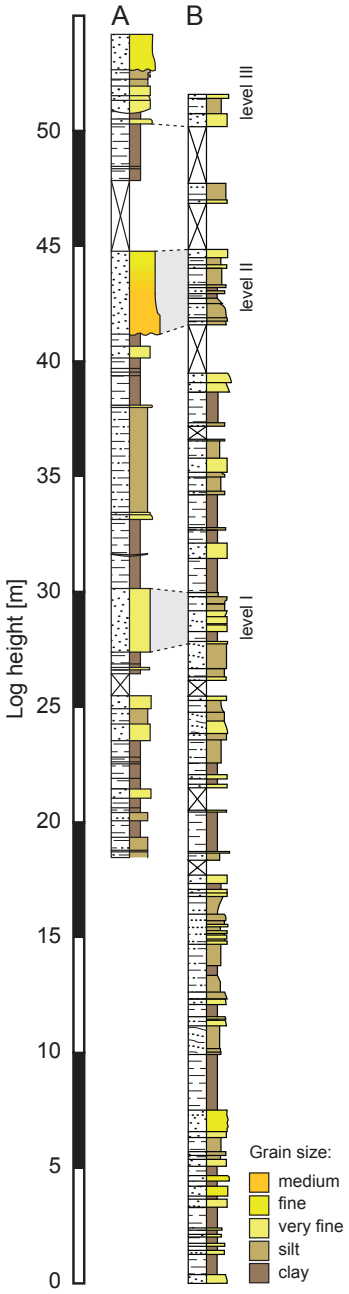

Figure 4.2: Correlation of the sedimentary type logs over a distance of approximately 2 km. (a) Sedimentary type log of the *Castillo de Montearagón* outcrop locality. (b) Sedimentary type log of the *Presa de Montearagón* outcrop locality.

racy using a *Trimble 5700* differential-GPS (dGPS) set (Parkinson and Enge, 1996). These were used in a least-squares regression analysis to estimate the orientation of the planar surface, yielding a structural dip of 0.96° with an azimuth of 227° towards the SW. This is consistent with earlier studies (e.g., Hirst, 1991) and compass validations. The corresponding coefficient of determination R^2 = 0.99 with a vertical standard deviation σ_z = 0.14 m, supporting the assumption that the reference paleosol is planar. The structural dip was used in conjunction with dGPS anchor points to stratigraphically correlate the outcrop localities, revealing a common stratigraphic interval of approximately 34 m (Figure 4.2).

Sedimentological logs comprising bed thickness, nature of contacts, grain size and colour, sedimentary structures, palaeoflow measurements, and bioturbation were recorded at a 1:50 scale. The apparent bed thickness on sloping sections was restored to true thickness. Log correlation was aided with digital photo panels, a laser range finder (>0.1 m accuracy), and dip-corrected dGPS measurements.

Samples were collected at 50-cm vertical increments from the top of selected intervals for grain-size analysis using a *Helos KR Sympatico* laser particle sizer (Blott et al., 2004). The polymodal grain-size distributions (GSDs) represent mixtures of overlapping components: i.e., bed-load (saltation) and suspended-load sediments. The GSDs were therefore decomposed by curve fitting using Weibull distribution functions (Sun et al., 2002; Weltje and Prins, 2007).

4.3. Facies description and interpretation

The sedimentary logs of both outcrop localities show similar lithologies within their common stratigraphic interval, particularly for intervals of stacked siltstone and sandstone sheets (Figure 4.2). The relative location of the outcrops (Figure 4.1b) is approximately parallel to the paleoflow direction measured in these deposits (Figure 4.3), suggesting that one is proximal to the other by ~1.6 km.

4.3.1. Thin-bedded sandstones (crevasse splays)

Ochre-to-grey thin-bedded siltstone and sandstone sheets are observed throughout the sections in both localities (Figure 4.2a,b), commonly exceeding outcrop dimensions in lateral extent. Their thickness ranges from 0.05–0.6 m with a sharp and locally undulating base. The tops are gradual, typically heavily bioturbated, and blue-grey in colour (Figure 4.4a). Individual beds fine upwards from fine-grained sand to silt and frequently contain <1 cm mud pebbles at their base. Climbing ripples and horizontal laminae are common, whereas cross bedding infrequently occurs where beds incise into underlying deposits. Sedimentary structures and scour orientations indicate a palaeocurrent direction towards the N to NW (Figure 4.3).

The facies described here are interpreted as crevasse-splay deposits. Individual crevasse splays originated from a breach point in the previously deposited levee of their feeder channel, forming lobate or elongated sheet sands with surface areas up to several square kilometres (Mjøs et al., 1993; Li and Bristow, 2015). Their sharp (and partly erosional) basal contact is indicative of a high flow energy directly after

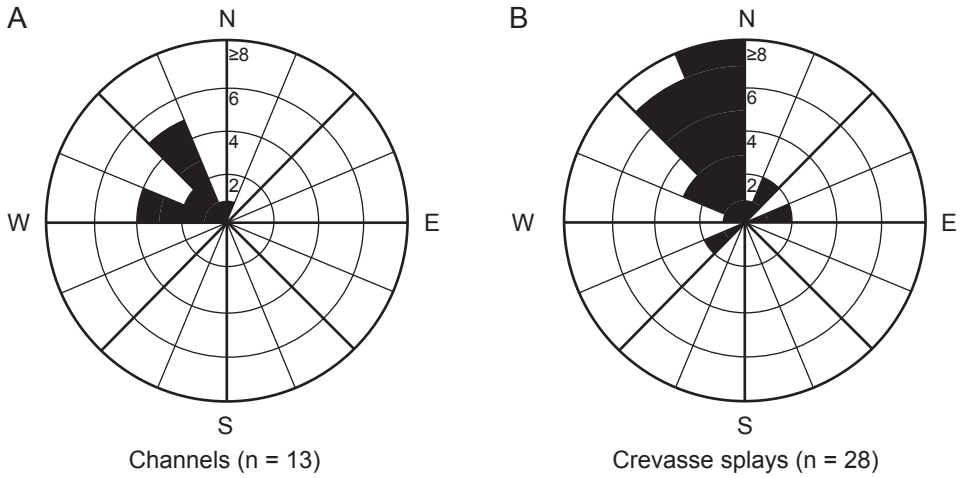

Figure 4.3: Current roses (levels II and III in Figure 4.2). (a) Paleoflow direction of ribbon-shaped sandstone bodies. (b) Paleoflow direction of thin-bedded siltstone and sandstone sheets.

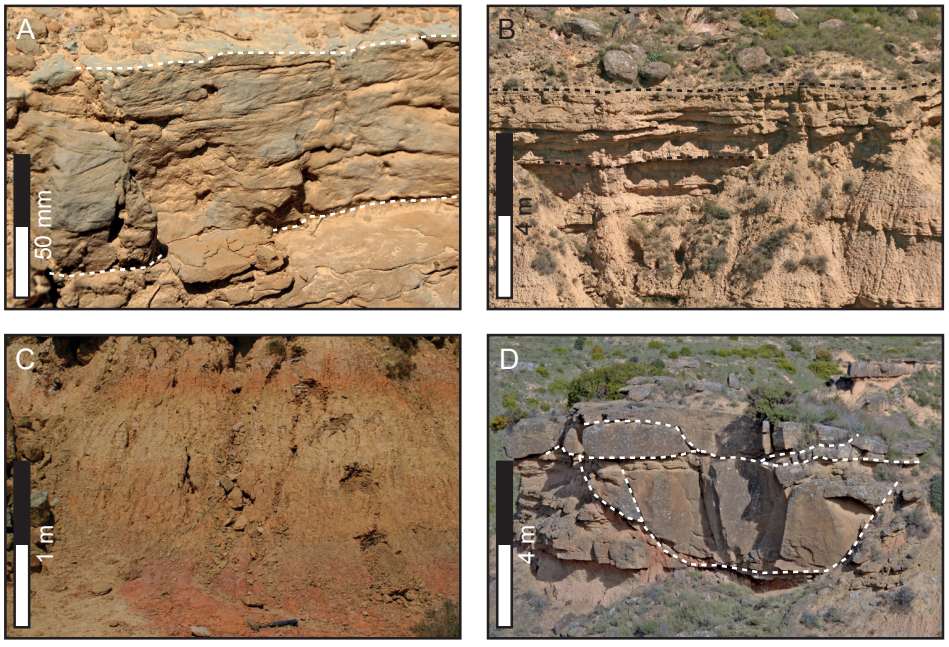

Figure 4.4: Lithofacies. (a) Thin-bedded siltstone and sandstone sheet with bed boundaries indicated in white dashed lines. Note the ripple foresets. (b) Stacked thin-bedded siltstone and sandstone sheets with interval boundaries indicated by white dashed lines. (c) Horizontally laminated claystones and siltstones with pink to purple-red structureless horizons. (d) Ribbon-shaped sandstone body with reactivation surfaces indicated by white dashed lines.

crevassing, when sediment-laden water entered the floodplain under a waxing flow regime. This is supported by the occurrence of rip-up mud clasts, which originated from the desiccated floodplain surface and underwent short-distance bedload transport (Rust and Nanson, 1989). Low sinuous crevasse-splay channels focussed the outflow and may have incised into the substrate (Ford and Pyles, 2014). Further downstream in the crevasse splay, they bifurcate (Donselaar et al., 2013) and end in subtle terminal mouth bars (Bridge, 2006). Abundant climbing ripples indicate that fine sand and silt were deposited under a waning flow regime. The gradual top suggests a gradual transition to deposition from suspension. This occurred when the floodplain was inundated and suspended-load sediment started to form conformable drapes of floodplain fines.

4.3.2. Variegated fines (floodplain)

Horizontally laminated claystone and siltstone constitute 50–60% of the total stratigraphy in the sedimentary logs (Figure 4.2). Continuous successions are up to 5 m thick (Figure 4.2) and often heavily weathered or vegetated. The colour of these deposits ranges from ochre to beige (Figure 4.4c), displaying abundant red mottling. Structureless horizons of claystone and fine siltstone with gradual contacts occur throughout the sections, varying in thickness (up to 0.5 m) and lateral extent. Their colour ranges from pink to purple-red and they are frequently overlain by a blue-grey or white top.

Laminated claystone and siltstone are interpreted as floodplain fines. These sediments settled out of suspension during floodplain inundation, forming a conformable drape on top of previous deposits. They were subsequently subaerially exposed, causing widespread mottling. Extended periods of pedogenesis formed paleosols, manifested as red to purple-red-coloured horizons. This required a prolonged absence of sediment influx, signifying local floodplain inactivity (Kraus, 2002). The paleosols in the study area match the descriptions of the *Bolea* (inceptisol) and *Erla* (entisol) pedotypes, as defined by Hamer et al. (2007). Their blue-grey tops have been attributed to burial gleization (Retallack, 1991).

4.3.3. Ribbon sandstones (channels)

Ribbon-shaped sandstone bodies range from 1.0 to 2.8 m in thickness, averaging 2 m (standard deviation σ = 0.8 m; n = 6) (Figure 4.5). They may be stacked up to 5 m in height with clear reactivation surfaces (Figure 4.4d). Their base is sharp and erosional, overlain by medium-to-coarse-grained poorly sorted sand and rip-up mud clasts. Trough cross bedding with set heights of 20–40 cm occur throughout the sandstone body. At the top, grain size decreases to fine-to-medium-grained sand with abundant bioturbation. The orientation of the low-sinuous ribbon axes and sedimentary structures indicate a paleoflow direction towards the W to NW (Figure 4.3), which is in accordance with earlier studies (e.g., Hirst, 1991) and oblique to the paleoflow direction of the crevasse splays (Figure 4.3). These sandstone ribbons typically truncate intervals of stacked thin-bedded crevasse splays

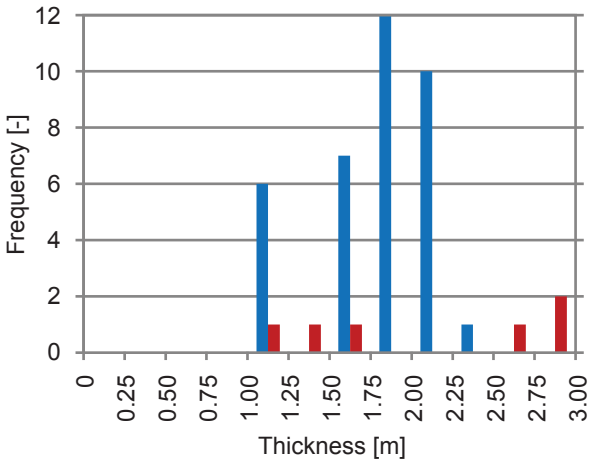

Figure 4.5: Left-closed histogram of thickness measurements of channel sandstone bodies (red) and intervals of stacked crevasse splays (blue). Note that channel thickness might be overestimated due to unidentified reactivation surfaces and that the population of measurements (n = 6) is not representative.

(Figure 4.4d), creating sand-on-sand contact at their erosional base.

Ribbon-shaped sandstone bodies are interpreted as fluvial channels whose low width-to-thickness ratios (<10) and lack of accretionary surfaces indicate limited lateral migration (Friend et al., 1979; Hirst, 1991; Nichols and Fisher, 2007). Their cross-bedded channel fill overlies an erosive base, suggesting incision and subsequent aggradation of channel-lag deposits up to 2.8 m thick. Vertical stacking of the channel ribbons into multi-storey sandstone bodies is caused by successive phases of intrachannel erosion and deposition. This can be attributed to fluctuations in flowrate or, in some instances, repeated reoccupation of the remnant channel depression (Slingerland and Smith, 2004). Friend et al. (1986), Hirst (1991), Fisher et al. (2007), and Nichols and Fisher (2007) have observed crevasse splays extending from the top of ribbon channels as 'wings', forming a continuous sandstone body. This could not be unambiguously verified in the outcrop localities of this study due to the poor exposure of these interfaces.

4.4. Crevasse-splay amalgamation

Individual crevasse splays are frequently found in amalgamated complexes of up to several metres in thickness. These levels correspond to nearby channel deposits and can be correlated between the outcrop localities in the study area.

4.4.1. Lateral amalgamation

In earlier studies, Donselaar et al. (2013) and Li et al. (2014) have observed compensational stacking of crevasse splays in the modern-day Río Colorado fluvial system (Altiplano Basin, Bolivia). The lobate geometry of crevasse splays forms a

dm-scale topography on the otherwise planar floodplain. Subsequent splays are deposited in the subtle topographic lows between adjacent crevasse splays. The proximally erosive base of the newly deposited splay truncates the finer-grained top of its previously deposited neighbours, creating sand-on-sand contact. Further away from the feeder channel, the depth of incision is less, preserving the finer-grained top of the underlying sheets in an onlapping geometry. This process of lateral amalgamation creates large areas of interconnected sand sheets up to ~10^7 m^2 (Li and Bristow, 2015), elevating the floodplain proximal to the feeder channel. The mechanism is generic, but its expression is difficult to unambiguously identify in the study area due to the limited extent of outcrop exposure and lack of grain-size contrast at lateral amalgamation surfaces.

4.4.2. Vertical stacking

Individual crevasse splays are frequently stacked (Figure 4.4b) to a combined thickness of up to 2.35 m, with a local average of 1.8 m (σ = 0.37 m; n = 36) (Figure 4.5). Such intervals are typically underlain by a red to purple-red paleosol with gradual contacts, separated by several centimetres of ochre to red laminated floodplain claystone and siltstone. The lowermost crevasse splay has a sharp planar base, whereas subsequent splays show an increasingly undulating base with an undulation relief of <30 cm (Figure 4.6). Proximal to the feeder channel, these bed bases cut tens of centimetres into underlying crevasse splays, having removed their fine-grained top and creating sand-on-sand contact. The grain-size contrast at these contacts is dependent on the depth of incision and the interface is frequently marked by <1 cm mud clasts separated by a sand matrix. The amalgamation surfaces exceed outcrop dimensions and are only locally interbedded with remnant drapes of floodplain fines. The depth of incision decreases in the paleocurrent direction, where the finer-grained top of the underlying sheet is preserved up to several hundreds of metres from its distal fringe. This results in a downstream separation of individual beds, which finger out and lose grain-size contrast with interbedded parallel-laminated floodplain fines (Figure 4.7). Laser particle size analysis of samples from these intervals reveals grain sizes ranging from 2–250 µm in diameter, i.e., clay to fine-grained sand (Wentworth, 1922). The grain-size distributions are decomposed into component 'A', ranging from clay to very-fine silt and displaying no obvious trends, and component 'B', ranging from medium silt to fine sand and showing a subtle coarsening-up trend within consecutive sheets (Figure 4.8).

4.4.3. Depositional mechanisms

Vertical stacking of crevasse splays (Figures 4.6 and 4.7) implies that the active channel belt has aggraded (i.e., super-elevated) above the surrounding floodplain. This aggradation of alluvial ridges characterises prograding fluvial systems, where successive avulsions cause the active channel belt to periodically shift and enter (previously inactive) lower-lying parts of the floodplain in a process of large-scale compensational stacking (Slingerland and Smith, 2004). As each newly

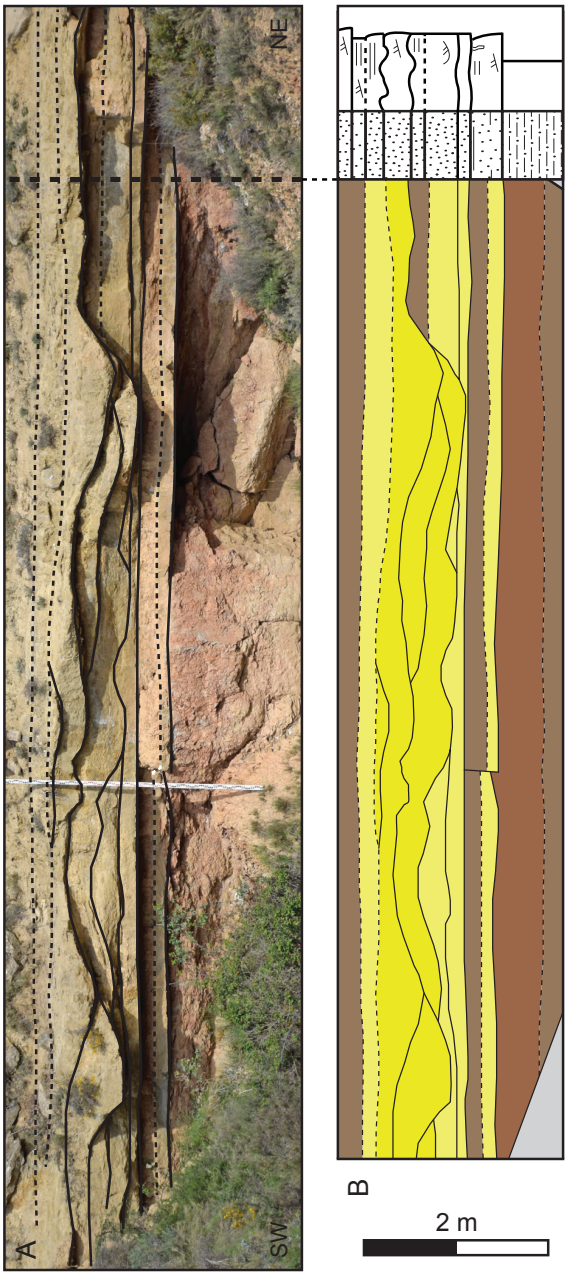

Figure 4.6: Section through stacked thin-bedded siltstone and sandstone sheets perpendicular to the paleoflow direction (level II in Figure 4.2). (a) Outcrop photo with bed boundaries marked in continuous (sharp) or dashed (gradual) black lines. Sedimentary log location indicated in black. (b) Interpretation panel including sedimentary log. Colours according to key in Figure 4.2.

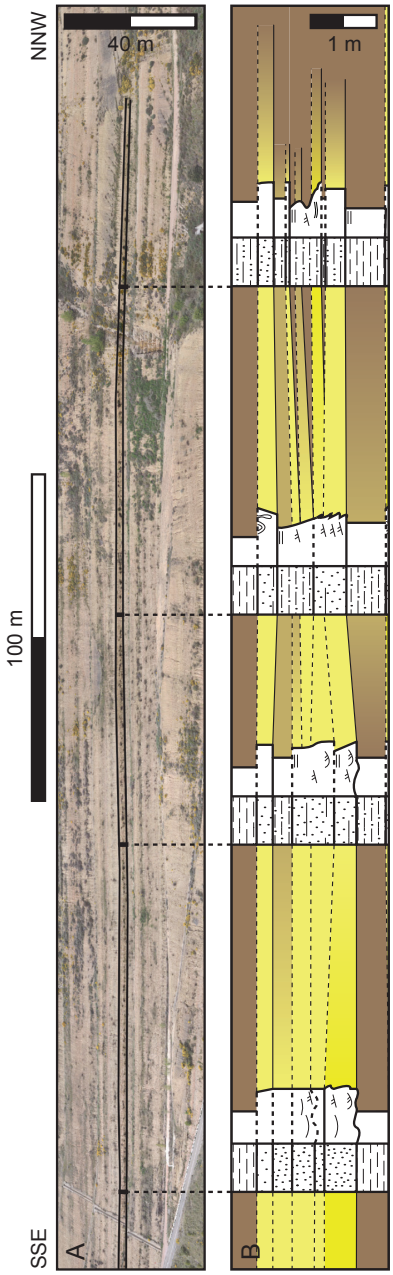

Figure 4.7: Section through stacked thin-bedded siltstone and sandstone sheets parallel to the paleoflow direction (level I in Figure 4.2). (a) Outcrop photo with interval of interest bounded by black lines. Sedimentary log locations indicated in black. (b) Interpretation panel including sedimentary logs. Colours according to key in Figure 4.2.

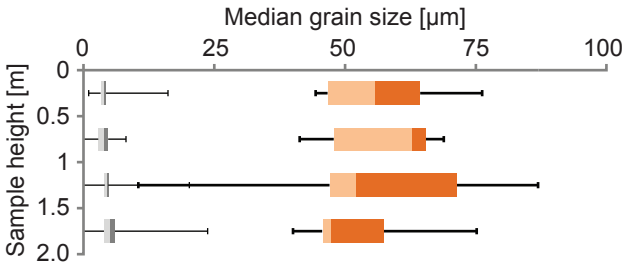

Figure 4.8: Distribution of median grain size in quartiles after decomposition at 0.5 m intervals from the top of stacked thin-bedded siltstone and sandstone sheets (level III in Figure 4.2). Component 'A' in grey; component 'B' in orange.

avulsed river tract adjusts towards the system equilibrium profile (Chapter 3), an alluvial ridge forms through the stacking of crevasse splays until a subsequent avulsion terminates the influx of sediment (e.g., Mohrig et al., 2000; Dalman et al., 2015).

Prolonged periods of local floodplain inactivity and subaerial exposure allow for extensive pedogenesis, resulting in mature paleosols (Kraus, 2002) (Figures 4.4c, 4.6, and 4.9a). Fluvial system dynamics (i.e., shifts in active river proximity) may cause periodical reactivation of the local floodplain, which is manifested by deposition of floodplain fines (Figures 4.4c and 4.6). Reactivation is occasionally followed by (partial) avulsion onto the local floodplain when a channel reaches a critical threshold for avulsion (e.g., Mohrig et al., 2000; Slingerland and Smith, 2004; Hajek and Wolinsky, 2012). Prolific crevasse splays prograde onto the lower-lying floodplain adjacent to the active fluvial ridge, receiving a gradually increasing share of the total discharge (Chapter 2). These preludes to avulsion have been termed 'associated non-coeval splays' by Ford and Pyles (2014). As their crevasse-splay channels stabilise and decrease in number, the increasing flow volume is accommodated through headward incision and levee development (Smith et al., 1989; Hajek and Wolinsky, 2012) (Figure 4.9b).

Even before this gradual avulsion is fully completed, levee build-up causes the bankfull height of the new channel to rise. This mimics the aggradation of the newly established channel when flow volumes stabilise and the hydraulic capacity becomes more or less constant (Figure 4.9c). Weak points in the levees are breached during peak discharge events, after which their sediment is reworked into crevasse splays (termed 'associated coeval splays' by Ford and Pyles (2014)). The initial crevasse splays are deposited onto a relatively flat floodplain surface, resulting in a planar base (Figures 4.6 and 4.9c). Amalgamation with adjacent lobes (Li et al., 2014) create an elevated rim extending up to several kilometres away from the active channel (Donselaar et al., 2013) (Figure 4.9d). Levees continue to build on top of the proximally aggraded floodplain during unconfined overbank flow and are in turn reworked into crevasse splays. These then stack on top of precursory splays and further raise the floodplain proximal to the active channel. The subsequent rise in bankfull height again mimics the aggradation of the channel thalweg. The

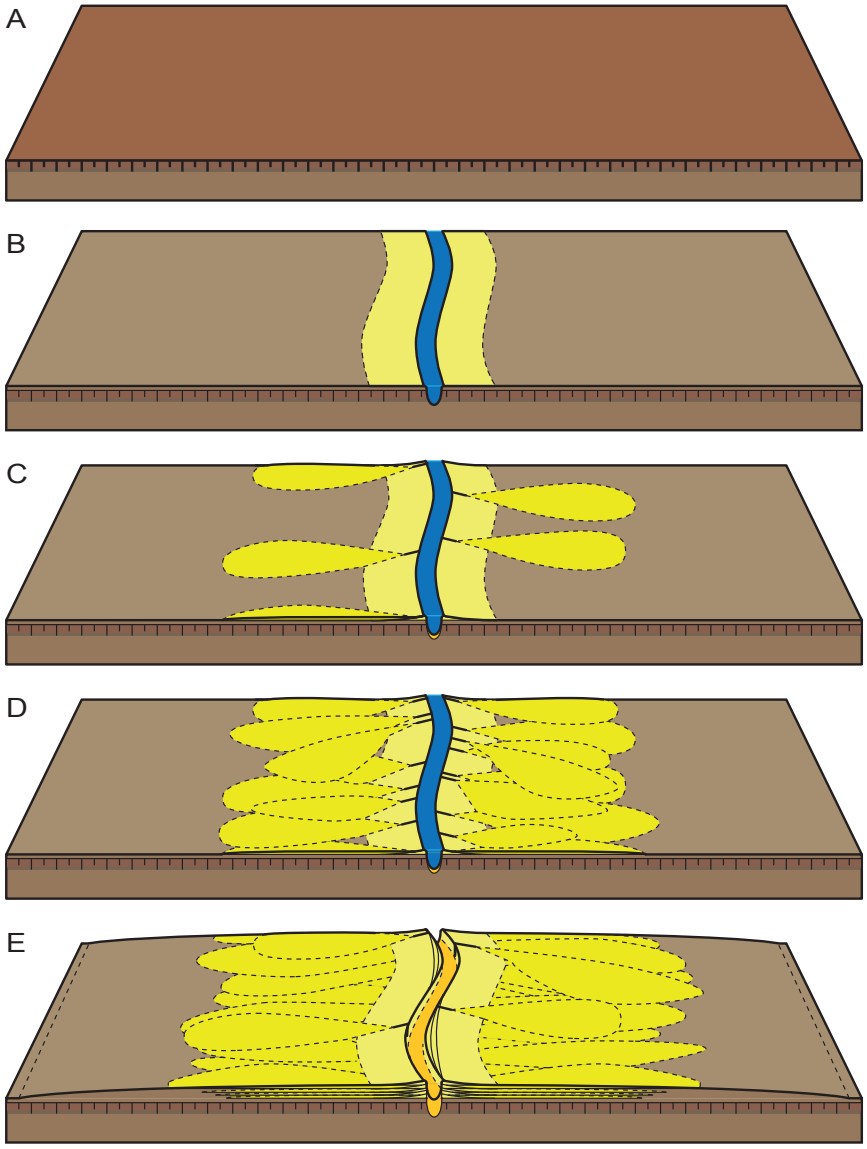

Figure 4.9: Schematic representation of the proposed mechanism for stacking of crevasse splays (not to scale). Colours according to key in Figure 4.2; water in blue. (a) Pedogenesis of the inactive floodplain, creating an extensive paleosol. (b) Increased deposition of floodplain fines announcing floodplain reactivation. Upon avulsing, the active channel incises into the substrate and starts building up levees through overbank deposition. (c) Levees are reworked into crevasse splays when they are breached. The rise in bankfull height mimics the elevation of the channel thalweg. (d) Lateral amalgamation of crevasse splays creates an elevated rim around the active channel. (e) Levees continue to build on top of the proximally aggraded floodplain and are in turn redeposited into crevasse splays, stacking on top of their precursors and building out further onto the floodplain, resembling a subaerial analogy of a prograding high-stand delta. The process terminates when an upstream avulsion occurs. Note that the thickness of the stacked crevasse-splay interval matches that of the aggraded channel lag (orange-yellow).

resulting increased overbank gradient causes successive crevasse spays to longer retain their energy. This is manifested by deeper incision of crevasse-splay channels close to their feeder channel (Figure 4.6), an increase in grain size (Figure 4.8), and sediment transport further onto the floodplain, resembling a subaerial analogue of a prograding delta (Figure 4.9e). This iterative process of channel-belt aggradation and widening (Figure 4.7) continued until an upstream avulsion occurred.

The expression of stacked crevasse splays in this study (Figures 4.6 and 4.7) and the proposed depositional mechanisms (Figure 4.9) are consistent with the work of, e.g., Slingerland and Smith (2004), Jerolmack and Mohrig (2007), and Dalman et al. (2015). These authors used a numerical model with subgrid parameterisation of channel evolution (crevasses, avulsions, bifurcations) to simulate super-elevation of a fluvio-deltaic system onto a low-gradient shelf as a result of progradation (regression), where accommodation is created through a lengthening of the fluvial equilibrium profile and a reduction of its gradient.

In fact, fluvial system aggradation (i.e., creation of accommodation) may occur throughout a supply-accommodation cycle (sequence), except when the equilibrium profile is lower than the surface gradient (i.e, when the base level falls below a shelf break; e.g., Koss et al., 1994). During this late stage of the falling stage systems tract (FSST), progradational units with a fundamentally different geometry are created, characterized by the absence of avulsions and an abundance of bifurcations (Karamitopoulos et al., 2014), stacking of crevasse splays owing to channel-belt aggradation is the rule in low-gradient fluvial systems (e.g., Hajek and Wolinsky, 2012; Dalman et al., 2015).

4.5. Implications for reservoir connectivity

Crevasse splays may have reservoir potential, comprising sand and silt in an otherwise fine-grained floodplain environment. They could, therefore, contribute to fluvial reservoir volumes and enhance connectivity, especially in the lower net-to-gross distal reaches of a fluvial system.

4.5.1. Connectivity

Despite their large areal extent (up to several km^2), the limited thickness (decimetre-scale) of individual crevasse splays only yields sediment volumes on the order of $\sim 10^5$ m^3. Lateral amalgamation connects individual splays into aerially extensive sand sheets (Donselaar et al., 2013; Li et al., 2014) (Figure 4.10a), increasing the aerial extent and, hence, connected sediment volumes by one order of magnitude, i.e., to $\sim 10^6$ m^3. Vertical stacking of crevasse splays creates sand-on-sand contact through local erosion of underlying beds (Figure 4.10b), mainly proximal to their feeder channel. In this study, two intervals of stacked crevasse splays have been correlated between the outcrop localities (Figure 4.2), well within the maximum areal extent of crevasse splays (Mjøs et al., 1993; Li and Bristow, 2015). Vertical stacking up to several metres thickness may increase the connected sediment volume of these intervals by another order of magnitude, i.e., to $\sim 10^7$ m^3.

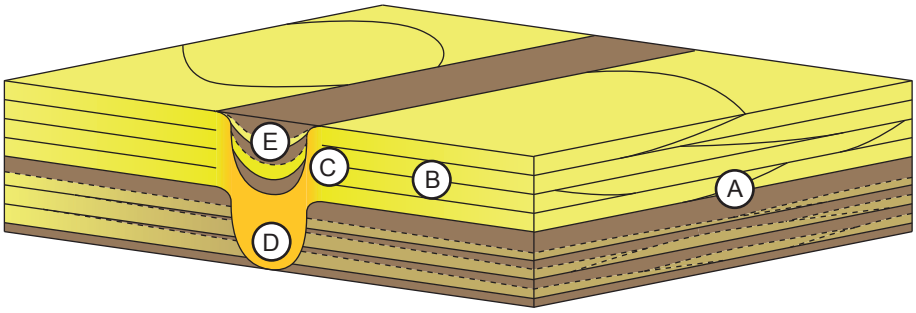

Figure 4.10: Conceptual diagram illustrating the nature and types of connectivity (not to scale). Colours according to key in Figure 4.2. Continuous lines indicate erosional surfaces; dashed lines indicate gradual bed boundaries. (a) Lateral amalgamation and (b) vertical stacking proximal to the feeder channel where bed bases are erosional, creating sand-on-sand contact. (c) Crevasse splays continuing into the top of aggraded channel-lag sandstone. (d) Truncation of crevasse splays by channel-lag sandstone, creating sand-on-sand contact. (e) Heterolithic channel-fill.

Crevasse splays are connected to channel-lag and heterolithic channel-fill deposits, which typically constitute the lithologies with best reservoir quality (e.g., Fielding and Crane, 1987; Pranter et al., 2008). Channel-lag deposits in the crevasse-splay channels connect as 'wings' to their coeval feeder-channel fill (Friend et al., 1986; Hirst, 1991; Mjøs et al., 1993; Nichols and Fisher, Fisher et al.; 2007, 2007) (Figure 4.10c). Truncation of previously deposited crevasse splays (i.e., non-associated or associated non-coeval splays; Ford and Pyles, 2014) by later channels may further increase connectivity (Mjøs et al., 1993) (Figure 4.10d). This contradicts the notion that laterally restricted fluvial reservoirs such as the channel ribbons in this study are isolated from each other by floodplain deposits (e.g., Fielding and Crane, 1987), despite their lower reservoir quality. Their contribution to producible volumes should therefore be considered in order to avoid an underestimation of net reservoir volume and long-term production rates. Similar issues are of concern in deep-marine systems, where thin-bedded lobate deposits contribute to connected reservoir volumes (De Ruig and Hubbard, 2006).

Effective connectivity may be limited to a channel-belt scale. Compensational stacking in an aggradational setting causes onlap of successive channel belts (Figure 3.9). The floodplain fines at their lateral fringes are likely to be preserved in absence of erosion. These floodplain fines form barriers to flow, effectively compartmentalising individual channel belts unless they are connected through their channel-lag deposits.

4.5.2. Secondary reservoir potential

Thin-bedded crevasse splays may constitute a secondary source of natural gas in areas where production is in decline, such as the Northwest European gas province. A prolongation of production by several percent at a low investment cost (e.g., Donselaar et al., 2011) would allow to postpone abandonment, significantly increasing the net present value (NPV) of a field. Existing well penetrations that produce from conventional reservoir intervals may be re-evaluated in order to detect complexes of amalgamated crevasse splays. Borehole image logs with a high spatial resolution contribute to an improved characterisation of these thin-bedded deposits (e.g., Donselaar and Schmidt, 2005), which are difficult to distinguish on conventional well logs (Bridge, 2006). Low-cost development scenarios may include reperforation of existing wells and side-track or infill drilling in order to unlock unswept volumes in low net-to-gross fluvial stratigraphy.

Intervals of amalgamated crevasse splays can also be used to estimate the dimensions of their feeder channel in intervals where the latter is not directly penetrated by a well. The proposed mechanism for the stacking of crevasse splays (Figure 4.9) implies that the maximum thickness of these crevasse splay complexes is approximately equal to the thickness of their aggraded trunk-channel lag, given that its hydraulic capacity was more or less constant. Thickness measurements in the Castillo de Montearagón outcrop locality are compliant with this proportionality (Figure 4.5). The ability to estimate subsurface channel dimensions in the absence of any direct penetrations provides a proxy for connectivity assessment. Larue and Hovadik (2006) have used channel dimensions and the net-to-gross ratio in wells to predict geobody connectivity. The findings presented here enable the use of a similar approach based on the interval thicknesses of crevasse splay complexes, which due to their lateral extent are significantly more likely to be penetrated by a well.

4.6. Conclusions

The studied stratigraphic interval comprises crevasse splays, floodplain fines, and low-sinuous channel sandstone ribbons, representing the distal part of the Huesca fluvial fan. Stacked crevasse splays are encountered in intervals of up to 2.35 m thick and can be correlated between outcrop localities over a distance of 2 km.

Vertical stacking of crevasse splays implies local aggradation of the active channel belt, which may have been induced by avulsion onto a lower-lying part of the floodplain. Levees were reworked into crevasse splays with surface areas of up to several square kilometres. Lateral amalgamation created an interconnected fringe around the active channel, raising its bankfull height and the feeder-channel thalweg. This process of channel-belt super-elevation repeated until an upstream avulsion occurred.

Lateral amalgamation and vertical stacking of crevasse splays significantly increases their connected reservoir volume up to $\sim 10^7$ m^3. Despite their lower reser-

voir quality, these thin-bedded sheets effectively connect channel deposits in low net-to-gross fluvial stratigraphy, and hence, their contribution to producible volumes should be considered. Unswept intervals of amalgamated crevasse splays may constitute a secondary source of natural gas in brown field development situations. Their interval thickness can serve as a proxy for feeder-channel dimensions, which can in turn be used to estimate the degree of stratigraphic connectivity.

5

Discussion and Conclusion

The aim of this study has been to investigate the role that crevasse splays play in the autogenic development of fluvial fans. A generic depositional model and a life cycle were proposed, which capture the full evolution of crevasse splays in both space and time within the context of their parent fluvial system. This led to the identification of depositional mechanisms that promote the aggradation of alluvial ridges, expressing the super-elevation of the active river in response to its progradation. Moreover, crevasse splays were shown to play a key role in the subsequent autogenic switching (i.e., avulsion) of river channels to a hydrodynamically more-favourable path. These findings supported quantitative reconstructions of the sedimentary architecture and properties of crevasse splays. Here, the main findings of the Thesis are briefly summarised, after which the relevance and limitations of the research are discussed and an outlook of future work is presented.

5.1. Synopsis

A generic life cycle applies to crevasse splays in prograding fluvial systems, typically ending in healing and abandonment. Crevasse-splay channels adjust to a graded equilibrium profile through proximal erosion and distal deposition, with their distal termini acting as a (prograding) local base level. When proximal incision advances to below the maximum flooding level, a reflux of floodwater occurs during the waning stage of flooding. The resultant decrease in gradient ultimately leads to the backfilling and abandonment of a crevasse splay, provided that the elevation at its distal fringe remains higher than that of the trunk channel floor. Consecutive crevasse splays form an alluvial ridge through lateral amalgamation and subsequent vertical stacking, perching the active river above the surrounding floodplain. Super-elevation of the channel thalweg above the distal termini of a prograding crevasse splay leads to avulsion.

A high-resolution morphological reconstruction of both the active (and recently abandoned) river(s) and the surrounding floodplain has been established to test the proposed life cycle of crevasse splays and evaluate its role in autogenic avulsion and organisation of the fluvial system. An avulsion can only occur when an overbank path of steepest descent reaches the system base level in a shorter distance (which may partially reuse the existing channel or remnant channel depressions) than the along-channel distance to its terminus. Crevasse splays prograde along this overbank flow path and capture an increasing portion of the total discharge, accelerating their development. When the crevasse apex incises down to or below its trunk channel thalweg, the avulsion is complete. The overbank path of steepest descent (i.e., avulsion path) is governed by floodplain topography, which is largely formed of abandoned alluvial ridges. This leads to compensational stacking of successive prograding channel belts, resulting in fan of amalgamated ridges.

5.2. Perspective and limitations

The work presented here was conceived to evaluate the hydrocarbon reservoir potential of crevasse splays in subsurface intervals with a high proportion of floodplain mudrock (i.e., low net-to-gross fluvial stratigraphy). Such intervals are common in, e.g., the Northwest European natural gas province, which dominantly produces from Permo-Triassic continental successions that were deposited along the margins of rift basins associated with the (early) breakup of the Pangea Supercontinent (Geluk, 2007a, 2007b; Williams and McKie, 2009; McKie, 2011a). Production from conventional fluvio-aeolian sandstone reservoirs in this mature area is currently in decline, and previously bypassed intervals of fluvial overbank stratigraphy could constitute additional reservoir capacity. These intervals may be economically developed using existing infrastructure at minimal reinvestment (e.g., Donselaar et al., 2011), thus prolonging production and postponing abandonment. In fact, a recent re-perforation by the *Nederlandse Aardolie Maatschappij* (NAM) in similar (Rotliegend) stratigraphy resulted in ~30 · 10^6 Sm^3 of additional gas production at an investment of merely ~50 k€ (Donselaar et al., 2011). Upon further study, NAM identified a number of wells that show secondary reservoir potential in the Permian (Rotliegend) Ten Boer Member (dr. C.A. Visser, NAM, pers. comm., 2018).

Preliminary studies as part of this research (Appendix B) indicate that crevasse splays indeed contribute to connected fluvial reservoir volumes and may qualify as (secondary) gas reservoirs. Moreover, crevasse splays may provide additional constraints for well-based palaeo-reconstructions of subsurface fluvial intervals. More research is needed to further investigate these findings and work towards their practical application in exploration and production.

The mechanisms proposed in this study are thought to be generic for prograding fluvial fans. However, factors such as the range of grain sizes available in the system, the nature of the substrate (e.g., gradient, flatness), base-level changes, and climate (e.g., discharge variation, vegetation) may significantly influence the expression of these sedimentary processes and their resultant deposits. Moreover, post-depositional diagenetic processes (e.g., cementation) can significantly deteriorate reservoir properties. The influence of such aspects should be carefully considered when applying the results of this Thesis to any fluvial system.

5.3. Outlook and recommendations

Future work may focus towards the application of the insights presented in this Thesis, specifically in combination with subsurface date of Permo-Triassic basin fringe successions in the northwest European natural gas province. Architectural reconstructions and reservoir assessment could be further enhanced by incorporating information on gas shows and well tests of correlated intervals, ultimately allowing to produce system-scale permeability-thickness (kh) maps that are valuable in exploration and de-risking of redevelopment. This could potentially prolong gas supply in mature areas, creating additional revenue and postponing the cost of

decommissioning.

The research could also serve to improve the parametrisation of crevassing and avulsions in (sedimentary process-based) forward models, improving their predictive value and allowing to better study system evolution. Additionally, the data collected from the Río Colorado fluvial fan form a basis for sediment budget models, and may be enhanced through, e.g., aerial LIDAR scanning of the system topography, the collection of additional dGPS ground control points, and river discharge measurements. Research boreholes at intervals along the system axis (i.e., from its apex towards the basin) could reveal the extent of lacustrine intercalations resulting from endorheic flooding cycles, supporting ongoing research aimed at correlating 'onset of flooding' surfaces based on well-log data. A system-scale chronostratigraphic mapping of the Huesca fluvial fan could be used as a validation.

A

Sediment dispersal patterns in crevasse splays

The figures in this Appendix are based on the M.Sc. thesis work of A.B. Sandén.

A

Introduction

Fluvial sedimentation is primarily dependent on aqueous flow energy, as stream power provides critical thresholds for the mobilisation and deposition of sediment (e.g., Miller et al., 1977; Bull, 1979). Channelised streams have more energy than unconfined flows, which decelerate through widening, shallowing, and increased surface drag. As a result, overbank deposits generally represent the lower spectrum of the total grain-size range available in a river system. Levees and crevasse splays comprise the coarsest of these floodplain sediments, forming where overbank flow maintains a sufficiently high stream power (i.e., preceding floodwater arrest by ponding or floodplain inundation).

Crevasse-splay deposits are commonly coarser-grained and thicker then levees (Bridge, 2006), comprising splay channels that facilitate higher overbank stream power. This channelised splay geometry bears resemblance to larger-scale fluvial fans (Nichols and Fisher, 2007) and prograding fan deltas (Van Dijk et al., 2009), where rivers control sediment dispersal patterns. Scarce accounts of the grain-size distribution in crevasse splays do not capture comparable patterns in detail, instead specifying a general fining trend from the crevasse apex towards its distal fringes (e.g., Burns et al., 2017).

This Appendix details the initial results of a study on sediment dispersal in crevasse splays based on grain-size samples from the modern-day Río Colorado dryland fluvial system (Altiplano Basin, Bolivia). Principal mechanisms for the distribution of fluvial sediment are proposed and subsequently tested using calibrated process-based models. Their scale independence is discussed, drawing from analogies to channelised lobes and fans. A thorough understanding of these depositional processes constrains detailed reconstructions of the resultant grain-size distribution.

Methodology

Data acquisition took place around the single active channel in the distal fan of the Río Colorado fluvial system during field campaigns in 2012 and 2014. Over 250 georeferenced sediment samples were collected from three well-developed crevasse splays and analysed using a *Helos KR Sympatico* laser particle sizer (Blott et al., 2004). Each polymodal grain-size distribution (GSD) was subsequently unmixed into end-member compositions by curve fitting of Weibull distribution functions (Sun et al., 2002; Weltje and Prins, 2007) (Figure A.1). The spatial distribution of median grain-size values for each genetic component was analysed for trends in sediment dispersal.

Process-based models in *Delft3D* served to simulate sediment dispersion in crevasse splays (Lesser et al., 2004), assuming non-stratified (i.e., two-dimensional) flow across a uniform 250x250 Cartesian grid with a 2 m resolution. The model setup comprised a river channel with adjoining levees on its left boundary, receiving sediment-laden inflow at the bottom and outflow from the top. An artificial depression in the rightmost levee was created to initiate crevassing onto the low-

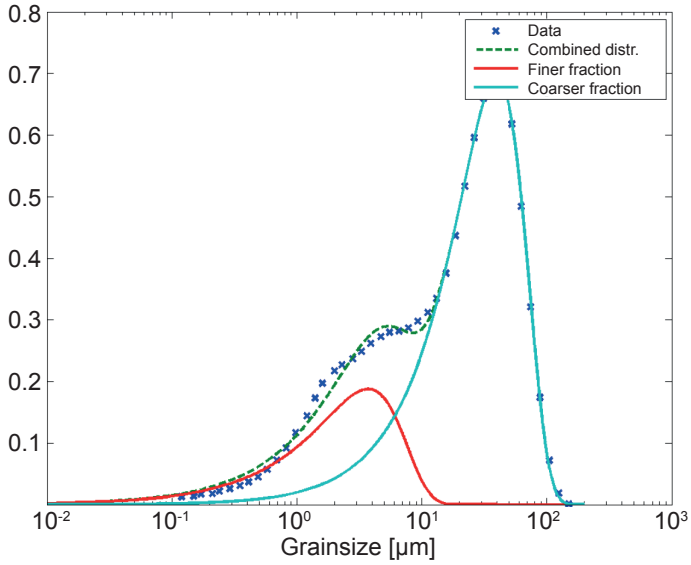

Figure A.1: Grain-size distribution measured through laser diffraction analysis (blue crosses) decomposed into end-member distributions (red and cyan lines) and their combined distribution (green dashed line) for one sample.

gradient floodplain that formed the bulk of the model (Figure A.2). Calibration of the model parameters was achieved using a discretised aggregation of sample GSDs for sediment input, and quantifications of discharge variation (Li et al., 2014) and fluvial morphology (Donselaar et al., 2013) for flow dynamics. The models were run for nine successive flooding cycles (Figure A.2).

Sediment dispersal patterns

The sample GSDs each consist of two main end-member compositions which display significant differences in the spatial distribution of their median grain size (Figure A.1). The finer fraction (median D_{50} = 5.3 ± median absolute deviation MAD = 3.2 µm) shows no unambiguous spatial patterns or trends and appears to be uniformly draped across the sampled areas. The coarser component (D_{50} = 30 µm ± MAD = 21 µm) exhibits a significantly higher spatial variation in median grain size. The differences in sediment size and distribution of the end-member compositions are attributed to their respective mode of deposition. The finer component represents sediment that settled from (near-)standing water during floodplain inundation. Dispersal of the coarser fraction is associated with flow competence, wherein grains are deposited when the stream power drops below a size-specific threshold. This stream power is largely a function of crevasse-splay morphology, as its channels facilitate higher and longer-retained flow energies than the non-channelised part of the splay. This implies that grain size is inversely correlated

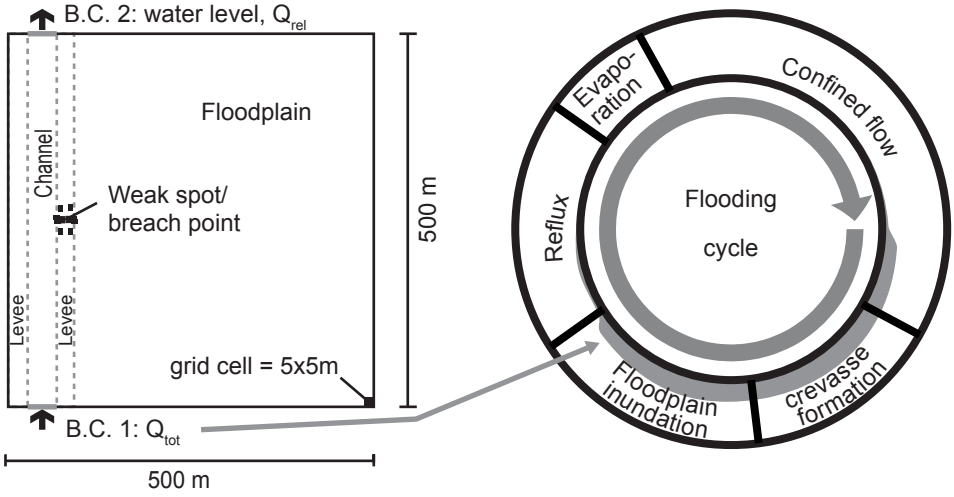

Figure A.2: Schematic representation of the process-based model setup (left) and the flooding cycle (right). B.C.: boundary condition; Q_{tot}: total influx; Q_{rel}: relative (to water level) outflux.

to both the along-channel distance and the distance travelled outside these channels (Figure A.3). Expressing these correlations in a simple parametrisation (i.e., a bivariate quadratic polynomial fitted using non-linear regression analysis) yields a significantly improved coefficient of determination ($r^2 > 0.95$) compared to the univariate correlation between grain size and distance from the crevasse apex ($r^2 < 0.2$) proposed in previous studies (Figure A.4). Despite this advancement, local divergences indicate that it is short of capturing the full complexity of sediment dispersal in crevasse splays.

Modelling

The process-based models show that initial sedimentation in crevasse splays occurs directly downstream of the crevasse incision, forming a relatively coarse-grained lobe (cf. Yuill et al., 2016). As the crevasse deepens and extends into a crevasse channel, sediment is deposited along its margins whilst the lobe at its terminus progrades further onto the floodplain. Once the lobe stabilises, it forces the crevasse channel to bifurcate around it, partially reworking its frontal part. The locus of deposition shifts to the termini of the second-order channels, repeating the sequence of events (Figure A.5). This shows that a crevasse splay is comprised of amalgamated lobes, overlain by crevasse levees and, ultimately, a drape of floodplain fines. This is in accordance with the conceptual model proposed by Mjøs et al. (1993).

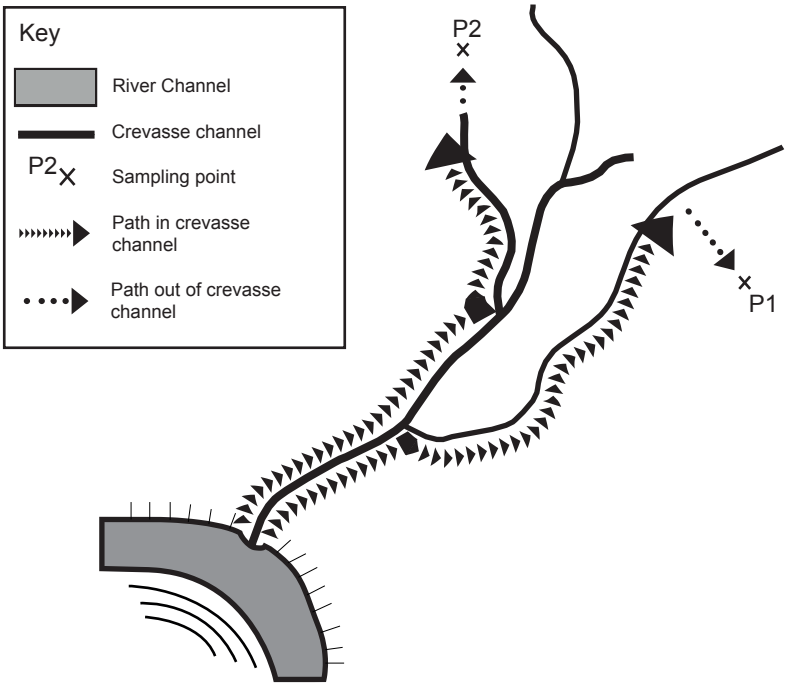

Figure A.3: Schematic representation of the inverse correlation of sediment size (of the coarser end member) to both the along-channel distance and the distance travelled outside these channels.

Scale-independent analogies

The sedimentary processes observed at the termini of splay channels are similar to the mechanisms proposed by, e.g., Edmonds and Slingerland (2007) and Fagherazzi et al. (2015) for river mouth bars. Likewise, crevasse splay levees are deposited following the same principles as those described by, e.g., Brierley et al. (1997) for fluvial levees. These similarities suggest that there are scale-independent analogies between fluvial processes.

Despite the often complex combination of factors controlling fluvial dynamics, individual grains may only experience hydraulic energy. The principles of flow competence apply regardless of system scale, governing the transport and deposition of sediment. The geometry of a crevasse splay can be described as a near-unconfined channelised lobe with a point-source apex. Apart from the spatial extent, this is analogous to both larger-scale fluvials fans (e.g., Nichols and Fisher, 2007) and fan deltas and small-scale lobes (similar to the experimental setups of, e.g., Whipple et al. (1998), Sheets et al. (2002) and Van Dijk et al. (2009)). As a result, sediment dispersal mechanisms at these different scales are fundamentally the same, other than their respective ratios.

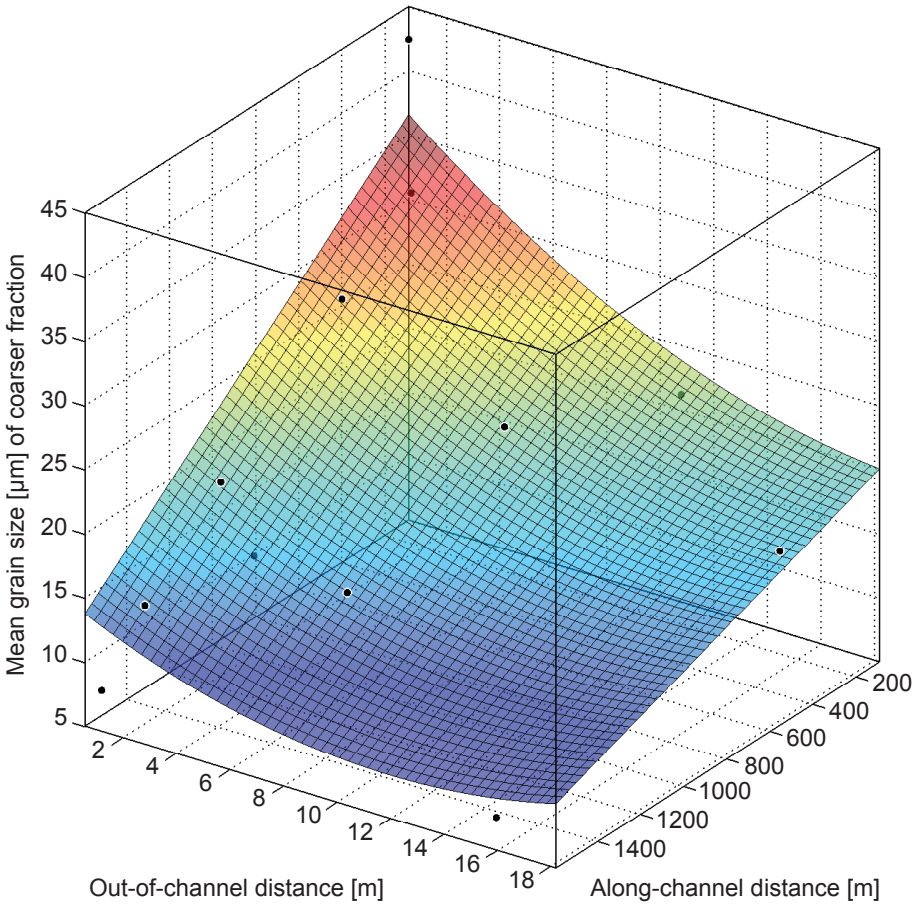

Figure A.4: Schematic diagram of along-channel distance and out-of-channel distance against the mean grain size (vertical), showing the correlation of the proposed parametrisation for sediment size. Black dots represent grain-size samples.

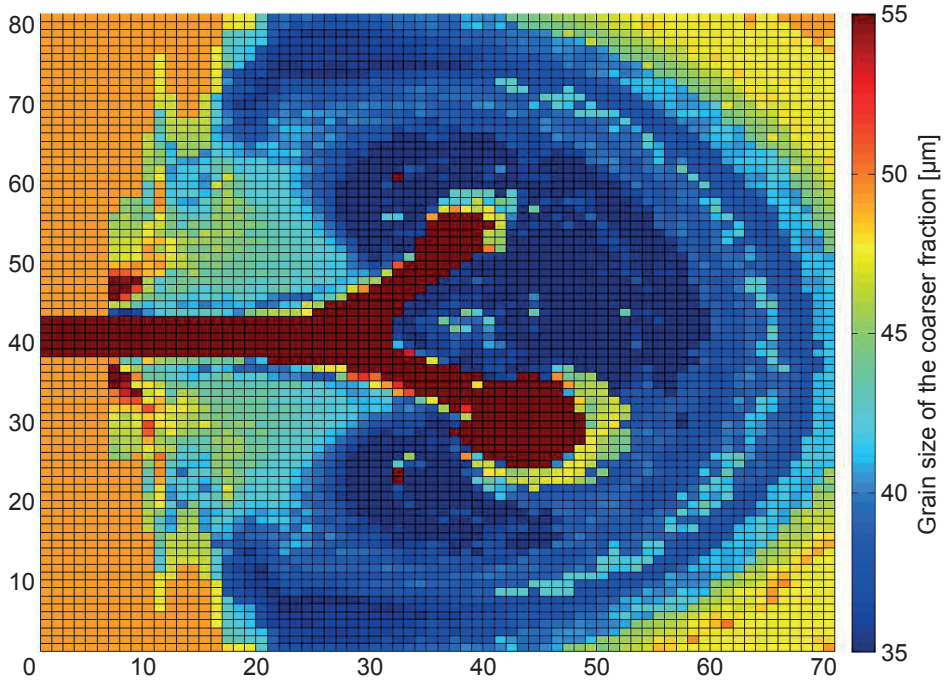

Figure A.5: Median sediment size of the coarser fraction at the end of eight flooding cycles in the process-based model. Note the accumulation of crevasse-channel levees and terminal mouth bars.

Conclusions

Crevasse splays comprise bimodal sediment distributions which are attributed to different modes of deposition: a coarser end-member is deposited as a function of flow competence, whereas a finer component only settles from suspension in standing water. As fluvial sedimentation is a function of flow competence, the dispersal of the coarser fraction can be described as a bivariate function of transport distance along-channel and outside the splay channels. Deposition of crevasse-splay sediment occurs as lobes at the termini and crevasse-splay levees alongside the crevasse channels, forming a complex amalgamation of sedimentary bodies. These fluvial processes are largely scale-independent and can be observed in both extensive channelised fans and small depositional lobes.

B

Subsurface reservoir properties and production potential

Part of the figures in this Appendix were originally published in the M.Sc. theses of H.T.W. Boerboom and C.G. Perdomo Figueroa.

Preliminary studies indicate that crevasse splays could qualify as (secondary) gas reservoirs, with porosities ranging from 5–15% and permeabilities on the order of 0.01–10 mD (core plug measurements; Figure B.1). These petrophysical properties are largely correlated with grain size (core description; Figure B.1), which means that the relatively coarser-grained crevasse channels could accommodate preferential flow paths throughout each splay (Appendix A and Figure B.2). Individual splays are interconnected through lateral amalgamation and vertical stacking in alluvial fans of up to several metres thick and kilometres wide (Chapter 3), and maintain connectivity with their parent channel (Chapter 4). Additional connectivity may result from compensational stacking, wherein consecutive alluvial ridges adjoin and onlap laterally, possibly creating sand-on-sand contact (Chapter 3). Incision of successive river paths into previously deposited fluvial sands also increases connectivity (Chapter 3).

Dynamic flow simulations in a static reservoir model based on this research (Figures B.3 and B.4) show a hierarchical organisation of streamlines analogous to a cardiovascular system, where the main rivers constitute 'arteries', crevasse channels form 'arterioles' and 'capillaries', and splay sediment represents permeable 'tissue' (Figure B.3). Random penetrations (i.e., hypothetically aimed at deeper-lying conventional reservoirs and subsequently reperforated in the modelled interval) each yield a ~10% chance of producing $\geq 10^5$ Sm^3 gas per day (assumed to approximate a minimum economic rate) for at least one year from a single interval of stacked crevasse splays (Figure B.5).

Crevasse splays in low net-to-gross fluvial intervals could help to constrain well-based (i.e., sub-seismic) reconstructions of their associated fluvial system, provided that individual river fans (up to several metres in thickness) can be reliably correlated between wells. Ongoing research with *Neptune Energy Netherlands* achieves a sufficiently high-resolution well correlation (3–5 m vertically) based on the identification of 'onset of flooding' surfaces in conventional gamma-ray logs (Figures B.6 and B.7). Within the correlated intervals, normalised well-log responses representative of sediment size (e.g., gamma ray and cross-correlated density-neutron logs) could be used to derive the relative position of each penetration within the system and estimate the associated river dimensions, based on the insights presented in this Thesis. This would ultimately help to constrain approximations of size, orientation, and connectivity of the fluvial fan, aiding exploration and productivity assessments.

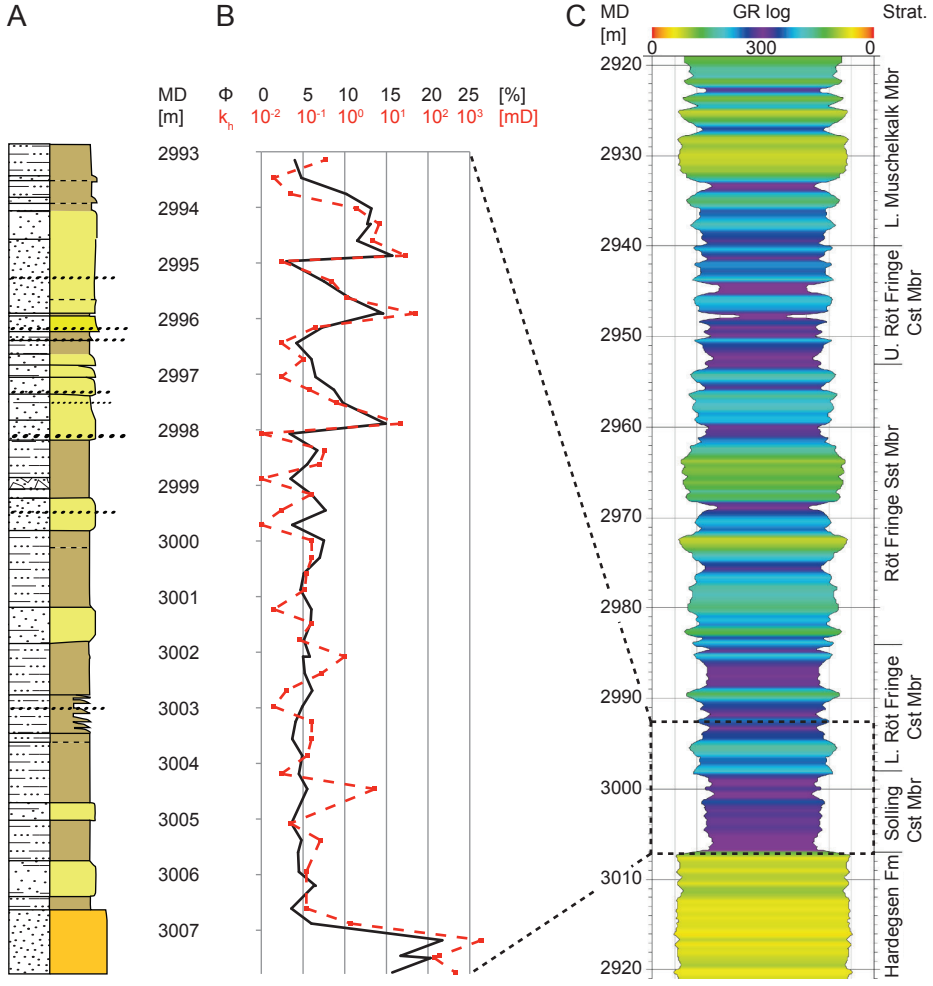

Figure B.1: Well Pernis West 1 (PRW-01) (a) Core description showing grain size and the occurrence of mud clasts. (b) Petrophysical data (i.e., porosity ϕ and horizontal permeability k_h from core plug analyses are plotted alongside the corresponding core interval. (c) Mirrored gamma-ray (GR) log showing the expression of low net-to-gross fluvial stratigraphy (Solling and Röt Formations) overlying the Lower Triassic Main Buntsandstein Subgroup in the West Netherlands Basin.

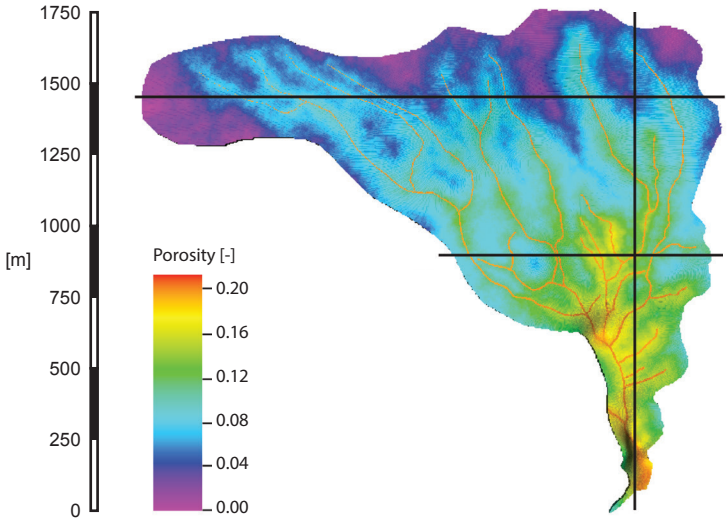

Figure B.2: Model of a crevasse splay in *Schlumberger Petrel* with porosity as a function of along-channel distance and distance from the crevasse channels based on the sediment dispersal patterns in Appendix A and a correlation between grain size and petrophysical properties from well data (e.g., Figure B.1).

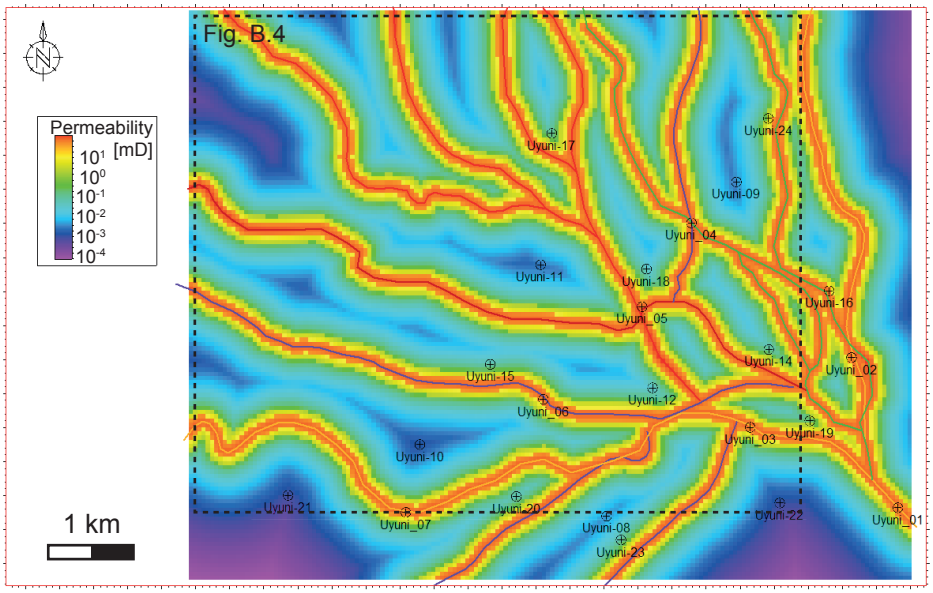

Figure B.3: Static reservoir model in *Schlumberger Petrel* showing permeability and random well locations. The model is based on the channel distribution in the Río Colorado fluvial system study and populated with petrophysical values from subsurface core plugs correlated with grain size (e.g., Figure B.1). Dashed line indicates outline of Figure B.4.

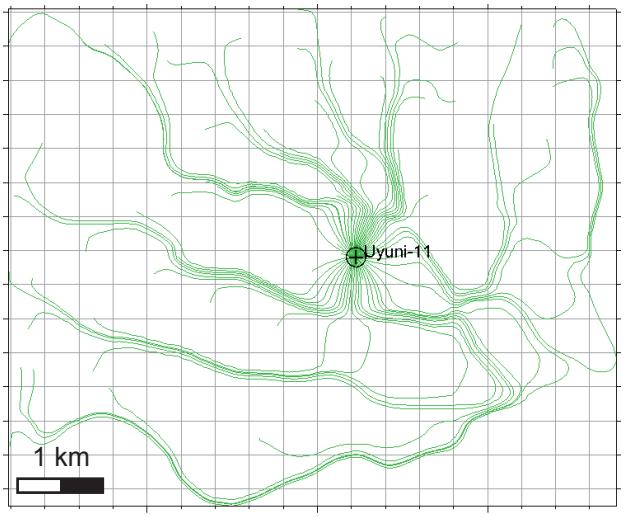

Figure B.4: Streamlines in *Schlumberger Eclipse* showing gas production through well Uyuni-11 (Figure B.3) assuming aquifer drive. Flow mainly follows the highly permeable channel facies, but also occurs in overbank deposits (i.e., crevasse splays).

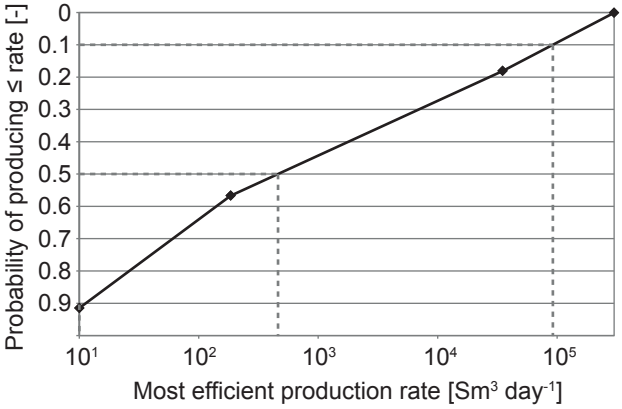

Figure B.5: Graph showing P90, P50, and P10 of most efficient production rates for randomly placed wells within the reservoir model (Figures B.3 and B.4). An economic rate is assumed to be $>10^5$ Nm^3 day^{-1}, although it should be noted that this is highly dependent on local parameters such as the operating expenditure (OPEX) of the production infrastructure.

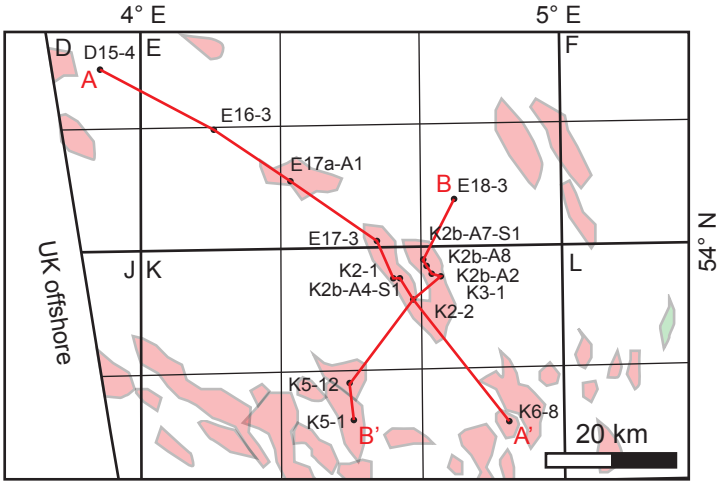

Figure B.6: Map view of (part of) the D, E, F, J, L, and L blocks offshore the Netherlands. Gas fields indicated in light red, oil fields indicated in light green. Wells are indicated in black dots. The correlation panels in Figure B.7 are indicated in red lines A-A' and B-B'.

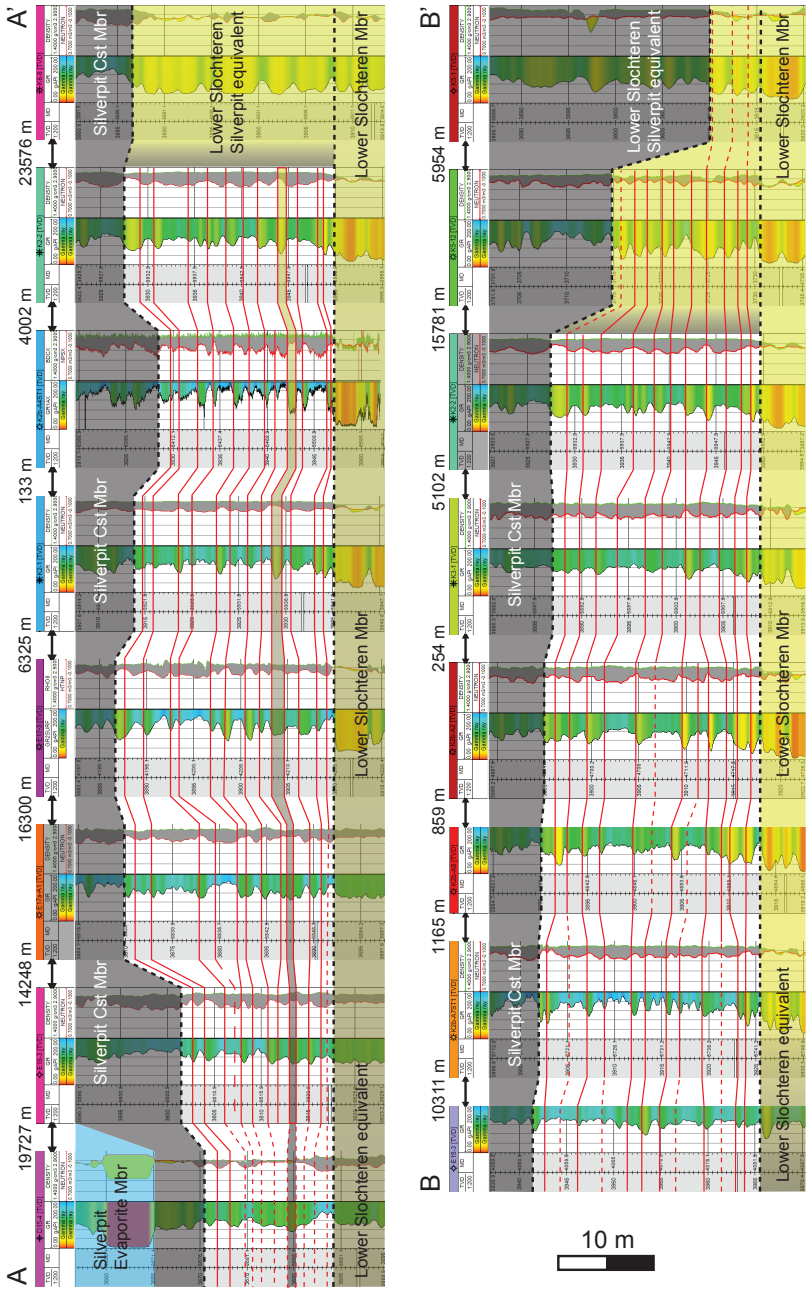

Figure B.7: Correlation panels A-A′ (A) and B-B′ (B) showing the gamma-ray and neutron porosity logs of wells (see Figure B.6) showing a south-to-north decrease in grain size and net-to-gross ratio (indicated in yellow-to-grey shading).

C

Vertical enhancement of a digital surface model

This is an Appendix to Chapter 3 of this Thesis.

An iterative approximation is used to resample a given DSM to the required vertical accuracy in exchange for a lower horizontal resolution. Input parameters include:

d = horizontal resolution of the original DSM [m]
$\sigma_{z,loc}$ = local vertical standard deviation of the original DSM, established using dGPS ground control points in the study area [m] (alternatively, a global vertical standard deviation σ_z may be used)
∇ = minimum surface gradient to be captured [-]
CI = confidence interval of elevation values in the resultant DEM [-] (from this follows the associated critical value (z-score) z^*)

Elevations in the original DSM are averaged within a search radius r, which is found by solving the system of equations below. The grid size D of the resultant DEM is defined such that the search area envelops the entire grid cell in order to avoid data loss (Figure C.1). Ideally, the search area would match the grid cell, but this was omitted for practical reasons.

$$MOE = \nabla \cdot D \tag{C.1}$$

$$N = \left(z^* \cdot \sigma_{z,loc}/MOE\right)^2 \tag{C.2}$$

$$r = \sqrt{N \cdot d^2/\pi} \tag{C.3}$$

$$D = 2 \cdot \sqrt{N \cdot r^2/2} \tag{C.4}$$

where:

MOE = margin of error [m]
D = horizontal resolution of the resultant DEM [m] (d may be used as an initial value)
N = amount of original DMS tiles to be sampled [-]
z^* = critical value (z-score) associated to the CI [-]
r = radius of the circle in which the original DSM elevation is averaged [-]

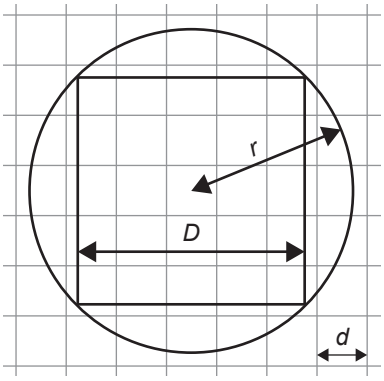

Figure C.1: Schematic representation of the original DSM grid (grey) with horizontal resolution d, the search area with radius r in which the original DSM is averaged, and the resultant DEM grid cell with resolution D.

References

Adams, P. N., Slingerland, R. L. and Smith, N. D. (2004). Variations in natural levee morphology in anastomosed channel flood plain complexes, *Geomorphology* **61**: 127–142.

Anderson, D. S. (2005). Architecture of crevasse splay and point-bar bodies of the nonmarine Iles Formation north of Rangely, Colorado: Implications for reservoir description, *The Mountain Geologist* **42**: 109–122.

Arenas, C. and Pardo, G. (1999). Latest Oligocene-Late Miocene lacustrine systems of the north-central part of the Ebro Basin (Spain): Sedimentary facies model and palaeogeographic synthesis, *Palaeogeography, Palaeoclimatology, Palaeoecology* **151**: 127–148.

Argollo, J. and Mourguiart, P. (2000). Late Quaternary climate history of the Bolivian Altiplano, *Quaternary International* **72**: 37–51.

Arndorfer, D. J. (1973). Discharge patterns in two crevasses on the Mississippi River delta, *Marine Geology* **15**: 269–287.

Baker, P. A., Rigsby, C. A., Seltzer, G. O., Fritz, S. C., Lowenstein, T. K., Bacher, N. P. and Veliz, C. (2001). Tropical climate changes at millennial and orbital timescales on the Bolivian Altiplano, *Nature* **409**: 698–701.

Bernal, C., Christophoul, F., Darrozes, J., Laraque, A., Bourrel, L., Soula, J. C., Guyot, J. L. and Baby, P. (2013). Crevassing and capture by floodplain drains as a cause of partial avulsion and anastomosis (lower Rio Pastaza, Peru), *Journal of South American Earth Sciences* **44**: 63–74.

Blott, S. J., Croft, D. J., Pye, K., Saye, S. E. and Wilson, H. E. (2004). Particle size analysis by laser diffraction, *in* K. Pye and D. J. Croft (eds), *Forensic Geoscience: Principles, Techniques and Applications*, Vol. 232, Geological Society of London Special Publication 232, pp. 63–73.

Bridge, J. S. (1984). Large-scale facies sequences in alluvial overbank environments, *Journal of Sedimentary Research* **54**: 583–588.

Bridge, J. S. (2003). *Rivers and floodplains: Forms, processes and sedimentary record*, Wiley-Blackwell.

Bridge, J. S. (2006). Fluvial facies models: recent developments, *in* H. W. Posamentier and R. G. Walker (eds), *Facies models revisited*, Society for Sedimentary Geology SEPM Special Publication 84, pp. 85–170.

Brierley, G. J., Ferguson, R. J. and Woolfe, K. J. (1997). What is a fluvial levee?, *Sedimentary Geology* **114**: 1–9.

Bristow, C. S., Skelly, R. L. and Ethridge, F. G. (1999). Crevasse splays from the rapidly aggrading, sand-bed, braided Niobrara River, Nebraska: Effect of base-level rise, *Sedimentology* **46**: 1029–1047.

Buehler, H. A., Weissmann, G. S., Scuderi, L. A. and Hartley, A. J. (2011). Spatial and temporal evolution of an avulsion on the Taquari River distributive fluvial system from satellite image analysis, *Journal of Sedimentary Research* **81**: 630–640.

Bull, W. B. (1979). Threshold of critical power in streams, *Geological Society of America Bulletin* **90**: 453–464.

Burns, C., Mountney, N. P., Hodgson, D. M. and Colombera, L. (2017). Anatomy and dimensions of fluvial crevasse-splay deposits: Examples from the Cretaceous Castlegate Sandstone and Neslen Formation, Utah, U.S.A., *Sedimentary Geology* **351**: 21–35.

Cahoon, D. R., White, D. A. and Lynch, J. C. (2011). Sediment infilling and wetland formation dynamics in an active crevasse splay of the Mississippi River delta, *Geomorphology* **131**: 57–68.

Chan, E. C. L. and Baciu, G. (2012). Differential GPS and assisted GPS, *in* E. C. L. Chan and G. Baciu (eds), *Introduction to Wireless Localization*, 1st edn, John Wiley & Sons Singapore Pte. Ltd., Singapore, pp. 157–184.

Chepstow-Lusty, A., Bush, M. B., Frogley, M. R., Baker, P. A., Fritz, S. C. and Aronson, J. (2005). Vegetation and climate change on the Bolivian Altiplano between 108,000 and 18,000 yr ago, *Quaternary Research* **63**: 90–98.

Colombera, L., Mountney, N. P. and Mccaffrey, W. D. (2013). A quantitative approach to fluvial facies models: Methods and example results, *Sedimentology* **60**: 1526–1558.

Dalman, R. A. F. and Weltje, G. J. (2008). Sub-grid parameterisation of fluvio-deltaic processes and architecture in a basin-scale stratigraphic model, *Computers and Geosciences* **34**: 1370–1380.

Dalman, R. A. F., Weltje, G. J. and Karamitopoulos, P. (2015). High-resolution sequence stratigraphy of fluvio–deltaic systems: Prospects of system-wide chronostratigraphic correlation, *Earth and Planetary Science Letters* **412**: 10–17.

De Ruig, M. J. and Hubbard, S. M. (2006). Seismic facies and reservoir characteristics of a deep-marine channel belt in the Molasse foreland basin, Puchkirchen, *AAPG Bulletin* **90**: 735–752.

Donselaar, M. E., Cuevas Gozalo, M. C. and Moyano, S. (2013). Avulsion processes at the terminus of low-gradient semi-arid fluvial systems: Lessons from the Río Colorado, Altiplano endorheic basin, Bolivia, *Sedimentary Geology* **283**: 1–14.

Donselaar, M. E., Cuevas Gozalo, M. C. and Wallinga, J. (2017). Avulsion history of a holocene semi-arid river System - Outcrop analogue for thin-bedded fluvial reservoirs in the Rotliegend Feather Edge, *79th EAGE Conference & Exhibition*, Paris, France, pp. 1–5.

Donselaar, M. E., Overeem, I., Reichwein, J. H. C. and Visser, C. A. (2011). Mapping of fluvial fairways in the Ten Boer Member, Southern Permian Basin, *in* J. Grötsch and R. Gaupp (eds), *The Permian Rotliegend of the Netherlands*, Society for Sedimentary Geology SEPM Special Publication 98, pp. 105–117.

Donselaar, M. E. and Schmidt, J. M. (2005). Integration of outcrop and borehole image logs for high-resolution facies interpretation: Example from a fluvial fan in the Ebro Basin, Spain, *Sedimentology* **52**: 1021–1042.

Edmonds, D. A. and Slingerland, R. L. (2007). Mechanics of river mouth bar formation: Implications for the morphodynamics of delta distributary networks, *Journal of Geophysical Research* **112**: 1–14.

Elger, K., Oncken, O. and Glodny, J. (2005). Plateau-style accumulation of deformation: Southern Altiplano, *Tectonics* **24**: TC4020.

Fagherazzi, S., Edmonds, D. A., Nardin, W., Leonardi, N., Canestrelli, A., Falcini, F., Jerolmack, D. J., Mariotti, G., Rowland, J. C. and Slingerland, R. L. (2015). Dynamics of river mouth deposits, *Reviews of Geophysics* **53**: 642–672.

Farrell, K. M. (2001). Geomorphology, facies architecture, and high-resolution, non-marine sequence stratigraphy in avulsion deposits, Cumberland Marshes, Saskatchewan, *Sedimentary Geology* **139**: 93–150.

Field, J. (2001). Channel avulsion on alluvial fans in southern Arizona, *Geomorphology* **37**: 93–104.

Fielding, C. R., Ashworth, P. J., Best, J. L., Prokocki, E. W. and Sambrook Smith, G. H. (2012). Tributary, distributary and other fluvial patterns: What really represents the norm in the continental rock record?, *Sedimentary Geology* **261-262**: 15–32.

Fielding, C. R. and Crane, R. C. (1987). An application of statistical modelling to the prediction of hydrocarbon recovery factors in fluvial reservoir sequences, *in* F. G. Ethridge, R. M. Flore and M. D. Harvey (eds), *Recent Developments in Fluvial Sedimentology*, Society for Sedimentary Geology SEPM Special Publication 39, pp. 321–327.

Fisher, J. A., Nichols, G. J. and Waltham, D. A. (2007). Unconfined flow deposits in distal sectors of fluvial distributary systems: Examples from the Miocene Luna and Huesca Systems, northern Spain, *Sedimentary Geology* **195**: 55–73.

Ford, G. L. and Pyles, D. R. (2014). A hierarchical approach for evaluating fluvial systems: Architectural analysis and sequential evolution of the high net-sand content, middle Wasatch Formation, Uinta Basin, Utah, *AAPG Bulletin* **98**: 1273–1304.

Fornari, M., Risacher, F. and Féraud, G. (2001). Dating of paleolakes in the central Altiplano of Bolivia, *Palaeogeography, Palaeoclimatology, Palaeoecology* **172**: 269–282.

Friend, P. F., Hirst, J. P. P. and Nichols, G. J. (1986). Sandstone-body structure and river process in the Ebro Basin of Aragon, Spain, *Cuadernos Geología Ibérica* **10**: 9–30.

Friend, P. F., Slater, M. J. and Williams, R. C. (1979). Vertical and lateral building of river sandstone bodies, Ebro Basin, Spain, *Journal of the Geological Society* **136**: 39–46.

Geluk, M. (2007a). Permian, *in* T. E. Wong, D. A. J. Batjes and J. de Jager (eds), *Geology of the Netherlands*, Royal Netherlands Academy of Arts and Sciences, Amsterdam, The Netherlands, pp. 63–83.

Geluk, M. (2007b). Triassic, *in* T. E. Wong, D. A. J. Batjes and J. de Jager (eds), *Geology of the Netherlands*, Royal Netherlands Academy of Arts and Sciences, Amsterdam, The Netherlands, pp. 85–106.

Ghazi, S. and Mountney, N. P. (2009). Facies and architectural element analysis of a meandering fluvial succession: The Permian Warchha Sandstone, Salt Range, Pakistan, *Sedimentary Geology* **221**: 99–126.

Gulliford, A. R., Flint, S. S. and Hodgson, D. M. (2014). Testing applicability of models of distributive fluvial systems or trunk rivers in ephemeral systems: Reconstructing 3-D fluvial architecture in the Beaufort Group, South Africa, *Journal of Sedimentary Research* **84**: 1147–1169.

Hajek, E. A. and Edmonds, D. A. (2014). Is river avulsion style controlled by floodplain morphodynamics?, *Geology* **42**: 199–202.

Hajek, E. A. and Wolinsky, M. A. (2012). Simplified process modeling of river avulsion and alluvial architecture: Connecting models and field data, *Sedimentary Geology* **257-260**: 1–30.

Hamer, J. M. M., Sheldon, N. D., Nichols, G. J. and Collinson, M. E. (2007). Late Oligocene – Early Miocene paleosols of distal fluvial systems , Ebro Basin , Spain, *Palaeogeography, Palaeoclimatology, Palaeoecology* **247**: 220–235.

Hampton, B. A. and Horton, B. K. (2007). Sheetflow fluvial processes in a rapidly subsiding basin, Altiplano plateau, Bolivia, *Sedimentology* **54**: 1121–1147.

Hirst, J. P. P. (1991). Variations in Alluvial Architecture Across the Oligo-Miocene Huesca Fluvial System, Ebro Basin, Spain, *in* A. D. Miall and N. Tyler (eds), *The three-dimensional facies architecture of terrigenous clastic sediments and its implications for hydrocarbon discovery and recovery*, Society for Sedimentary Geology SEPM Concepts in Sedimentology and Paleontology 3, pp. 111–121.

Hornung, J. and Aigner, T. (1999). Reservoir and aquifer characterization of fluvial architectural elements: Stubensandstein, Upper Triassic, southwest Germany, *Sedimentary Geology* **129**: 215–280.

Horton, B. K., Hampton, B. A. and Waanders, G. L. (2001). Paleogene synorogenic sedimentation in the Altiplano plateau and implications for initial mountain building in the central Andes, *GSA Bulletin* **113**: 1387–1400.

Jerolmack, D. J. and Mohrig, D. (2007). Conditions for branching in depositional rives, *Geology* **35**: 463–466.

Jerolmack, D. J. and Paola, C. (2007). Complexity in a cellular model of river avulsion, *Geomorphology* **91**: 259–270.

Joeckel, R. M., Tucker, S. T. and McMullin, J. D. (2016). Morphosedimentary features from a major flood on a small, lower-sinuosity, single-thread river: The unknown quantity of overbank deposition, historical-change context, and comparisons with a multichannel river, *Sedimentary Geology* **343**: 18–37.

Jones, H. L. and Hajek, E. A. (2007). Characterizing avulsion stratigraphy in ancient alluvial deposits, *Sedimentary Geology* **202**: 124–137.

Jones, L. S. and Schumm, S. A. (1999). Causes of avulsion: an overview, *in* N. D. Smith and J. Rogers (eds), *Fluvial Sedimentology VI*, Blackwell Science Ltd., Oxford, United Kingdom, pp. 171–178.

Jordan, D. W. and Pryor, W. A. (1992). Hierarchical levels of heterogeneity in a Mississippi River meander belt and application to reservoir systems, *AAPG Bulletin* **76**: 1601–1624.

Karamitopoulos, P., Weltje, G. J. and Dalman, R. A. F. (2014). Allogenic controls on autogenic variability in fluvio-deltaic systems: inferences from analysis of synthetic stratigraphy, *Basin Research* **26**: 767–779.

Keeton, G. I., Pranter, M. J., Cole, R. D. and Gustason, E. R. (2015). Stratigraphic architecture of fluvial deposits from borehole images, spectral-gamma-ray response, and outcrop analogs, Piceance Basin, Colorado, *AAPG Bulletin* **99**: 1929–1956.

Keller, E. A. and Swanson, F. J. (1979). Effects of large organic material on channel form and fluvial processes, *Earth Surface Processes and Landforms* **4**: 361–380.

Kleinhans, M. G., Ferguson, R. J., Lane, S. N. and Hardy, R. J. (2013). Splitting rivers at their seams: Bifurcations and avulsion, *Earth Surface Processes and Landforms* **38**: 47–61.

Kleinhans, M. G., Jagers, H. R. A., Mosselman, E. and Sloff, C. J. (2008). Bifurcation dynamics and avulsion duration in meandering rivers by one-dimensional and three-dimensional models, *Water Resources Research* **44**: 1–31.

Koss, J. E., Ethridge, F. G. and Schumm, S. A. (1994). An experimental study of the effects of base-level change on fluvial, coastal plain and shelf systems, *Journal of Sedimentary Research* **B64**: 90–98.

Kraus, M. J. (2002). Basin-scale changes in floodplain paleosols: Implications for interpreting alluvial architecture, *Journal of Sedimentary Research* **72**: 500–509.

Larue, D. K. and Hovadik, J. (2006). Connectivity of channelized reservoirs: a modelling approach, *Petroleum Geoscience* **12**: 291–308.

Leeder, M. R. (1975). Pedogenic carbonates and flood sediment accretion rates: a quantative model for alluvial arid-zone lithofacies, *Geological Magazine* **112**: 257–270.

Lesser, G. R., Roelvink, J. A., Van Kester, J. A. T. M. and Stelling, G. S. (2004). Development and validation of a three-dimensional morphological model, *Coastal Engineering* **51**: 883–915.

Li, J. and Bristow, C. S. (2015). Crevasse splay morphodynamics in a dryland river terminus: Río Colorado in Salar de Uyuni Bolivia, *Quaternary International* **377**: 71–82.

Li, J., Donselaar, M. E., Hosseini Aria, S. E., Koenders, R. and Oyen, A. M. (2014). Landsat imagery-based visualization of the geomorphological development at the terminus of a dryland river system, *Quaternary International* **352**: 100–110.

Li, J., Luthi, S. M., Donselaar, M. E., Weltje, G. J., Prins, M. A. and Bloemsma, M. R. (2015). An ephemeral meandering river system: Sediment dispersal processes in the Río Colorado, Southern Altiplano Plateau, Bolivia, *Zeitschrift für Geomorphologie* **59**: 301–317.

Li, J., Menenti, M., Mousivand, A. and Luthi, S. M. (2014). Non-vegetated playa morphodynamics using multi-temporal landsat imagery in a semi-arid endorheic basin: Salar de Uyuni, Bolivia, *Remote Sensing* **6**: 10131–10151.

Mackin, J. H. (1948). Concept of the graded river, *Geological Society of America Bulletin* **59**: 463–512.

McKie, T. (2011a). A comparison of modern dryland depositional systems with the Rotliegend group in the Netherlands, *in* J. Grötsch and R. Gaupp (eds), *The Permian Rotliegend of the Netherlands*, Society for Sedimentary Geology SEPM Special Publication 98, pp. 89–103.

McKie, T. (2011b). Architecture and behavior of dryland fluvial reservoirs, Triassic Skagerrak Formation, Central North Sea, *in* S. K. Davidson, S. Leleu and C. P. North (eds), *From River to Rock Record: The Preservation of Fluvial Sediments and Their Subsequent Interpretation*, Society for Sedimentary Geology SEPM Special Publication 97, pp. 189–214.

McMahon, T. A., Finlayson, B. L., Haines, A. and Srikanthan, R. (1987). Runoff variability: a global perspective, *in* S. I. Solomon, M. Beran and W. Hogg (eds), *The influence of climate change and climate variability on the hydrologic regime and water resources*, International Association of Hydrological Sciences Publication 168, pp. 3–12.

Meselhe, E. A., Georgiou, I., Allison, M. A. and McCorquodale, J. A. (2012). Numerical modeling of hydrodynamics and sediment transport in lower Mississippi at a proposed delta building diversion, *Journal of Hydrology* **472-473**: 340–354.

Miall, A. D. (2014). *Fluvial depositional systems*, Springer International Publishing.

Millard, C., Hajek, E. A. and Edmonds, D. A. (2017). Evaluating controls on crevasse-splay size: Implications for floodplain-basin filling, *Journal of Sedimentary Research* **87**: 722–739.

Miller, M. C., McCave, I. N. and Komar, P. D. (1977). Threshold of sediment motion under uinidirectional currents, *Sedimentology* **24**: 507–527.

Mjøs, R., Walderhaug, O. and Prestholm, E. (1993). Crevasse splay sandstone geometries in the Middle Jurassic Ravenscar Group of Yorkshire, UK, *in* M. Marzo and C. Puigdefabregas (eds), *Alluvial Sedimentation*, International Association of Sedimentologists Special Publication 17, pp. 167–184.

Mohrig, D., Heller, P. L., Paola, C. and Lyons, W. J. (2000). Interpreting avulsion process from ancient alluvial sequences: Guadalope-Mantarranya system (northern Spain) and Wasatch Formation (western Colorado), *Geological Society of America Bulletin* **112**: 1787–1803.

Nicholas, A. P. and Walling, D. E. (1997). Modelling flood hydraulics and overbank deposition on river floodplains.

Nichols, G. J. and Fisher, J. A. (2007). Processes, facies and architecture of fluvial distributary system deposits, *Sedimentary Geology* **195**: 75–90.

Nienhuis, J. H., Törnqvist, T. E. and Esposito, C. R. (2018). Crevasse splays versus avulsions: a recipe for land building with levee breaches, *Geophysical Research Letters* **45**: 4058–4067.

North, C. P. and Warwick, G. L. (2007). Fluvial fans: myths, misconceptions, and the end of the terminal-fan model, *Journal of Sedimentary Research* **77**: 693–701.

O'Brien, P. E. and Wells, A. T. (1986). A small, alluvial crevasse splay, *Journal of Sedimentary Research* **56**: 876–879.

Parkinson, B. W. and Enge, P. K. (1996). Differential GPS, *in* B. W. Parkinson and J. J. Spilker Jr. (eds), *Global Positioning System: Theory and Applications 2*, American Institute of Aeronautics and Astronautics, Reston (VA), USA, pp. 3–50.

Passey, Q. R., Dahlberg, K. E., Sullivan, K. B., Yin, H., Xiao, Y. H. and Brackett, R. A. (2004). A systematic approach to evaluate hydrocarbons in thinly bedded reservoirs, *SPWLA 45th Annual Logging Symposium*, Noordwijk, The Netherlands, pp. 1–12.

Pérez-Arlucea, M. and Smith, N. D. (1999). Depositional patterns following the 1870s avulsion of the Saskatchewan River (Cumberland Marshes, Saskatchewan, Canada), *Journal of Sedimentary Research* **69**: 62–73.

Placzek, C., Quade, J. and Patchett, P. J. (2006). Geochronology and stratigraphy of late Pleistocene lake cycles on the southern Bolivian Altiplano: Implications for causes of tropical climate change, *GSA Bulletin* **118**: 515–532.

Platt, N. H. and Keller, B. (1992). Distal alluvial deposits in a foreland basin setting - the Lower Freshwater Molasse (Lower Miocene), Switzerland: sedimentology, architecture and palaeosols, *Sedimentology* **39**: 545–565.

Pranter, M. J., Cole, R. D., Panjaitan, H. and Sommer, N. K. (2009). Sandstone-body dimensions in a lower coastal-plain depositional setting: Lower Williams Fork Formation, Coal Canyon, Piceance Basin, Colorado, *AAPG Bulletin* **93**: 1379–1401.

Pranter, M. J., Vargas, M. F. and Davis, T. L. (2008). Characterization and 3D reservoir modelling of fluvial sandstones of the Williams Fork Formation, Rulison Field, Piceance Basin, Colorado, USA, *Journal of Geophysics and Engineering* **5**: 158–172.

Retallack, G. J. (1991). Untangling the effects of burial alteration and ancient soil formation, *Annual Review of Earth and Planetary Sciences* **19**: 183–206.

Rigsby, C. A., Bradbury, J. P., Baker, P. A., Rollins, S. M. and Warren, M. R. (2005). Late Quaternary palaeolakes, rivers, and wetlands on the Bolivian Altiplano and their palaeoclimatic implications, *Journal of Quaternary Science* **20**: 671–691.

Risacher, F. and Fritz, B. (2009). Origin of salts and brine evolution of Bolivian and Chilean salars, *Aquatic Geochemistry* **15**: 123–157.

Roberts, H. H. (1997). Dynamic changes of the Holocene Mississippi River delta plain: the delta cycle, *Journal of Coastal Research* **13**: 605–627.

Rust, B. R. and Nanson, G. C. (1989). Bedload transport of mud as pedogenic aggregates in modern and ancient rivers, *Sedimentology* **36**: 291–306.

Sahoo, H., Gani, M. R., Hampson, G. J., Gani, N. D. and Ranson, A. (2016). Facies- to sandbody-scale heterogeneity in a tight-gas fluvial reservoir analog: Blackhawk Formation, Wasatch Plateau, Utah, USA, *Marine and Petroleum Geology* **78**: 48–69.

Santillan, J. R. and Makinano-Santillan, M. (2016). Vertical accuracy assessment of 30-M resolution ALOS, ASTER, and SRTM global DEMS over Northeastern Mindanao, Philippines, *International Archives of the Photogrammetry, Remote Sensing and Spatial Information Sciences - ISPRS Archives* **41**: 149–156.

Schumm, S. A. (1993). River response to baselevel change: Implications for sequence stratigraphy, *Journal of Geology* **101**: 279–294.

Servant, M., Fournier, M., Argollo, J., Servant-Vildary, S., Sylvestre, F., Wirrmann, D. and Ybert, J. P. (1995). La dernière transition glaciaire/interglaciaire des Andes tropicales sud (Bolivie) d'après l'Étude des variations des niveaux lacustres et des fluctiations glaciaires, *Comptes Rendus de l'Académie des Sciences, Paris, Séries II* **320**: 729–736.

Sheets, B. A., Hickson, T. A. and Paola, C. (2002). Assembling the stratigraphic record: Depositional patterns and time-scales in an experimental alluvial basin, *Basin Research* **14**: 287–301.

Shen, Z., Törnqvist, T. E., Mauz, B., Chamberlain, E. L., Nijhuis, A. G. and Sandoval, L. (2015). Episodic overbank deposition as a dominant mechanism of floodplain and delta-plain aggradation, *Geology* **43**: 875–878.

Simon, A. and Collinson, A. J. C. (2002). Quantifying the mechanical and hydrological effects of riparian vegetation on streambank stability, *Earth Surface Processes and Landforms* **27**: 527–546.

Slingerland, R. L. and Smith, N. D. (2004). River avulsions and their deposits, *Annual Review of Earth and Planetary Sciences* **32**: 257–285.

Smith, J. S., Chandler, J. and Rose, J. (2009). High spatial resolution data acquisition for the geosciences: kite aerial photography, *Earth Surface Processes and Landforms* **34**: 155–161.

Smith, N. D., Cross, T. A., Dufficy, J. P. and Clough, S. R. (1989). Anatomy of an avulsion, *Sedimentology* **36**: 1–23.

Smith, N. D. and Pérez-Arlucea, M. (1994). Fine-grained splay deposition in the avulsion belt of the lower Saskatchewan River, Canada, *Journal of Sedimentary Research* **64**: 159–168.

Smith, N. D., Slingerland, R. L., Pérez-Arlucea, M. and Morozova, G. S. (1998). The 1870s avulsion of the Saskatchewan River, *Canadian Journal of Earth Sciences* **35**: 453–466.

Straub, K. M., Paola, C., Mohrig, D. and Wolinsky, M. A. (2009). Compensational stacking of channelized sedimentary deposits, *Journal of Sedimentary Research* **79**: 673–688.

Sun, D., Bloemendal, J., Rea, D. K., Vandenberghe, J., Jiang, F., An, Z. and Su, R. (2002). Grain-size distribution function of polymodal sediments in hydraulic and aeolian environments, and numerical partitioning of the sedimentary components, *Sedimentary Geology* **152**: 263–277.

Sylvestre, F., Servant, M., Servant-Vildary, S., Causse, C. and Fournier, M. (1999). Lake-level chronology on the Southern Bolivian Altiplano (18°–23° S) during Late-Glacial Time and the Early Holocene, *Quaternary Research* **51**: 54–66.

Tadono, T., Nagai, H., Ishida, H., Oda, F., Naito, S., Minakawa, K. and Iwamoto, H. (2016). Generation of the 30 M-MESH global digital surface model by ALOS PRISM, *International archives of the photogrammetry, remote sensing and spatial information sciences XLI-B4*, Prague, Czech Republic, pp. 157–162.

Tooth, S. (2000). Process, form and change in dryland rivers: a review of recent research, *Earth-Science Reviews* **51**: 67–107.

Tooth, S. (2005). Splay formation along the lower reaches of ephemeral rivers on the northern plains of arid Central Australia, *Journal of Sedimentary Research* **75**: 636–649.

Törnqvist, T. E. and Bridge, J. S. (2002). Spatial variation of overbank aggradation rate and its influence on avulsion frequency, *Sedimentology* **49**: 891–905.

Van Dijk, M., Postma, G. and Kleinhans, M. G. (2009). Autocyclic behaviour of fan deltas: An analogue experimental study, *Sedimentology* **56**: 1569–1589.

Van Gelder, A., Van den Berg, J. H., Cheng, G. and Xue, C. (1994). Overbank and channelfill deposits of the modern Yellow River delta, *Sedimentary Geology* **90**: 293–305.

Van Toorenenburg, K. A., Donselaar, M. E., Noordijk, N. A. and Weltje, G. J. (2016). On the origin of crevasse-splay amalgamation in the Huesca fluvial fan (Ebro Basin, Spain): Implications for connectivity in low net-to-gross fluvial deposits, *Sedimentary Geology* **343**: 156–164.

Van Toorenenburg, K. A., Donselaar, M. E. and Weltje, G. J. (2018). The life cycle of crevasse splays as a key mechanism in the aggradation of alluvial ridges and river avulsion, *Earth Surface Processes and Landforms* **43**: 2409–2420.

Weissmann, G. S., Hartley, A. J., Nichols, G. J., Scuderi, L. A., Olson, M., Buehler, H. and Banteah, R. (2010). Fluvial form in modern continental sedimentary basins: Distributive fluvial systems, *Geology* **38**: 39–42.

Weltje, G. J. and Prins, M. A. (2007). Genetically meaningful decomposition of grain-size distributions, *Sedimentary Geology* **202**: 409–424.

Wentworth, C. K. (1922). A scale of grade and class terms for clastic sediments, *Journal of Geology* **30**: 377–392.

Whipple, K. X., Parker, G., Paola, C. and Mohrig, D. (1998). Channel dynamics, sediment transport, and the slope of alluvial fans: experimental study, *The Journal of Geology* **106**: 677–694.

Williams, B. P. J. and McKie, T. (2009). Preface: Triassic basins of the Central and North Atlantic Borderlands: models for exploration, *Geological Journal* **44**: 627–630.

Wright, P. V. and Marriott, S. B. (1993). The sequence stratigraphy of fluvial depositional systems: the role of floodplain sediment storage, *Sedimentary Geology* **86**: 203–210.

Yuill, B. T., Khadka, A. K., Pereira, J., Allison, M. A. and Meselhe, E. A. (2016). Morphodynamics of the erosional phase of crevasse-splay evolution and implications for river sediment diversion function, *Geomorphology* **259**: 12–29.

Zwoliński, Z. (1992). Sedimentology and geomorphology of overbank flows on meandering river floodplains, *Geomorphology* **4**: 367–379.

Acknowledgements

If it were not for Rick and Gert Jan, I would have never even contemplated pursuing a Ph.D. degree. Rick, throughout the years we have shared countless meals, travelled around the globe, and had many constructive discussions, not limited to sedimentology alone. I hugely appreciate your mentorship, companionship, and, above all, your trust. Gert Jan, you dazzled me with numerous ideas, then taught me how to properly write, and were ready with advice whenever I needed it. You made as good team of mentors as I could wish for, with a distinctly social angle to supervision. Many thanks for talking me into this.

This study was funded by *ENGIE E&P NL* (now *Neptune Energy Netherlands*) and *Energiebeheer Nederland* (EBN), following a project start within *TKI Gas* as part of the *Topsector Energie* programme. The project greatly profited from the continual involvement of Leo van Borren, Jan Lutgert, Mat de Jong, and Bastiaan Jaarsma, most notably in joining a sponsor excursion to our fieldwork area in Spain. I hope to continue our pleasant collaboration in the future, working towards the practical applicability of this work. Additional support to individual project contributions was awarded several times by the *Molengraaff Foundation* and the *University Fund Delft*. My employer, the *TNO Advisory Group for Economic Affairs* (TNO-AGE), kindly contributed to printing the Thesis books and allowed me time to write up.

The work presented here has significantly benefitted from several additional contributions. The *Nederlandse Aardoliemaatschappij* (NAM) provided full access to its core-viewing facility in Assen through the involvement of Frank Pardoel, Clemens Visser, Richard Porter, and Jan Tillema. Hans Reichwein (*Shell International*) and Clemens have also been very helpful in finding out more about reperforations of gas-charged low net-to-gross fluvial stratigraphy. At the *Politecnico di Torino*, Costanzo Peter, Giulia Codegone, and Francesco Marzano greatly assisted in building static reservoir models. The *Free University* (VU) of Amsterdam facilitated grain-size analyses under the auspices of Maarten Prins and Martine Hagen. Joep Storms and Helena van der Vegt co-supervised the M.Sc. project of Axel, involving forward modelling in *Delft3D*. Hans van der Marel was instrumental in his support for the acquisition and processing of dGPS data, which more than proved its worth. Pierre Lesage and Hans Elbers gave me experience-based advice on a suitable setup for kite-aerial photography on the Bolivian Altiplano. Guido Hoetz gave me tangible recommendations for the future application of this work. On a scholarly level, I much appreciated the constructive feedback and reviews of fellow researchers, such as Gary Nichols, Cathryn Amos, Colin North, and Tom McKie. I also value the time and effort put into assessing this Thesis and forming part of the doctoral committee by Christopher Fielding, Alessando Amorosi, Elizabeth Hajek, Rory Dalman, Allard Martinius, Giovanni Bertotti, and, naturally, my Ph.D. advisors.

It would have been impossible to explore so many leads and integrate them into this study without the contributions of an army of students. Niels and Lisanne, you got to it even before I did. Niels, I very much enjoyed your pleasant company (and remarkable competence) on no less than four fieldworks together. Lisanne, the great amount of work you did is second only to your dancing skills in *el Tubito*. Marloes, we made a great team together, even if we never did get that DJ to play *Haus am See*. "Here's looking at you, kid…". Shelley, I am still amazed by your independence in research. No surprise that you ended up pursuing a Ph.D. degree yourself. Eren, despite an early ending, your efforts have most certainly not been in vain. You'll get there. Axel and Thore, I am still occasionally startled awake at night by flashbacks to your truly appalling level of humour. Axel, I thoroughly enjoyed your sharp mind, even if it was slightly intimidating at times. Thore, your focus in work is rarely matched and something to be jealous of. *Ella elle l'a*, i.e., an eye for wild orchids whilst navigating the rugged fieldwork area (and outwitting me for carrying the dGPS rover). Thank you for dragging me along. Christian, thank you for the good times in dusty Uyuni and helping me bring everything together. Nos vemos luego. Rosmar and Carlos, many thanks for your efforts to help out us gringos in Bolivia.

As a final through, I would like to thank those who have had an indirect (but perhaps equally important, if not more) impact on my personal development as a doctoral student. Of course, our academic staff, insofar not mentioned yet: Jan Kees, Maaike, Hemmo, Karl-Heinz, David, Auke, Nico, Salle, and Gerhard. Thank you for the occasional chats and especially for involving me in teaching. Stefan, many thanks for the way in which you fulfilled your advisory role in the initial stages of the research. Everybody knows (or should know) that the academic world comes to a grinding halt without support staff. Lydia, Marlijn, Margot, Marijke, Marja, Myrthe, Hannie, Asha, and last, but not least, Ralf, I hugely appreciate your help and friendliness over these last few years. Last, but not least, I would like to thank my friends, family, and close colleagues in the sections of Applied Geology, Applied Geophysics & Petrophysics, and Petroleum Engineering, and the department of Remote Sensing & Geoscience. Kevin and Rahul, this baby face will now finally become a baby doctor. Many thanks for your lasting friendship, counselling (both solicited and unsolicited), and dressing up as penguins for my defence. Rémi, Helena, and Cees, I regard you as friends, rather than colleagues. Thank you for the ten-to-ten coffee breaks, toy wars, and dinner parties. Not to forget Sid, Santosh, Quinten, Runhai, Navid, Rahul, Stephan, Youwei, Martha, Thaís, Rodolfo, Andrea, Menno, and Liang; one small gang of indomitable geoscientists holding out against the army of engineers in Delft. I am indebted to my parents, Theo and Birgit, and brothers, Roel and Thijs, whom I can always count on. And finally: Lisanne, thank you for your endless patience and loving support, especially in this last, hectic year. I am sure you will remind me of it when it is your turn to wrap up.

Curriculum Vitæ

Koen Arnoldus VAN TOORENENBURG

22-08-1988 Born in Leiden, The Netherlands.

Education

2000–2006	Grammar School Rijnlands Lyceum Oegstgeest
2004–2006	Pre-University College Leiden University
2006–2009	B.Sc. Applied Earth Sciences Delft University of Technology
2009–2012	M.Sc. Petroleum Engineering & Geosciences Delft University of Technology
2013–2018	Ph.D. Applied Geology Delft University of Technology

List of Publications

Journal publications

2. **Van Toorenenburg, K. A.**, Donselaar, M. E., Weltje, G. J. (2018). The life cycle of crevasse splays as a key mechanism in the aggradation of alluvial ridges and river avulsion, *Earth Surface Processes and Landforms* **43**: 2409–2420.

1. **Van Toorenenburg, K. A.**, Donselaar, M. E., Noordijk, N. A., Weltje, G. J. (2016). On the origin of crevasse-splay amalgamation in the Huesca fluvial fan (Ebro Basin, Spain): Implications for connectivity in low net-to-gross fluvial deposits, *Sedimentary Geology* **343**: 156–164.

Conference proceedings

18. Donselaar, M. E., Cuevas Gozalo, M. C., **Van Toorenenburg, K. A.**, Wallinga, J. (2018). Self-organizing avulsions in an endorheic dryland river system, *20th International Sedimentological Congress*, Quebec City, Canada, pp. 1–1.

17. Donselaar, M. E., Cuevas Gozalo, M.C., **Van Toorenenburg, K. A.**, Wallinga, J. (2017). OSL-based absolute age dating of alluvial ridge formation and associated river avulsion in a Holocene low-gradient dryland-river system: Altiplano Basin, Bolivia, *33rd International Meeting of Sedimentology*, Toulouse, France, pp. 1–1.

16. Donselaar, M. E., De Jong, M. G. G., Boerboom, H. T. W., **Van Toorenenburg, K. A.**, Weltje, G. J., Van Borren, L. (2017). Reservoir potential of thin-bedded fluvial terminal-splay sandstone at the interface with the endorheic Silverpit lake, Rotliegend, offshore The Netherlands, *11th International Conference on Fluvial Sedimentology*, Calgary, Canada, pp. 1–1.

15. Donselaar, M. E., Cuevas Gozalo, M. C., **Van Toorenenburg, K. A.**, Wallinga, J. (2017). Timing and processes of alluvial-ridge network formation in an endorheic, semi-arid river system: Holocene Río Colorado (Altiplano Basin, Bolivia), *11th International Conference on Fluvial Sedimentology*, Calgary, Canada, pp. 1–1.

14. De Jong, M. G. G., Donselaar, M. E., Boerboom, H. T. W., **Van Toorenenburg, K. A.**, Weltje, G. J., Van Borren, L. (2017). High-Resolution Reservoir Architecture Modelling of Thin-bedded Fluvial Terminal-splay Sandstone in the Rotliegend Feather-edge Area, *79th EAGE Conference and Exhibition 2017*, Paris, France, pp. 1–5.

13. **Van Toorenenburg, K. A.**, Donselaar, M. E., Weltje, G. J. (2017). The potential of fluvial crevasse splays as (secondary) reservoirs, *AAPG Annual Convention and Exhibition 2017*, Houston, USA, pp. 1–1.

12. **Van Toorenenburg, K. A.**, Donselaar, M. E., Weltje, G. J. (2016). The role of floodplain aggradation in building low-gradient dryland river stratigraphy, *AAPG Annual Convention and Exhibition 2016*, Calgary, Canada, pp. 1–1.

11. Sandén, A. B., Boerboom, H. T. W., Donselaar, M. E., Storms, J. E. A., **Van Toorenenburg, K. A.**, Van der Vegt, H., Weltje, G. J. (2016). Process-based modelling of sediment distribution in fluvial crevasse splays, *78th EAGE Conference and Exhibition 2016*, Vienna, Austria pp. 1–5.

10. Boerboom, H. T. W., Sandén, A. B., **Van Toorenenburg, K. A.**, Donselaar, M. E., Weltje, G. J. (2016). High-resolution reservoir architecture modelling of crevasse splay deposits in low-net-to-gross fluvial stratigraphy, *78th EAGE Conference and Exhibition 2016*, Vienna, Austria, pp. 1–5.

9. **Van Toorenenburg, K. A.**, Donselaar, M. E., Weltje, G. J. (2016). Floodplain aggradation as a dominant control on autocyclic switching of low-gradient dryland rivers in endorheic basins, *5th EAGE Shale Workshop*, Catania, Italy, pp. 1–5.

8. **Van Toorenenburg, K. A.**, Donselaar, M. E., Weltje, G. J. (2016). Stacked crevasse splays in the semi-arid Huesca fluvial fan (Ebro Basin, Spain) - Implications for connectivity, *5th EAGE Shale Workshop*, Catania, Italy, pp. 1–5.

7. Sandén, A. B., Donselaar, M. E., Storms, J. E. A., **Van Toorenenburg, K. A.**, Van der Vegt, H., Weltje, G. J. (2016). Process-based modelling of sediment distribution in fluvial crevasse splays, *2nd EAGE Conference on Forward Modelling of Sedimentary Systems*, Trondheim, Norway, pp. 1–5.

6. **Van Toorenenburg, K. A.**, Donselaar, M. E., Weltje, G. J. (2016). Stacked crevasse splays in the semi-arid Huesca fluvial fan (Ebro Basin, Spain): implications for connectivity, *Nederlands Aardwetenschappelijk Congres 13*, Veldhoven, The Netherlands, pp. 1–1.

5. Donselaar, M. E., Bouman, L. S., Noordijk, N. A., **Van Toorenenburg, K. A.**, Weltje, G. J. (2015). Reservoir potential of thin-bedded sandstone in continental mudrock successions - The search for hidden treasures, *77th EAGE Conference and Exhibition 2015*, Madrid, Spain, pp. 1–5.

4. **Van Toorenenburg, K. A.**, Donselaar, M. E., Weltje, G. J. (2015). Reservoir architecture and tough gas reservoir potential of fluvial crevasse-splay deposits, *77th EAGE Conference and Exhibition 2015*, Madrid, Spain pp. 1–5.

3. **Van Toorenenburg, K. A.**, Donselaar, M. E., Weltje, G. J. (2015). Reservoir architecture of fluvial crevasse splay deposits, *AAPG Annual Convention and Exhibition 2015*, Denver, USA, pp. 1–1.

2. **Van Toorenenburg, K. A.**, Donselaar, M. E., Weltje, G. J. (2015). Tough gas reservoirs in fluvial crevasse splay sandstones, *AAPG Annual Convention and Exhibition 2015*, Denver, USA, pp. 1–1.

1. **Van Toorenenburg, K. A.**, Donselaar, M. E., Weltje, G. J. (2014). Characterizing thin-bedded, low-N/G tough gas reservoirs through reservoir-analogue and core studies, *Nederlands Aardwetenschappelijk Congres 12*, Veldhoven, The Netherlands, pp. 1–1.

Other publications

3. **Van Toorenenburg, K. A.**, Donselaar, M. E., Weltje, G. J. (2018). Cover image, *Earth Surface Processes and Landforms* **43**(11): i–i.

2. **Van Toorenenburg, K. A.**, Donselaar, M. E., Weltje, G. J. (2014). Tough gas targeting through high-resolution characterisation of fine-grained sedimentary rock, *Public Report TKI Gas*, TKIG01024, pp. 1–3.

1. **Van Toorenenburg, K. A.**, Donselaar, M. E., Weltje, G. J. (2014). Tough gas targeting through high-resolution characterisation of fine-grained sedimentary rock, *Confidential Report TKI Gas*, TKIG01024, pp. 1–11.